2008

The effect of demand, tank parameters, and pumping stations on energy use in municipal drinking water distribution systems

Santosh Raj Ghimire
Michigan Technological University

Follow this and additional works at: https://digitalcommons.mtu.edu/etds
Part of the Civil and Environmental Engineering Commons

The Effect of Demand, Tank Parameters, and Pumping Stations on Energy Use in Municipal Drinking Water Distribution Systems

By

Santosh Raj Ghimire

A DISSERTATION

Submitted in partial fulfillment of the requirements

For the degree of

DOCTOR OF PHILOSOPHY

(Environmental Engineering)

MICHIGAN TECHNOLOGICAL UNVIERSITY

2008

The Dissertation, "The Effect of Demand, Tank Parameters, and Pumping Stations on Energy Use in Municipal Drinking Water Distribution Systems" is hereby approved in partial fulfillment of the requirement for the degree of DOCTOR OF PHILOSOPHY in the field of (Environmental Engineering).

Program: Environmental Engineering

Dr. Brian D. Barkdoll, Dissertation Advisor — Date

Dr. Judith A. Perlinger, Program Chair — Date

Dr. Neil J. Hutzler, Committee Member — Date

Dr. David W. Hand, Committee Member — Date

Dr. Leonard J. Bohmann, Committee Member — Date

Abstract

Two of the indicators of the UN Millennium Development Goals ensuring *environmental sustainability* are energy use and per capita carbon dioxide emissions. The increasing urbanization and increasing world population may require increased energy use in order to transport enough safe drinking water to communities. In addition, the increase in water use would result in increased energy consumption, thereby resulting in increased greenhouse gas emissions that promote global climate change. The study of multiple Municipal Drinking Water Distribution Systems (MDWDSs) that relates various MDWDS aspects—system components and properties—to energy use is strongly desirable. The understanding of the relationship between system aspects and energy use aids in energy-efficient design. In this study, components of a MDWDS, and/or the characteristics associated with the component are termed as MDWDS aspects (hereafter—system aspects). There are many aspects of MDWDSs that affect the energy usage. Three system aspects (1) system-wide water demand, (2) storage tank parameters, and (3) pumping stations were analyzed in this study. The study involved seven MDWDSs to understand the relationship between the above-mentioned system aspects in relation with energy use. A MDWDSs model, EPANET 2.0, was utilized to analyze the seven systems.

Six of the systems were real and one was a hypothetical system. The study presented here is unique in its statistical approach using seven municipal water distribution systems.

The first system aspect studied was system-wide water demand. The analysis involved analyzing seven systems for the variation of water demand and its impact on energy use. To quantify the effects of water use reduction on energy use in a municipal water distribution system, the seven systems were modeled and the energy usage quantified for various amounts of water conservation. It was found that the effect of water conservation on energy use was linear for all seven systems and that all the average values of all the systems' energy use plotted on the same line with a high R^2 value. From this relationship, it can be ascertained that a 20% reduction in water demand results in approximately a 13% savings in energy use for all seven systems analyzed. This figure might hold true for many similar systems that are dominated by pumping and not gravity driven.

The second system aspect analyzed was storage tank(s) parameters. Various tank parameters: (1) tank maximum water levels, (2) tank elevation, and (3) tank diameter were considered in this part of the study. MDWDSs use a significant amount of electrical energy for the pumping of water from low elevations (usually a source) to higher ones (usually storage tanks). The use of electrical energy has an effect on pollution emissions and, therefore, potential global climate change as well. Various values of these tank parameters were modeled on seven MDWDSs of various sizes using a network solver and the energy usage recorded. It was found that when averaged over all seven analyzed systems (1) the reduction of maximum tank water level by 50% results in a 2% energy reduction, (2) energy use for a change in tank elevation is system specific, and (2) a reduction of tank diameter of 50% results in approximately a 7% energy savings.

The third system aspect analyzed in this study was pumping station parameters. A pumping station consists of one or more pumps. The seven systems were analyzed to understand the effect of the variation of pump horsepower and the number of booster stations on energy use. It was found that adding booster stations could save energy depending upon the system characteristics. For systems with flat topography, a single main pumping station was found to use less energy. In systems with a higher-elevation neighborhood, however, one or more booster pumps with a reduced main pumping station capacity used less energy. The energy savings for the seven systems was dependent on the number of boosters and ranged from 5% to 66% for the analyzed five systems with higher elevation neighborhoods (S3, S4, S5, S6, and S7). No energy savings was realized for the remaining two flat topography systems, S1, and S2.

The present study analyzed and established the relationship between various system aspects and energy use in seven MDWDSs. This aids in estimating the amount of energy savings in MDWDSs. This energy savings would ultimately help reduce Greenhouse gases (GHGs) emissions including per capita CO_2 emissions thereby potentially lowering the global climate change effect. This will in turn contribute to meeting the MDG of ensuring environmental sustainability.

Acknowledgements

First, my heart-felt acknowledgement goes to my Advisor Dr. Brian D. Barkdoll, whose continuous advice and support have always been a source of inspiration and encouragement and without which the research would not have been possible. I would like to thank and appreciate him for all his support.

I sincerely acknowledge, appreciate, and thank my advisory committee members: Dr. Neil J. Hutzler, Dr. David W. Hand, and Dr. Leonard J. Bohmann, for their valuable advice and comments on my research work.

I would like to thank all of the professors and instructors in various departments of Michigan Technological University—Department of Civil and Environmental Engineering, Department of Physics, Department of Social Sciences, and Department of Computer Sciences, who imparted an excellent education to me. I would like to thank all the professors associated with Michigan Tech's Sustainable Futures Institute and Southern University and A & M College, Nelson Mandela School of Public Policy and Urban Affairs, Baton Rouge, LA, who trained me for a quality education of sustainability. I would like to thank all of the staff within my department, the Graduate School, and in the rest of the campus community for their direct and indirect support. I gratefully acknowledge the valuable input from Dr. Anne Faith Mareck and Mrs. Sylvia

Matthews to improve the quality of the text in the dissertation, and wish to thank them for their help. In addition, I sincerely thank Dr. Debra D. Charlesworth for her valuable suggestions to improve the quality of the dissertation.

The author gratefully acknowledges support from the Sustainable Futures *Integrative Graduate Education and Research Traineeship* (IGERT) project sponsored by the National Science Foundation (NSF) (under Grant No. DGE 0333401). The research outcomes are the views of the author and not those of the NSF. The work would not have been possible without the financial support of the Department of Civil and Environmental Engineering and Sustainable Futures Institute, Michigan Technological University, and the NSF. I would like to thank them.

Finally, I would like to extend thanks and appreciation to my family members and friends for their continuous support. I thank my wife Pramila, and my daughter Angela who have been always a source of joy and inspiration. In addition, I thank my parents, my brother Shankar, his wife Stuti and their daughter Avani, who have been always a source of inspiration.

Dedication

To my parents Tek Raj Ghimire & Shobha Devi Ghimire—who nurtured me,

and

Janardan Acharya & Mina Devi Acharya—who nurtured my wife Pramila.

Table of Contents

List of Figures

List of Tables

Chapter 1

Introduction

1.1 Background

Two of the indicators of the UN Millennium Development Goals (MDG) ensuring "environmental sustainability" are energy use and per capita carbon dioxide (CO_2) emissions (Millennium Development Goals, 2000). According to the UN Population Division, the projected population of the world will exceed 9 billion by 2050 (United Nations Secretariat, 2007). The increasing world population will result in an increased demand for water. The rise in drinking water demands will increase the global warming agents, energy use and per capita CO_2 emissions, thereby posing a major challenge to meeting the MDG. Global warming is a huge challenge not only to the US (Levin et al., 2002) but also to the world.

Municipal drinking water distribution systems (MDWDS) come into play when a safe water supply is needed. In the US, more than 85% of the total drinking water is supplied by municipal water systems (Vickers, 2001). The electricity necessary for water processing and distribution in municipal water systems accounts for up to 80% of the cost (EPRI, 2002). Thus, the study of municipal drinking water distribution systems can be helpful in meeting the MDG of ensuring "environmental sustainability." If the energy use associated with the MDWDSs is studied, it will be a helpful contribution to achieving the MDGs. If water distribution systems were designed based upon a generalized rule developed from multiple systems, it will be useful to any system thereby helping to mitigating global warming. This means understanding the relationships between various aspects of multiple MDWDSs,—system components and system properties (hereafter—system aspects), and energy use will promote energy efficient design. The system components are the objects associated with MDWDSs, which include nodes (junctions), tanks, reservoirs, pumps, pipes, and valves; whereas properties are the characteristics of the objects. For example, water demand of a junction is a system property, while the junction itself is a system component. However, understanding energy sensitivity to create a better design is difficult due to the complex interactions among the system components (Lansey, 2000).

There are many researchers working in various aspects of water distribution systems. Some of the traditional research conducted in water distribution systems are highlighted in Table 1.1 on page 4 below. Most of the traditional research concentrates on least-cost design (Table 1.1 S# 7-12, p. 4). More specifically, the majority of research focus is least-cost optimization of pipe diameter (Savic and Walters, 1997). The other components of research influencing energy consumption considered in water distribution systems are pump scheduling (Table 1.1, S# 4-6) and control valve location (Reis el al., 1997). In particular, energy consumption has been examined through optimum pump scheduling (Brion and Mays, 1991, Farmani et al., 2004, Pezeshk and Helweg, 1996, Tarquin and

Dowdy, 1989) and through optimal system design to minimize energy consumption (Gyergyek and Presern, 1982).

The traditional methods of analyzing water distribution systems are valuable and can be applied successfully only to the specific water distribution system that was studied as described above. The major purpose of those studies was to provide system-specific information on optimal capital cost of design of MDWDS components to ensure economic benefit. The past two and a half decades of research on MDWDSs are mostly focused on capital costs (Zecchin et al., 2007). Importantly, this research was conducted on a limited number of systems—most of them were conducted on one system (N=1) (see Table 1.1, p. 4). The application of a limited number of systems as a benchmark has become a tradition in municipal water distribution research. In contrast, the current study will seek to develop a trend of application of multiple numbers of systems in the MDWDSs research arena by using seven systems for the analysis. This use of seven systems (N=7) is a new attempt to use a bigger sample size, N>7, for MDWDS analysis. The study will invite researchers to continue using higher N values to obtain robust and generalizable results applicable to any system. This will ultimately contribute to the development of a set of standards for efficient design for MDWDS design that are applicable to all systems.

In addition, there are some researchers working on broader economic and environmental aspects of MDWDSs design and management. For example, minimization of energy cost (Table 1.1 S# 4-6, p. 4), eco-efficiency analysis of water supply expansions, life-cycle energy analysis of pipe replacements frequency (Table 1.1 S# 1-2,

p. 4), whole life costing of water distribution systems (Skipworth et al., 2002), and life cycle analysis of water use in multi occupant buildings (Arpke and Hutzler, 2005). Researchers are also focusing to integrate issues such as water conservation (Ellis, 1978) in MDWDSs. Albuquerque, New Mexico's successful attempt at reducing per capita water consumption by 20% in 9 years (1995-2004) is exemplary in this regard (Vickers, 2001). However, the relationship between MDWDS aspects and the associated energy use has not been studied. It is strongly desirable to study the relationship between the MDWDS aspects and energy use based upon multiple MDWDSs. The current study will address the challenge of studying the relationship between system aspects and associated energy use. This will aid in energy efficient design of MDWDSs and in turn will help to meet the MDG of ensuring environmental sustainability.

Table 1.1 Current approaches of analysis of MDWDSs

S #	References/ Summary	Systems	Comments
1	**Mohapatra et al. (2002):** Eco-efficiency analysis of Amsterdam water supply expansion was performed.	1	Paper concluded that the conventional energy use is one of the major contributors to environmental impact. This indicates that energy use in municipal water systems is a major concern for GHG emissions.
2	**Filion et al. (2004):** Life-cycle energy analysis of pipe replacement frequency of a water distribution system was performed.	1	The 50-year replacement plan yielded the minimum energy expenditure in comparison to the remaining 10-, 20-, and 100-year frequencies.
3	**Meier and Barkdoll (2000):** The genetic algorithm was applied to optimize the sampling design for network calibration.	1	Calibration is needed to simulate more accurate results.
4	**Yu et al. (1994):** Generalized reduced gradient method was applied to optimize pump scheduling.	1	The method was recommended as a general method for any water distribution system with multiple pumping stations and sources.

			However, it was demonstrated only in one system.
5	**Lansey and Awumah (1994):** Dynamic programming was used for optimal pump scheduling	1	The paper studied the minimization of energy cost with a limitation of mid size systems.
6	**Ulanicki, B. et al (2007):** Dynamic optimization was used for optimal scheduling of pumps.	1	The method was demonstrated in one system as a case study.
7	**Colombo and Karney (2001):** A study of energy costs due to leaky pipes was presented.	1	The paper stated that the cost due to leaks depends on system complexity.
8	**Savic and Walters (1997):** A potential use of genetic algorithms for least cost design of a pipe in a water distribution system was presented.	3	The results of the paper were compared with seven other studies.
9	**Simpson et al. (1994):** Study of application of genetic algorithms, complete enumeration, and non-linear programming in a water system was presented.	1	The optimization of least-cost expansion of a pipe network has to be tested on any system.
10	**Zecchin et al. (2007)**: Application of ant colony optimization algorithms to water systems design (pipe) was presented.	4	This algorithm was demonstrated in four systems.
11	**Babayan et al. (2007):** Least cost design of pipes of water system using genetic algorithms was presented.	1	Authors stated that their optimization methods have to be tested on more networks.
12	**Cunha and Sousa (2001):** Simulated annealing heuristics to find least-cost design of pipes for water systems are presented.	2	The authors stated that more research should be done on complex systems.

1.2 Research Objectives and Scope

The motivation underlying this study is to aid the research in MDWDSs to incorporate current issues such as water conservation, environmental impacts, and energy consumption in MDWDS planning to help to meet the MDG of ensuring environmental sustainability. Congruent with the motive, there are two main objectives of the study:

(1) To begin a trend of using a larger number of systems (N>4) in MDWDSs research

(2) To analyze seven MDWDSs (N=7) to understand the effect of variation in system aspects on energy use as described below:

- Variation in water demand
- Variation in tank parameters (maximum water levels, tank locations, and tank diameters)
- Variation in pump horsepower, pumping stations, and their locations

1.3 Hypothesis

Recently, much valuable research is being done focusing on optimal design of municipal water distribution systems as described previously in Section 1.1 (p. 1). The relationships between various aspects and energy use will aid the researcher in energy-efficient design of MDWDSs. The system aspects of the seven diverse MDWDSs are as follows:

- Variation in water demand and the impact on energy use

- Variation in tank parameters (maximum water levels, tank locations, and tank diameter) and the impact on energy use
- Variation in pump horsepower, pumping stations, and their locations and the impact on energy use

The relationships indicating the effect of variation of several system aspects of water networks on energy use is yet to be addressed. To fill the current gap using multiple numbers of systems (N>4) in MDWDSs to study the relationships between various systems aspects, the following hypotheses have been developed.

(1) Water conservation by reducing water demand in MDWDSs will reduce energy consumption.

(2) Reduction of MDWDS storage tank parameters (maximum tank water level, tank elevation, and tank diameter) will reduce energy consumption.

(3) The addition of booster pumping stations can reduce energy usage.

1.4 Dissertation Organization

The dissertation is organized as follows:

(1) Chapter 1—Introduction

(2) Chapter 2—Description of Systems and System Modeling

(3) Chapter 3—Energy Savings through Water Conservation in Municipal Water Distribution Systems

(4) Chapter 4—Impact of Tank Parameters on Energy Conservation in Municipal Water Distribution Systems

(5) Chapter 5—The Role of Pumping Stations in the Reduction of Energy Use in Municipal Drinking Water Distribution Systems

(6) Chapter 6— Summary and Conclusions

(7) Appendices

(8) References

Chapter 2 will describe the seven systems analyzed. It will also include the common approach used for the analysis.

Chapter 3 will investigate the relationship between water demands of each of the analyzed systems and the corresponding energy use and state the findings. This study found that energy savings is realized through the reduction of water demand. The average energy savings for the systems for 20% water conservation was estimated to be approximately 13%, which might have a significant effect on the reduction of GHG emissions.

Chapter 4 will describe the relationship between storage tank parameters: tank maximum water levels, tank elevation (locations), tank diameter, and corresponding energy use. It was found that the alteration of tank water levels has very little impact on energy use in comparison to the alteration of the remaining two parameters, tank elevation and tank diameter. It was found that the reduction of tank water level by 50% saved approximately 2% of the average energy use, and the reduction of tank diameter by 50% would save approximately 7% of average energy use for the seven systems. The energy savings by tank parameter variation was not as effective as other system aspect variations.

Chapter 5 presents the analysis of the seven systems to identify the role of pump stations in the reduction of energy use. The impact of variation in pump horsepower, number of pumping stations (boosters), and their location was studied. It was found that the role of boosters is more important than pump horsepower. The optimal number of booster stations, however, may vary depending upon the systems' characteristics. There were no energy savings from booster additions in two of the analyzed systems, S1 and S2 due to the system topography and head values. However, the optimal energy savings for the five systems analyzed was found to range from 5% to 66 %.

Chapter 6 will describe the summary and conclusions. The research findings showed that there is a tremendous potential to save energy in municipal water distribution systems. The understanding of relationships between system aspects,-components and properties- and energy use is important to save energy. The saving in energy thus leads to protection of the global environment by reducing GHG emissions. However, a further study is recommended in order to quantify a more accurate amount of GHG emissions reductions through MDWDSs energy savings. This is a separate study and is left open as a future work to be addressed.

1.5 New Contributions

The general contribution of the current study is to help mitigate GHG emissions and thus move towards the MDG of “environmental sustainability”. The results of this study will aid researchers and/or water utility managers in understanding the relationship between the above-mentioned system aspects, thus enabling them to design MDWDSs more efficiently.

More specifically, the new contributions of the current study are twofold: (1) to initiate the tradition of multi-systems approach of MDWDSs research, and, (2) to formulate relationships between system aspects as described below:

- Formulation of the relationship between water demand reduction and energy use
- Formulation of the relationship between tank parameters: storage tank maximum water levels, tank elevation (location), and tank diameter, and energy use
- Formulation of the relationship between pumping stations: pump horsepower, number of pumping stations (boosters) and their locations, and energy use

The study presented here is based upon seven municipal water distribution systems of which six are real systems and one is hypothetical. The research initiates a tradition of multi system approach in the MDWDSs research arena.

Chapter 2

Description of Systems and System Modeling

2.1 Background Information of Distribution Systems

Six of the seven systems used for the analysis are realistic, having been based on actual municipal systems; the seventh system is a hypothetical system. The names of the municipalities have been omitted for security reasons. Table 2.1 (p. 12) summarizes the system characteristics, where the difference between the minimum water level in the system (usually the source water elevation) and the maximum system-wide water elevation (usually the maximum tank level in the system) serves as a surrogate for the elevation head that the pumps have to overcome. In addition, the system-wide frictional loss values are represented by the surrogate, *F*. The loss values, *F*, are given in the last column in Table 2.1. The *Hazen-Williams* equation was used to match the data sets for the distribution systems modeled, since all seven systems had *Hazen-Williams C* values rather than *Darcy-Wiesbach f* values.

The system-wide friction loss was computed using the Hazen-Williams Equation given as follows (Haestad Methods, 2004, Ghimire and Barkdoll, 2008):

$$\frac{h_L}{Q^{1.852}} = \frac{C_f L}{C^{1.852} D^{4.87}} = F \tag{2.1}$$

where,

h_L	=	head loss due to friction (ft, m)
Q	=	pipeline flow rate (ft^3/s, m^3/s)
C_f	=	unit conversion factor (4.73 English, 10.7 SI)
L	=	pipe length (ft, m)
C	=	Hazen-Williams C-factor
D	=	pipe diameter (ft, m)
F	=	system-wide friction index ($s^{1.852}/ft^{4.556}$), ($s^{1.852}/m^{4.556}$) (§Units)

Table 2.1 Summary of system characteristics (After Ghimire and Barkdoll, 2008)

System	Junctions	Pipes	Pumps	Reservoirs	Tanks	Valves	Headloss: Static	Headloss: Friction	Headloss: % Static	Headloss: % Friction	(F) System-wide Friction loss
	(#)	(#)	(#)	(#)	(#)	(#)	(Δz_{max}) m (ft)	m (ft)			§Units
S1	6	8	1	1	1	0	39.6 (130)	52.7 (173)	42.9%	57.1%	451.1 (108,767.7)
S2	44	62	1	1	1	0	33.7 (110.5)	3.0 (9.9)	91.8%	8.2%	2,695.3 (649,894.3)
S3	126	168	2	1	2	8	217 (712.1)	1.2 (4.1)	99.6%	0.4%	252.8 (60,953.3)
S4	126	144	6	2	2	4	93.0 (305)	48.0 (157.4)	66.0%	34.0%	7,602.1 (1,833,024.0)
S5	347	394	8	1	2	1	100.3 (329)	79.0 (259.3)	55.9%	44.1%	16,354.9 (3,943,504.6)
S6	873	958	3	1	1[#]	6	27.4 (90)	87.8 (288.1)	23.8%	76.2%	79,291.4 (19,118,852.9)
S7	12,525	14,824	6	2	4	5	73.7 (241.7)	267.7 (878.4)	21.6%	78.4%	1,928,561.4 (465,017,213.8)

[#] *S6 was later modified by adding a second tank for the rest of the analysis.*

In Table 2.1 above, Δz_{max} is the elevation difference between the highest point (typically the maximum water level of the highest tank) of a system and the lowest point (source reservoir).

The static friction of all the systems was computed based upon the elevation difference between the storage tank and the reservoir (source). Usually the lowest elevation in a system is at the reservoir (source), and the highest elevation occurs at the storage tank. However, S3 has several junctions near Pumping station 1 with the elevation lower than the reservoir. The difference in elevation between the reservoir and the pumping station of S3 is 425 ft (129.5m).

In Table 2.1 (p. 12), the percentage of headlosses due to friction and static head were calculated as follows:

$$\text{\% Headloss due to friction} = \frac{\text{Headloss due to friction}}{(\text{static loss} + \text{friction friction})} x100\% \qquad (2.2)$$

$$\text{And, \% of static head} = \frac{\text{static head}}{\text{static loss} + \text{friction loss}} x100\% \qquad (2.3)$$

Thus, it can be seen in Table 2.1 that the systems comprise a range of sizes from 6 up to 12,525 junctions; 6 to 14,824 pipes (both a range of more than three orders of magnitude); 1 to 8 pumps; 1 to 2 reservoirs; 0 to 8 valves; 1 to 4 tanks; 27 to 201 m of change in water elevation, Δz; and from 252.8 to 1,928,561.4 (SI units) or 60,953 to 465,017,213.8 (English units) (a range of more than 700 orders of magnitude) of system-wide friction losses, F—thus comprising a wide range of system characteristics. In addition, the energy required to overcome losses due to friction and the static head of each system for peak daily demand hour can be found in Table 2.1 (p. 12). The minor head loss due to fittings and pump mounts is not included in the calculation. The headloss due to friction was calculated using the Hazen-Williams Equation (2.1) as described on page 12 above.

All systems used are pump-driven rather than gravity driven. Systems that exclusively use a large amount of gravity are not of interest here since they do not use a significant amount of energy.

2.1.1 Pump Efficiency

Pump efficiency is the ratio of power input to power output. Power input means the amount of power supplied to the motor. Output power may be subdivided into two terms: (1) *brakepower,* and (2) *waterpower,* depending upon several stages of energy input and output (Haestad Methods, 2004).

The amount of power supplied to the pump is called *brakepower,* whereas power supplied to water is termed *waterpower*. Thus, pump efficiency can be defined based upon the brakepower, waterpower, or a combination of both. The combined efficiency is known as *wire-to-water* or *overall* efficiency and is used in this water distribution system modeling. For water distribution systems analysis, an overall efficiency is used in two ways: (1) fixed efficiency and (2) efficiency curve. A fixed *wire-to-water* efficiency of 75% may be used for all the pumps for each system analysis. However, a typical wire-water efficiency curve may be generated using the following two typical curves: (1) typical pump efficiency (Crowe et. al., 2001, Daugherty and Franzini, 1957), (2) typical motor efficiency (Upper Peninsula Power Company, 2007). The wire-to-water curve (Figure 2.1, p. 15) thus may be generated by using the following relationship (Finnemore and Franzini, 2002):

$$E = \frac{\text{output power}}{\text{input power}} \tag{2.4}$$

Assuming a typical pump as 86% efficient on average (Crowe et. al., 2001, Daugherty and Franzini, 1957), and the average efficiency of standard-efficiency motors at average rated load as 86% (Upper Peninsula Power Company, 2007), the fixed wire-to-water pump efficiency can be estimated as approximately 75%.

A fixed wire-to-water pump efficiency of 75% was used for the first two aspects, demand variation and tank parameter variation of MDWDS, of this study. However, a typical pump efficiency curve (Figure 2.1 below) was used for the third aspect, pumping station analysis.

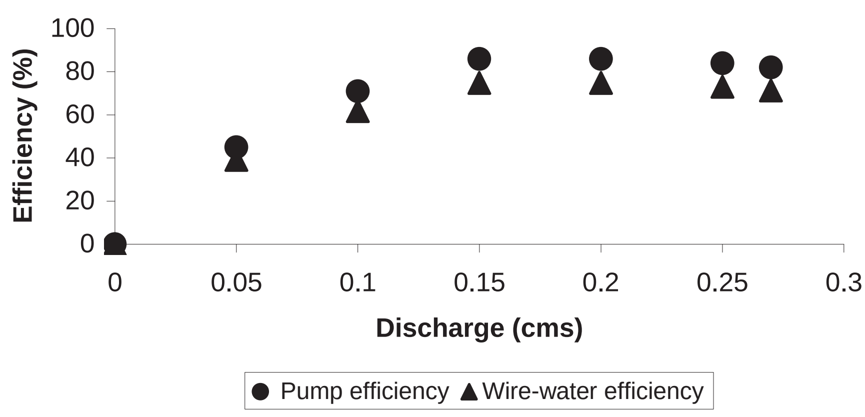

Figure 2.1 Typical wire-water pump efficiency curve:
Modified after Crowe et al., (2001)

2.1.2 Diurnal Demand Curve

Different water systems have their own water use pattern. The nature of water usage in a water distribution system may be represented by a water demand pattern or a diurnal curve. A global demand pattern may be used to address the stochastic nature of demand throughout a system or an individual pattern may be assigned for a junction. The nature of the curves could vary depending upon the water usage. Water usage in businesses, factories, single-family homes, and restaurants may have their own demand patterns (Haestad Methods, 2004). In general, the diurnal curves for residential areas have two peaks, the first during 7:00 to 13:00, and the second during 17:00 to 21:00 hours (Viessman and Hammer, 1998, and Wolff, 1961). A diurnal curve (Fig 2.2 below) was used for S1, S2, S4, and S6. The maximum daily demand of the curve in Figure 2.2 occurred at 18:00 hours, whereas it occurred at slightly different hours for the rest of the curves in systems S3, S5 and S7 (Figures 2.3, 2.5, and 2.6, p. 17-19).

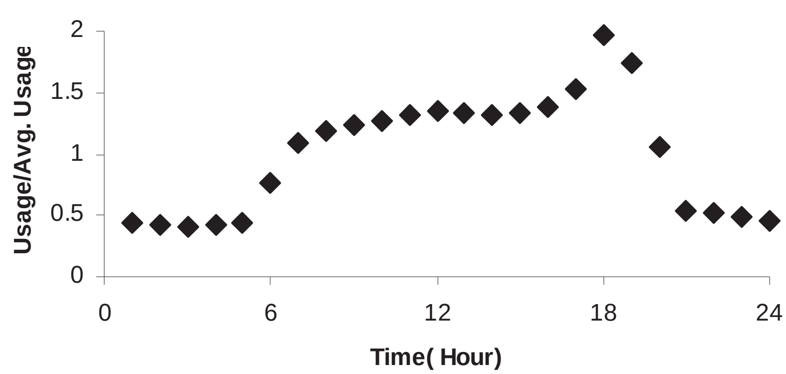

Figure 2.2 Demand pattern used for systems S1, S2, S4, and S6 (Approximately calculated from Viessman and Hammer, 1998; and Wolff, 1961)

Two diurnal curves were used in S3. The first curve (Figure 2.3 below) was used for all except five junctions.

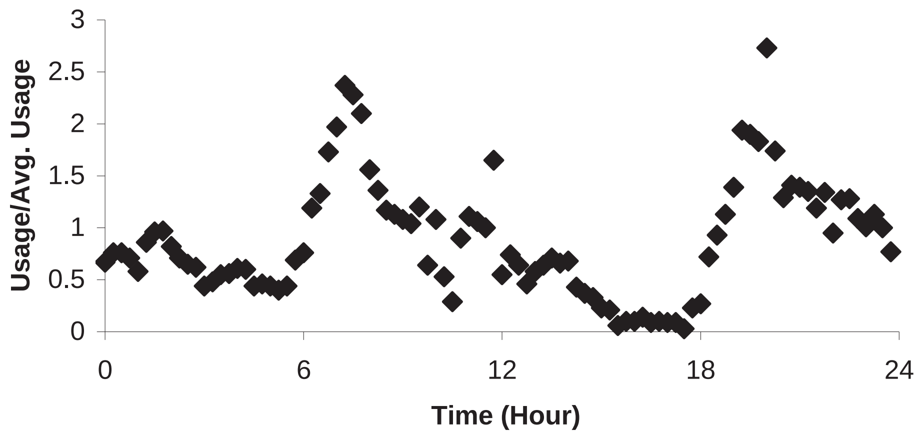

Figure 2.3 Demand pattern used for S3
(Approximately plotted from Ostfeld et al., 2006)

These five junctions used a second diurnal curve as shown in Fig 2.4 (p. 18). Even though the type of curve was not explicitly known, the nature of the curve matches with a typical diurnal curve for a factory (Haestad Methods, 2004), suggesting that S3 could incorporate five industrial junctions (Figure 2.10, p. 22).

S3 used an additional pattern (Figure 2.4) that matches with the demand pattern of a factory (Haestad Methods, 2004). It should be noted that since the diurnal curve in Fig. 2.4 was obtained directly from the original system data file from Ostfeld et al. (2006), it was not modified even though the integrated value of the curve does not sum to 1.0 as logic would dictate.

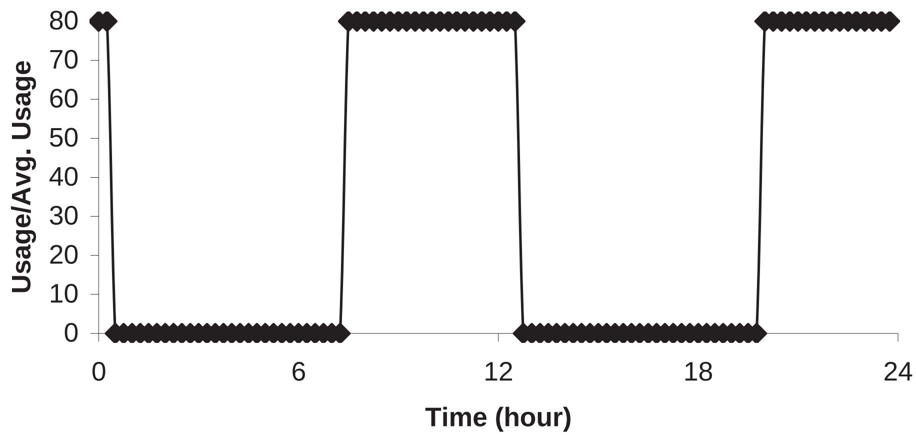

Figure 2.4 Demand pattern used in five junctions of S3
(Re-plotted from Ostfeld et al., 2006)

The Figure 2.5 following was the diurnal curve used for S5.

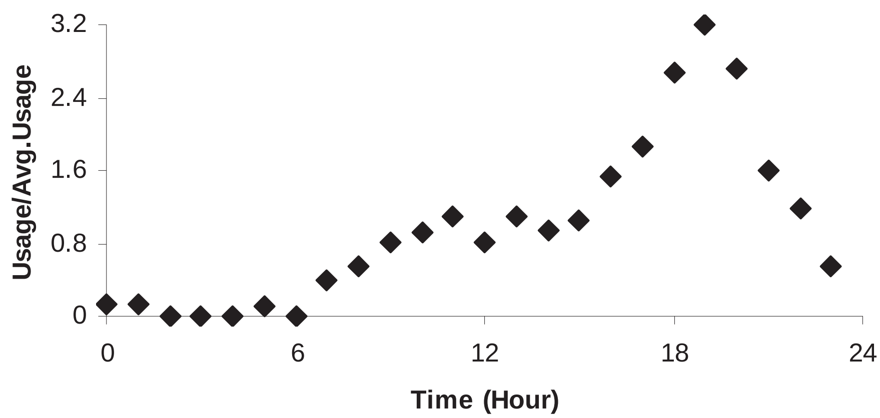

Figure 2.5 Demand pattern of S5

The curve shown below (Figure 2.6) represents a part of the original curve used for system S7, which had a 936-hour hydrograph. However, only 96 hours of the pattern have been shown here to match the simulation time for this study.

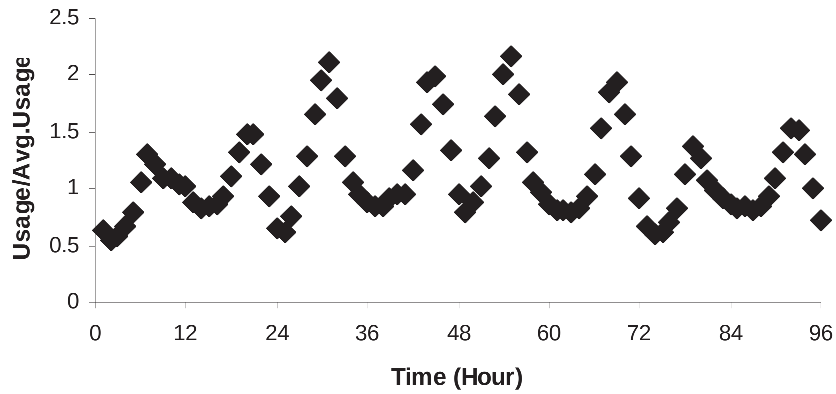

Figure 2.6 Demand pattern of S7
(Re-plotted from Ostfeld et al., 2006)

All of the junctions except reservoir "R3" (see Figure 2.14, p. 26) used the pattern represented by the curve at Figure 2.6 above. R3 used a different diurnal curve of a steady demand as given in Figure 2.7 below. Like the pattern in Figure 2.6, the second pattern applied to S7 is a segment of a 936-hour hydrograph. However, this pattern is just a steady demand for the first 592 hours. Thus, the second applied curve for the simulations of S7 is a straight line as shown below in Figure 2.7.

Reservoir, R3, has a negative demand of 3,078 gpm with the pattern as shown in Figure 2.7 below, indicating that S7 has another water source entering the system.

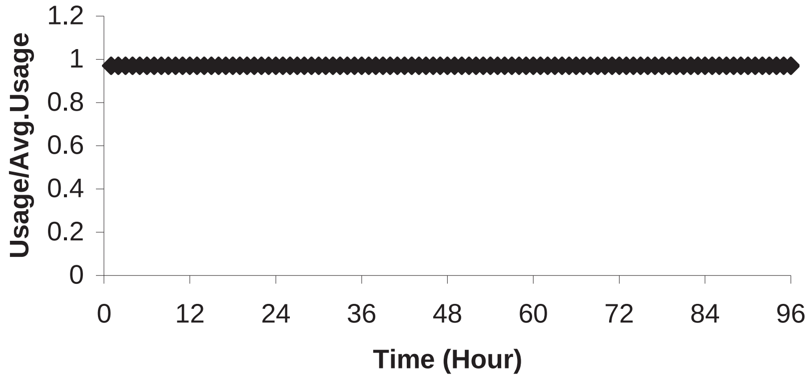

Figure 2.7 Demand pattern of S7 used for a water source, R3 (Re-plotted from Ostfeld et al., 2006)

2.2 Overview of Distribution Systems

The system-specific details of each of the seven systems are presented next. The systems are presented in the order of their complexity from simplest to the most complex. A diurnal demand curve was included, as described above, to make simulations more realistic.

2.2.1 System 1 (S1)

S1 is the first and simplest system used for the analysis. It was taken from the EPANET manual (EPA 2000) example problem (Figure 2.8 below). The system consists of six junctions, eight pipes, a pump, a reservoir, a tank, and no valves (see Table 2.1, p. 12). S1 used a typical diurnal curve as shown in Figure 2.2, p. 16 above.

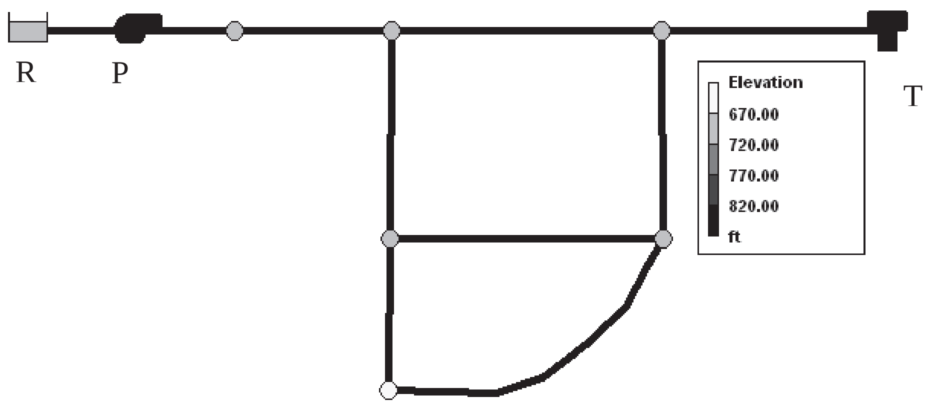

Figure 2.8 System 1 network map (Figure created from data from EPA, 2000)
Note: R = Reservoir, T = Tank, P = Pump house map

2.2.2 System 2 (S2)

S2 is a moderately sized system with 44 junctions, 62 pipes, a pump, a reservoir, and a tank, (Figure 2.9 below). It uses the same diurnal curve (Figure 2.2, p. 16) as S1.

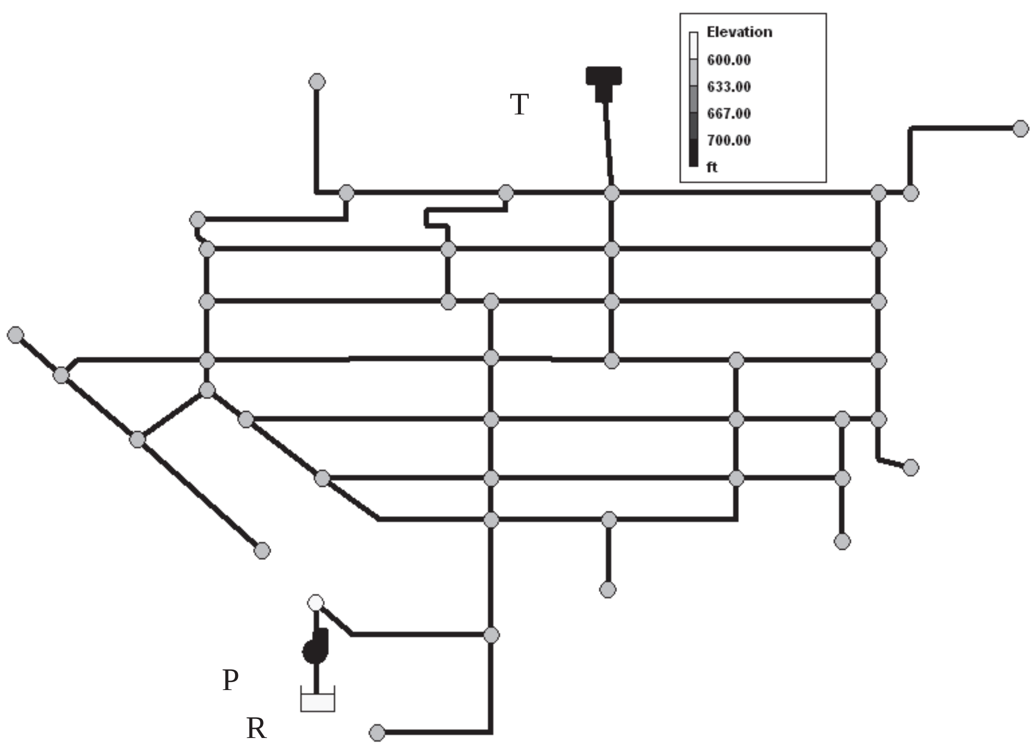

Figure 2.9 System 2 network map
Note: R = Reservoir, T = Tank, P = Pump house

2.2.3 System 3 (S3)

The third system, S3 (shown in Figure 2.10 below) taken from Ostfeld et al. (2006) consists of 126 junctions, 168 pipes, two pumps, one reservoir, two tanks, and eight valves. S3 used two different diurnal curves as described earlier in Section 2.1.2 on p. 16. The majority of junctions used a diurnal curve as shown in Figure 2.3 (p. 17). However, five of the junctions (highlighted in Figure 2.10 below) used a pattern as shown in Figure 2.4 (p. 18). S3 could have five industrial junctions due to the nature of the diurnal curve as described in Section 2.1.2 (p. 16).

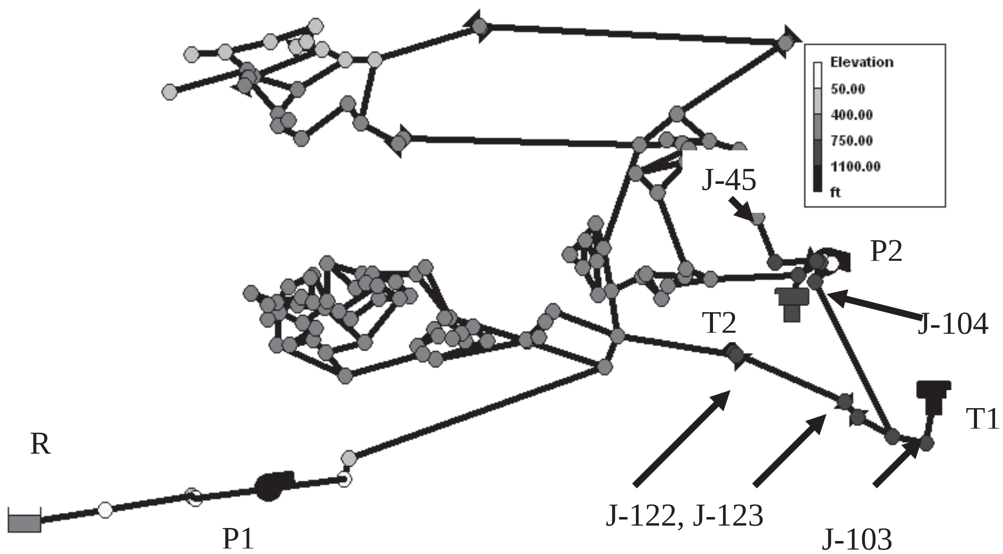

Figure 2.10 System 3 network map (Figure created from data from Ostfeld et al., 2006)
Note: R = Reservoir, T = Tank, P = Pump house (highlighted are five industrial junctions J-45, J- 103, J-104, J 122, and J- 123, which used the diurnal curve shown in Figure 2.4 while the rest used that shown in Figure 2.3).

2.2.4 System 4 (S4)

S4 (Figure 2.11 below) is similar in size to S3. It has 126 junctions, 144 pipes, six pumps (two pumps in operation and four on standby), two reservoirs, two tanks, and four valves. S4 used a diurnal curve as shown in Figure 2.2 (p. 16).

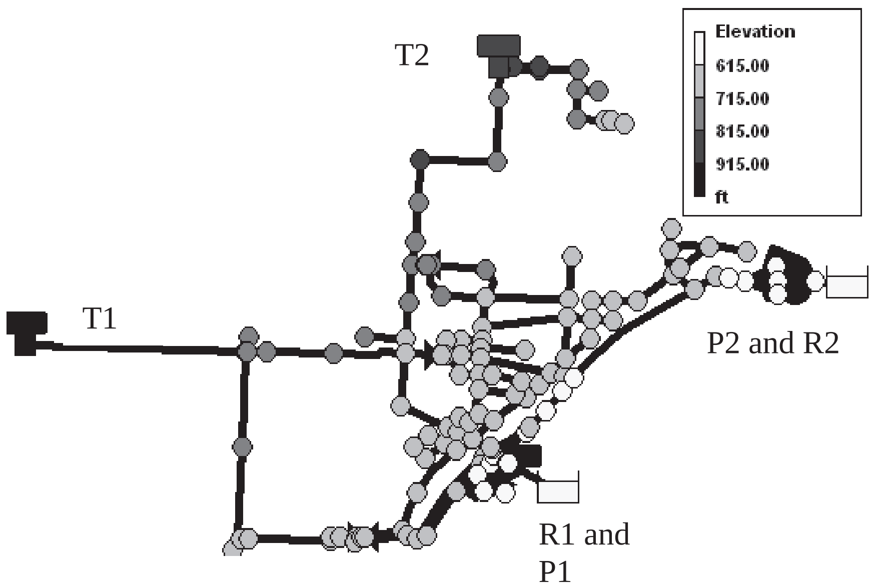

Figure 2.11 System 4 network map
Note: R = Reservoir, T = Tank, P = Pump house

2.2.5 System 5 (S5)

S5 is a moderately bigger system (Figure 2.12 below). It consists of 347 junctions, 394 pipes, eight pumps (four in operation and four for on standby), a reservoir, two tanks, and a valve. It has a diurnal curve as shown in Figure 2.5 (p. 18).

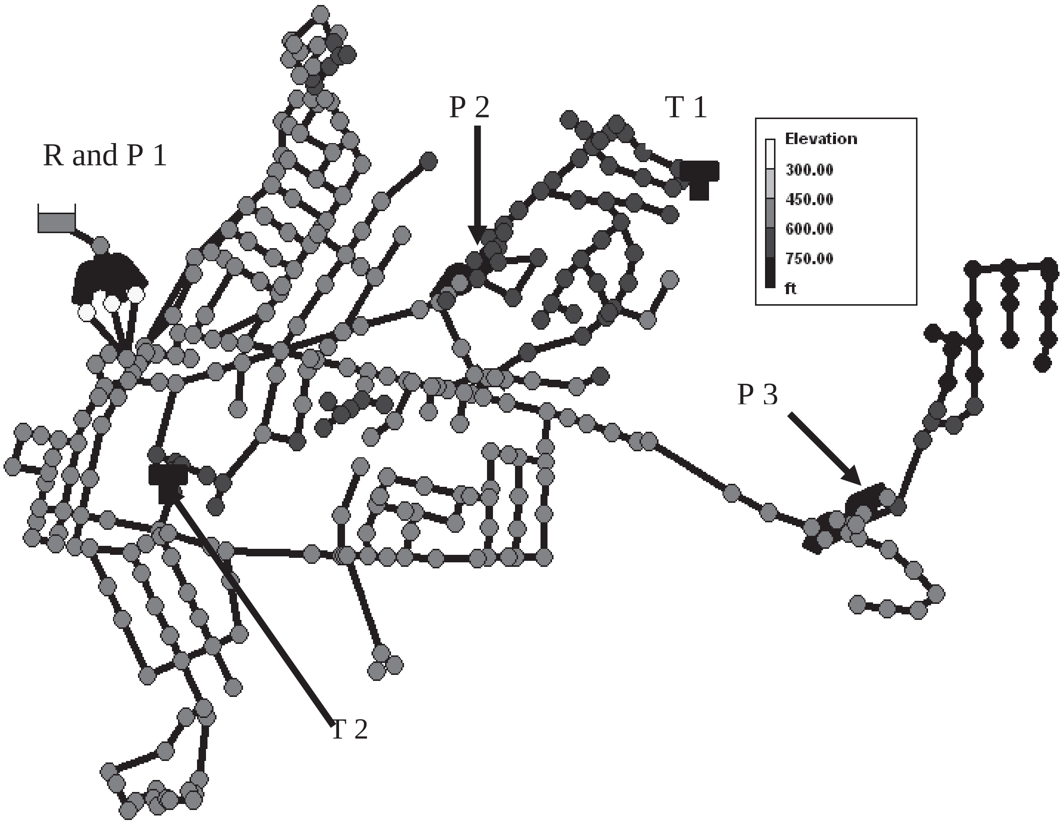

Figure 2.12 System 5 network map
Note: R = Reservoir, T = Tank, P = Pump house

2.2.6 System 6 (S6)

The sixth system, S6 used for the analysis, consists of 873 junctions, 958 pipes, 3 pumps (one operating and two on standby), a reservoir, two tanks, and six valves (Figure 2.13 below). The system used the typical diurnal curve as described in Figure 2.2 (p. 16).

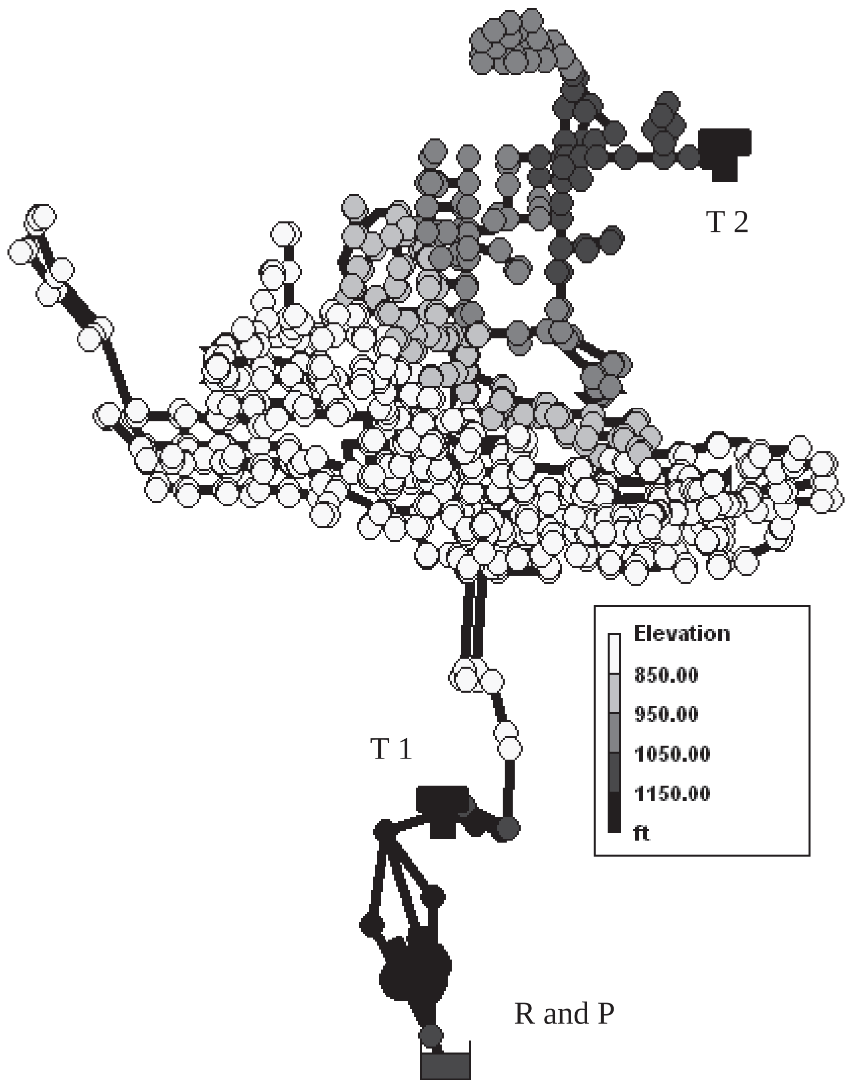

Figure 2.13 System 6 network map
Note: R = Reservoir, T = Tank, P = Pump house

2.2.7 System 7 (S7)

S7 is the biggest system, taken from Ostfeld et al. 2006 as seen in Figure 2.14 below. The system consists of 12,525 junctions, 14,824 pipes, six pumps (three in use: two at pump house P1 and one at pump house P2, and three on standby: one at pump house P3 and two at pump house P4), two reservoirs, four tanks, and five valves. There is an additional water source, R3, that supplies water to S7 (see Figure 2.14). S7 used two different types of diurnal curves as shown above in Figure 2.6 (p. 19) and Figure 2.7 (p. 20). The additional water source, R3, used the demand pattern of Figure 2.7, and the rest of the system used the pattern as shown in Figure 2.6 (p. 19).

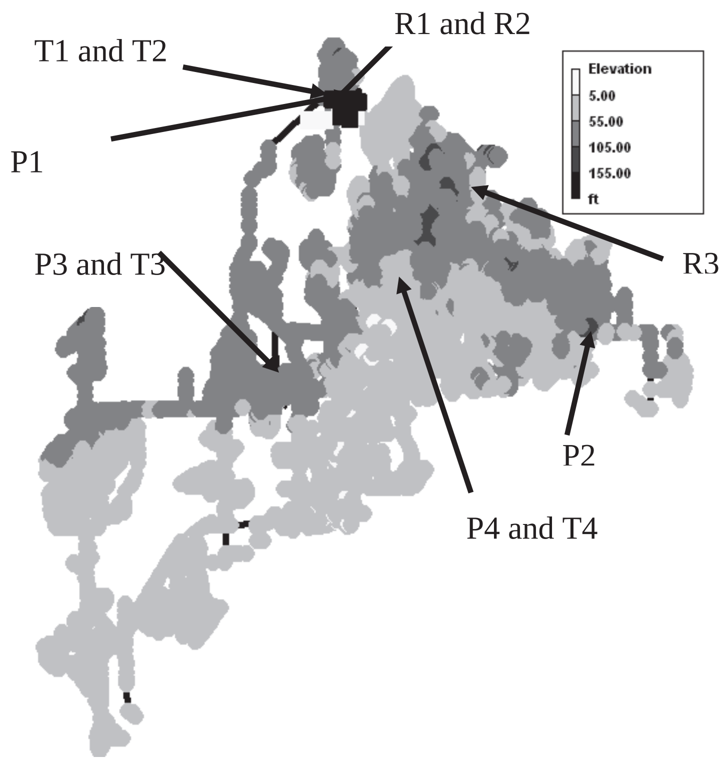

Figure 2.14 System 7 network map (Figure created from data from Ostfeld et al., 2006)
Note: R = Reservoir, T = Tank, P = Pump house

2.3 Hydraulic Grade Line (HGL) and Energy Grade Line (EGL) of Systems

In order to get a better feeling for each system, the concepts of Hydraulic Grade Line and Energy Grade Line are helpful. These will be reviewed here, followed by EGL plots for each of the systems.

The concept of hydraulic grade line (HGL) and energy grade line (EGL) can be understood from Bernoulli's theorem (Finnemore and Franzini, 2002) for steady and incompressible fluid along a stream line:

$$\left[\frac{p}{\gamma} + z + \frac{V^2}{2g}\right] = \text{Constant} \tag{2.5}$$

For the case when energy is added to a system and friction is considered, Equation (2.5) may be expanded as below (Finnemore and Franzini, 2002):

$$\left[\frac{p_1}{\gamma} + z_1 + \frac{V_1^2}{2g}\right] + h_p = \left[\frac{p_2}{\gamma} + z_2 + \frac{V_2^2}{2g}\right] + h_L \tag{2.6}$$

where,

p = static fluid pressure (N/m^2 or Pa, lb/ft^2 or psi)

γ = specific weight of fluid (in this case, water) = (N/m^3, lb/ft^3)

z = elevation of a point above a datum (m, ft)

V = average velocity of fluid ((m/s, f/s)

h_p = head added to fluid by a pump (in this case centrifugal pump), defined as energy per unit weight of fluid (N.m/N, lb.ft/lb)

h_L = Sum of all head losses (pipe wall friction, minor fittings losses), (m, ft)

Equation (2.6) does not include the internal energy of the fluid.

In Equation (2.6), the terms in the left hand side are defined as follows:

$\frac{p}{\gamma}$ = *pressure head* (m, ft)

z = *potential or elevation head* (m, ft)

$\frac{V^2}{2g}$ = *velocity head* (m, ft)

The line connecting the *piezometric* reading for a system of flowing water is known as the ***HGL*** of the system. A piezometer reads the quantity $\frac{p}{\gamma}+z$, the first two terms in Equation (2.5). If the additional term of velocity head is included, the quantity is defined as the ***EGL***.

Figure 2.15 below depicts the HGL and EGL of a simple water flow system (Crowe et al., 2001).

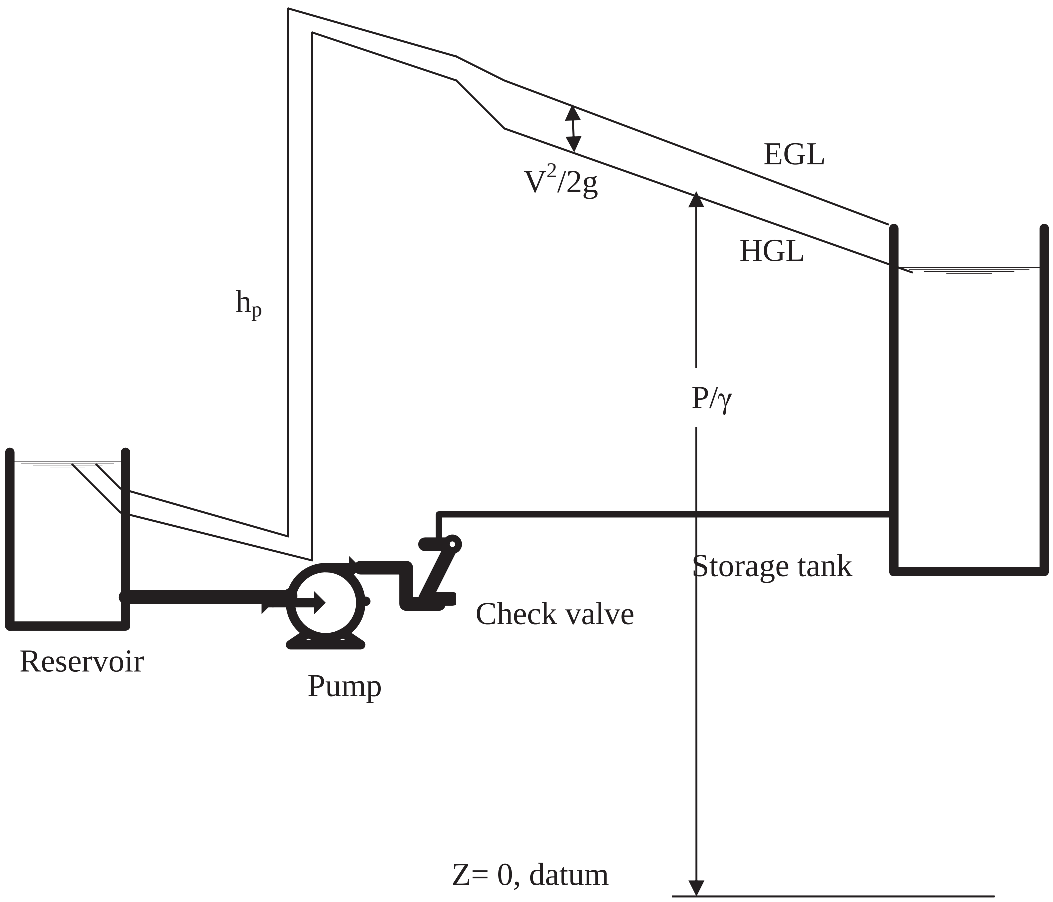

Figure 2.15 Definition sketch of HGL and EGL

The HGL and EGL are the same at the reservoir, and at the storage tank, as the velocity head at these locations goes to zero. In addition, it can be seen that the kinetic or velocity head is larger in the smaller pipe flow. The smaller pipe diameter forces the flow to have a larger velocity, as can be seen from the continuity equation (Equation 2.7):

$$V=Q/A \tag{2.7}$$

where, Q = pipe flow, (m^3/s, f^3/s)

The cross sectional area of the pipe,

$$A = (\pi D^2)/4 \tag{2.8}$$

in which, D is the diameter of the pipe, (m, ft).

The following figures will depict the EGL of the seven systems at their maximum demand hours. EPANET defines the "head" of each junction as the sum of all three terms in the bracketed quantity in Equation (2.5) (EPA, 2000), thereby making it equal to the EGL. The EGL of the seven systems defined as "head" are shown next.

2.3.1 System 1 (S1)

The head of S1 at the maximum demand hour 18:00 ranges from 750 ft to 850 ft as seen in Figure 2.16 below. The arrows in the map indicate the flow direction at the maximum hour.

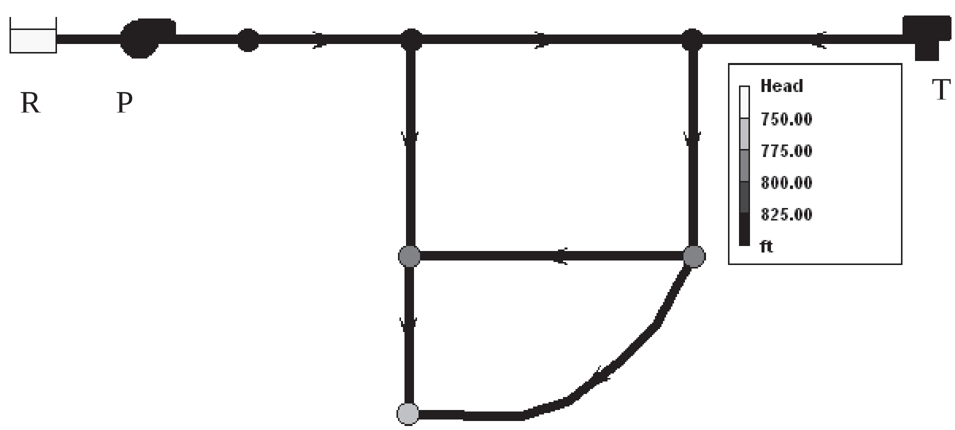

Figure 2.16 Head of S1 at normal operating condition at maximum demand hour (18:00)
(Figure created from data from EPA, 2000)
Note: R = Reservoir, T = Tank, P = Pump house

2.3.2 System 2 (S2)

The head of S2 at maximum demand hour 18:00 is ranging from 700 ft to 725 ft (Figure 2.17). The arrows in the map indicate the flow direction at the maximum hour.

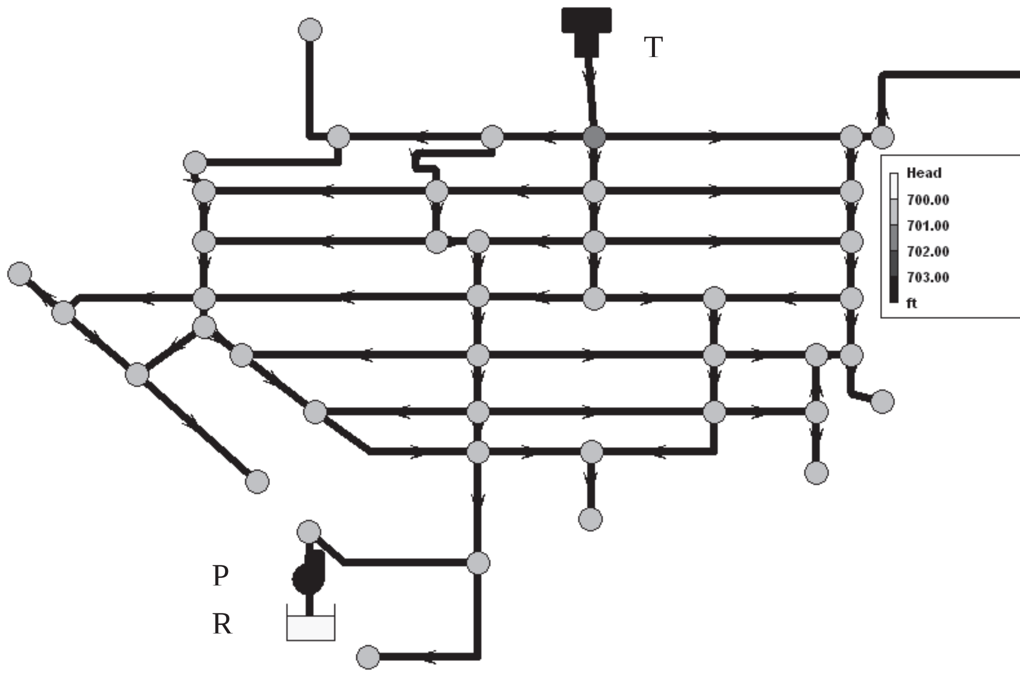

Figure 2.17 Head of S2 at normal operating condition at maximum demand hour (18:00)
Note: R = Reservoir, P = Pump house, T = Tank

2.3.3 System 3 (S3)

In contrast to the previous two systems, S1 andS2, the head of S3 at the maximum demand hour 20:00 ranges widely (Figure 2.18, p. 32). Arrows in the map show the flow direction at the maximum hour.

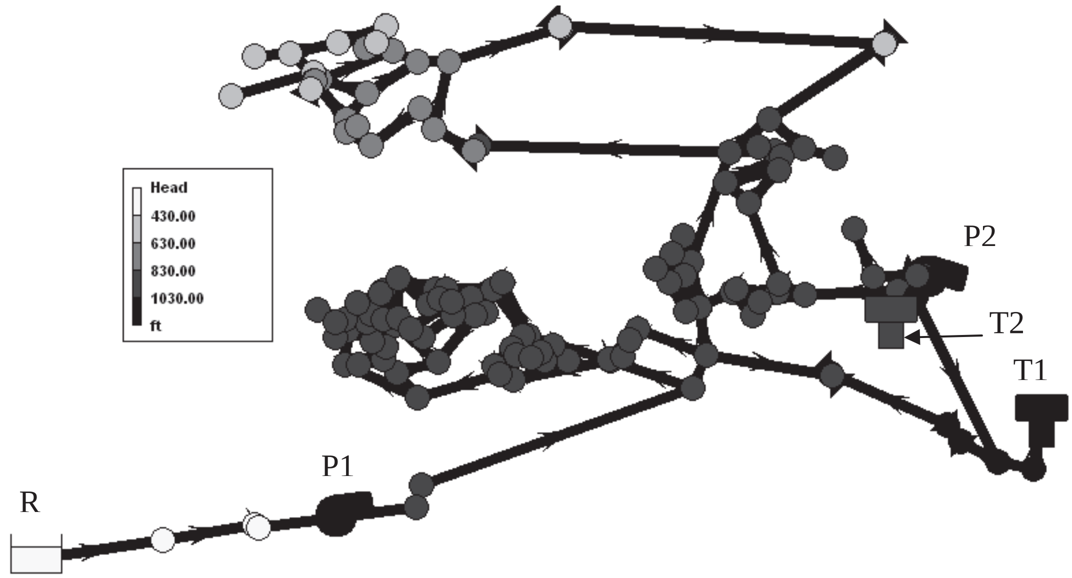

Figure 2.18 Head of S3 at normal operating condition at maximum demand hour (20:00)
(Figure created from data from Ostfeld et al., 2006)
Note: R = Reservoir, P = Pump house, T = Tank

2.3.4 System 4 (S4)

The head range of S4 at the maximum demand hour of 18:00 is wider, similar to S3, as can be seen from Figure 2.19 below. The flow direction is shown by arrows in the map at the maximum demand hour.

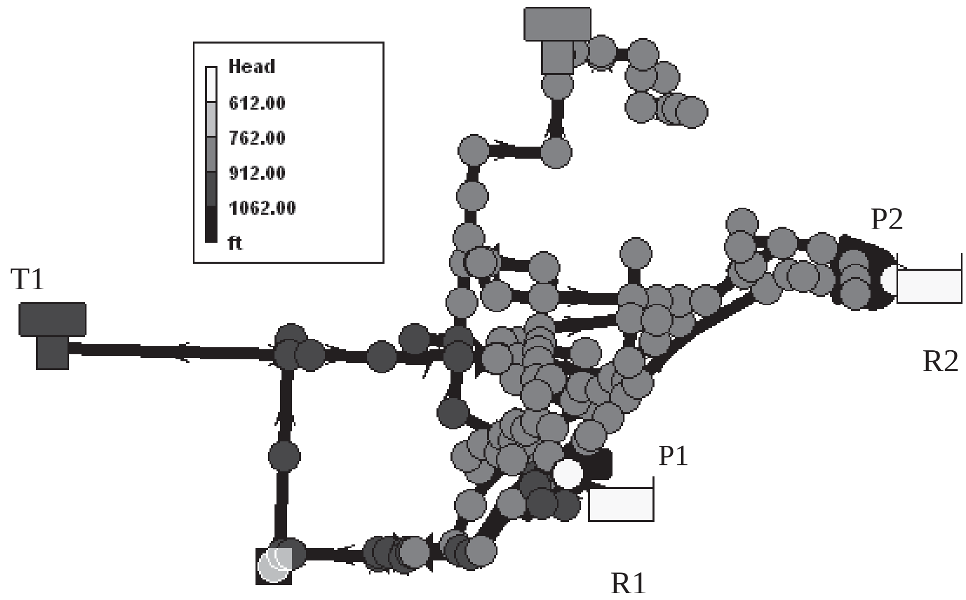

Figure 2.19 Head of S4 at normal operating condition at maximum demand hour (18:00)
Note: R = Reservoir, T = Tank, P = Pump house

2.3.5 System 5 (S5)

The head range of S5 at the maximum demand hour 20:00 is also wider, similar to S3 and S4, as can be seen from Figure 2.20 below. In addition, the flow direction is indicated by arrows on the map. The flow at every pipe is not clearly visible due to the size of the system.

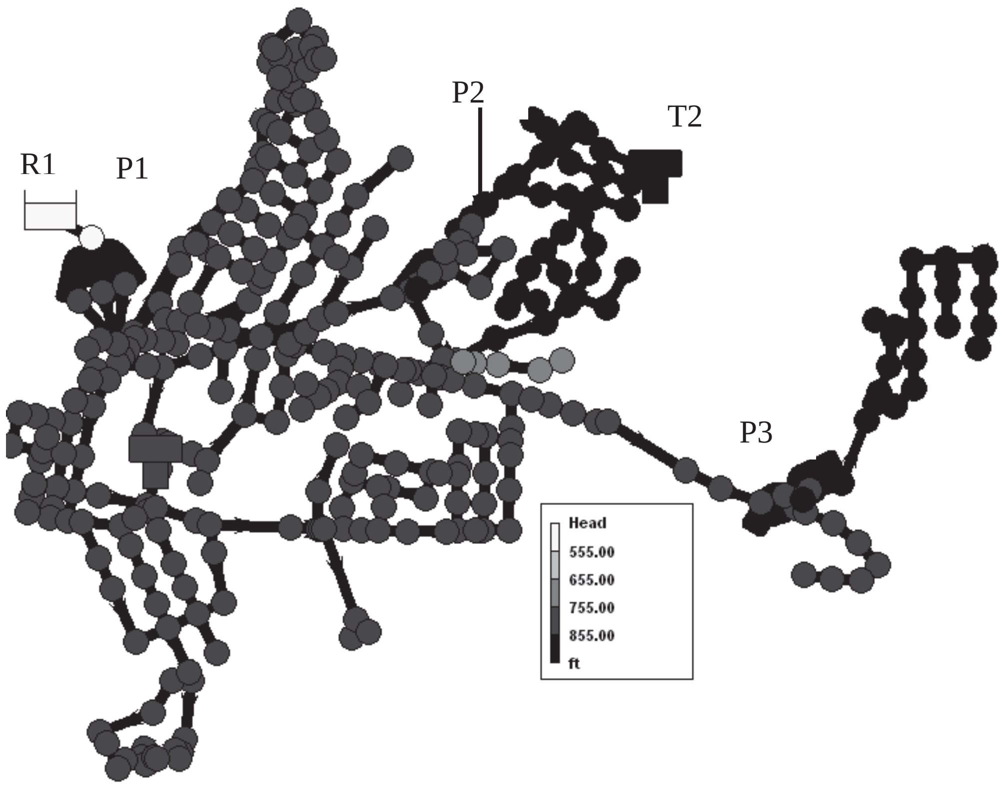

Figure 2.20 Head of S5 at normal operating condition at maximum demand hour (20:00)
Note: R = Reservoir, T = Tank, P = Pump house

2.3.6 System 6 (S6)

The head range of S6 at the maximum demand hour of 18:00 is different from the rest of systems. All the system junctions fall within the range of 1,200 ft to 1,300 ft of head except the storage tank, T1, and pumping station, as can be seen from Figure 2.21 below. Flow arrows except the main line near the storage tank T1 are not clearly visible due to the size of the system.

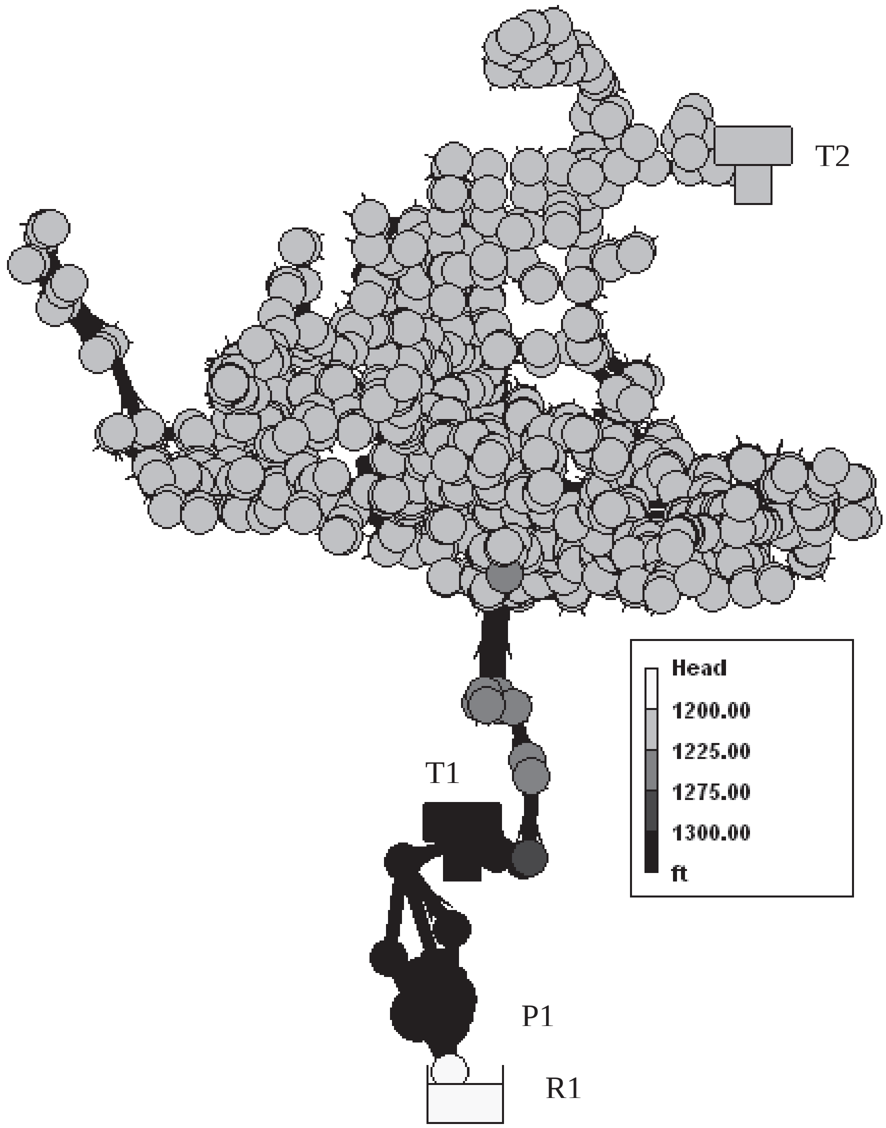

Figure 2.21 Head of S6 at normal operating condition at maximum demand hour (18:00)
Note: R = Reservoir, T = Tank, P = Pump house

2.3.7 System 7 (S7)

The head range of S7 at the maximum demand hour of 20:00 is different from the rest of systems. The head of S7 at this hour ranges from 0 ft to 400 ft for all of the locations as seen from Figure 2.22 below. The flow direction at the maximum hour is not shown due to the size of the system.

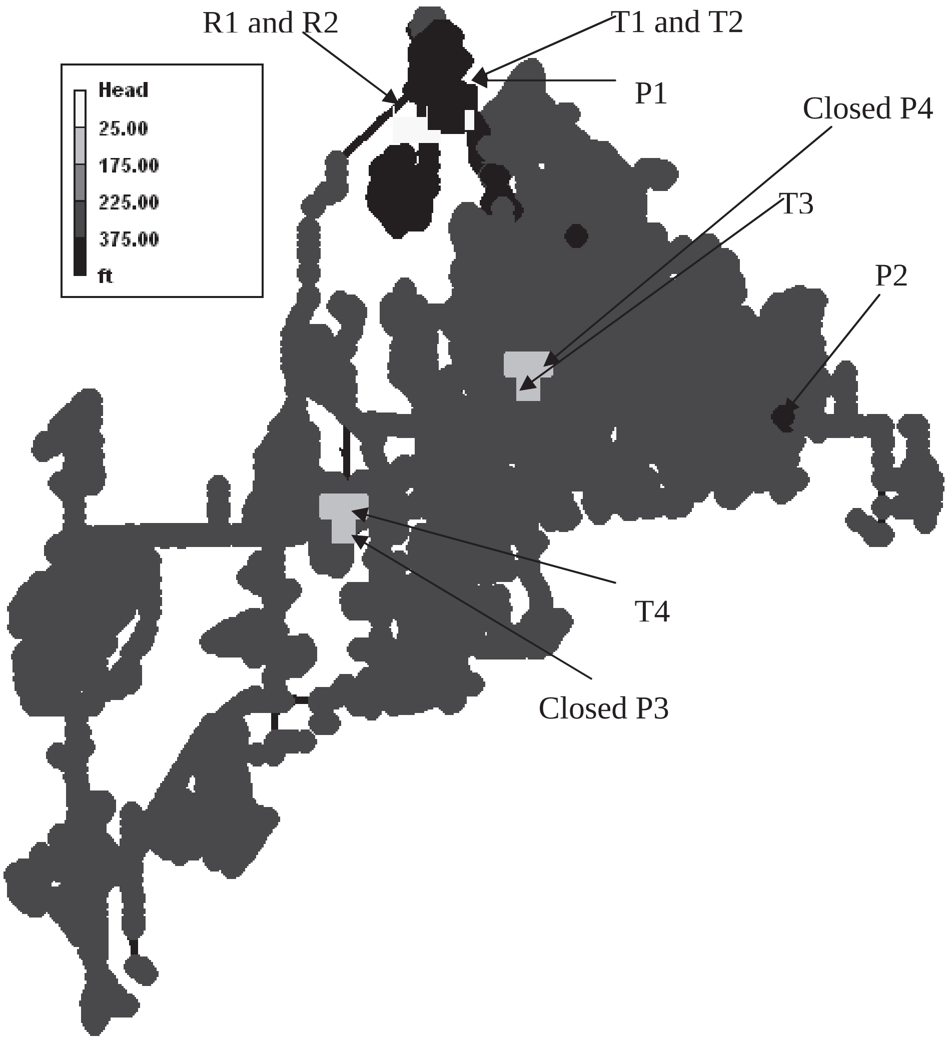

Figure 2.22 Head of S7 at normal operating condition at maximum demand hour (20:00)
(Figure created from data from Ostfeld et al., 2006)
Note: R = Reservoir, T = Tank, P = Pump house

2.4 System Modeling

Seven MDWDSs were modeled as described in the following chapters (Chapters 3-5, see Procedure section in each Chapter) for the analysis of energy use using a network solver

EPANET 2.0. Six of the systems were real existing systems and one was a hypothetical system.

2.4.1 EPANET 2.0

EPANET 2.0 is a free-for-download network solver developed by USEPA (EPA 2000) to simulate water distribution systems for various analyses including hydraulics and water quality. Some of the important features include the computation of system pressure, flow, and pumping energy cost. The capability of analyzing water quality includes modeling of chemical loss or growth and water age throughout the systems. Among several capabilities of EPANET, the modeling of energy use in a water distribution system was utilized in this research. EPANET models the energy utilized to pump water. In order to compute the energy usage, assigning a pump efficiency curve or a fixed power in lieu of the curve (see Section 2.1.1, p. 14) and a price rate of electricity are required as an input to the model. The monetary price/kWh of electricity is assigned to estimate the energy utilized by a pump. In this research, the average typical price of $0.0887/kWh was used to estimate the energy used for each of the seven systems (Energy Information Administration, 2007). This price is irrelevant; however, since energy usage will be normalized, as will be described later.

2.4.2 Analyzed System Components

A municipal distribution system consists of several components and associated properties. Typically, water sources, storage tanks, pipes, pipe intersections (junctions:

water enters or leaves the system), pumping stations, and valves are considered to be system components. Associated parameters such as demand associated with a junction are termed system properties. A system property (demand) and two system components (storage tanks, and pumping stations) were analyzed for their effect on energy use of the systems. These system properties and components (hereafter—system aspects) are described below:

2.4.2.1 Demand

Each junction of a system has specific required properties while modeling in EPANET 2.0. These include elevation, water demand, and initial quality (for water quality analysis, not used here). For the analysis of this research, the water demand of each junction was varied for a wide range: zero to 1.4 times the normal operating demand. Various diurnal curves (Figure 2.2 to Fig 2.7, p. 16-20) were used to simulate the systems to address the diurnal variation of demand of the systems.

2.4.2.2 Storage Tanks

Every water distribution system uses storage tanks to guarantee the reliability of system requirements such as equalization, pressure, flow, emergency storage such as fire protection, power outage, and transmission line breakage (Walski 2000). Designing a storage tank could be challenging due to various factors such as water quality, landscape (location of tanks), levels, and volume. In this research, a tank is referred to as a storage-service tank in MDWDSs.

EPANET can simulate any shape tank (EPA, 2000). In this research, cylindrical tanks were considered. The required properties to model a tank parameter using EPANET are tank diameter, tank bottom elevation (elevation), water levels (initial, minimum, and maximum), and initial quality of water (for water quality analysis). The variation of tank parameters: elevation, maximum water level, and diameter were considered in order to study the effect of tank parameters on energy use.

2.4.2.3 Pumping Stations

A pumping station in a MDWDS may consist of one or more pumps that adds head to the water. To analyze MDWDS energy use using EPANET, each pump needs a pump curve or pump power (EPA, 2000). A pump curve is the relationship between head supplied by the pump and flow through the pump. In EPANET, a pump curve can be assigned in four different ways: (1) *Single-Point* curve, (2) *Three-Point* curve, (3) *Multiple-Point* curve, and (4) *Variable-Speed* pump curve (EPA, 2000).

A Single-Point curve is a pump curve generated by EPANET based upon a single coordinate of a pump curve (flow and head) (EPA, 2000). EPANET generates two more coordinates to complete the curve: zero flow at the *shutoff head* (133% of *design head*), and a maximum flow (twice the design flow) at the zero head.

A Three-Point curve is a curve based on three coordinates of a pump curve.

A Multiple-Point curve is produced by EPANET based on a pair of coordinates or more than three points.

A Variable-Speed pump curve is produced based on the principle of the affinity law. The affinity law relates the flow through the pump (Q), revolutions of pump (rpm) (N), and head (H) added by the pump as given below (EPA, 2000):

$$\frac{Q_1}{Q_2} = \frac{N_1}{N_2} = \left(\frac{H_1}{H_2}\right)^{0.5} \tag{2.9}$$

In this research, pump curves as well as constant horsepower values were used in different aspects of the analysis. Pump curves were used for the first two aspects—demand variation and tank parameter variation (Chapter 3, p. 41 and Chapter 4, p. 54), whereas pump curve and constant pump horsepower were used for the third aspect—pump analysis (Chapter 5, p. 77).

Chapter 3

*Energy Savings through Water Conservation in Municipal Water Distribution Systems**

3.1 Introduction

Eighty-seven percent of the US total residential water use is supplied by public water sources with the average residential water demand being more than 1137 m^3/s, or 26—billion gallons per day (Vickers, 2001). The increasing population and water demand will compel MDWDS utilities to lower water consumption in order to minimize energy usage. In turn, minimization of energy use will reduce carbon emissions that cause global warming.

Water processing and distribution are the major costs in municipal water systems, using up to 80% of the total electric cost (EPRI, 2002). The cost of electricity can be reduced in several ways, including the efficient pumping of water and reducing water

* A conference paper summarizing the results of this chapter is published in the Proceedings of *ASCE, EWRI World Water and Environmental Resources Congress*, 2008.
The author acknowledges the valuable comments provided by three anonymous reviewers for this chapter of the dissertation.

demand or using water conservation techniques. Methods of water conservation include rainwater harvesting, low-flow home appliances such as toilets and showerheads, underground irrigation for lawns and gardens, and the use of grey-water for non-consumptive purposes. There are growing interests in water conservation. Albuquerque, New Mexico's successful attempt at reducing per capita water consumption by 20% in nine years from 1995 to 2004 is exemplary in this regard (Vickers, 2001).

In spite of all the valuable related studies described previously in Section 1.1 (p. 1), there is a need to directly study the sensitivity of energy use for pumping in relation to the total user demands for a wide variety of MDWDSs. This study focuses on water conservation and assumes that the current demands can be reduced by conservation. This study uses network modeling to analyze seven municipal water distribution systems (in which six systems are realistic and one is hypothetical) for the effect of water conservation on energy use.

3.2 Procedure

It has been commonly assumed in previous studies that MDWDSs are so complex that each one has to be analyzed independently and that a general rule-of-thumb, therefore, could not be applied to a wide array of systems. In contrast to this approach, however, this study analyzes seven systems and finds a common rate of energy savings for a reasonable reduction of global user demand.

First, each of the seven MDWDSs (See Chapter 2, p. 11) was modeled using the network solver EPANET 2.0 (EPA 2000). The analysis was based on a simulation period of 96 hours. To test the sensitivity of energy use to changes in water demand, several values of global system demand were modeled, and the corresponding value of energy usage was recorded. The recorded energy usage was based on a fixed pump wire-to-water efficiency of 75% (see Section 2.1.1, p. 14). The global demand variation range for the analysis was from zero to 1.4 times the normal operating condition demands. For values of demand higher than the normal operating condition value, some system modifications were necessary due to the inadequacy of some pumps to supply the higher demand. In addition, some valves had to be altered to ensure adequate pressures greater than 138 kPa (20 psi) throughout the system. Reservoirs, tanks and a few junctions near the tanks were exceptions to this pressure requirement. As a rule-of-thumb, the minimum pressure of 138 kPa (20 psi) was the criteria for most of the system junctions for emergencies such as fire (Chase, 2000). In general, the pressure range for a system should be 207 kPa (30psi) to 689 kPa (100 psi) (Chase, 2000). The details of the system modification can be found in Section 3.3.1.1 (p. 44 below).

3.3 Results and Discussions

The results were analyzed in two ranges of data: (1) analysis for a wide range of demand values, and (2) analysis of 20% demand reduction range, as described in the following two sections.

3.3.1 Analysis for a Wide Range of Demand Values

From Figure 3.1 below, it can be seen that the energy consumption by each of the systems increases with increasing demand. For the largest system, S7, the energy usage was two orders of magnitudes greater than any of the other systems. In addition, for values of normalized demand higher than 1.0 the energy usage for S7 rapidly increases, while for the remaining systems the rate of energy use remains constant for the entire range of normalized demand. The normalized demand, Q_D*, is defined as the ratio of the simulated demand divided by the existing demand (see Section 3.3.1.1 below).

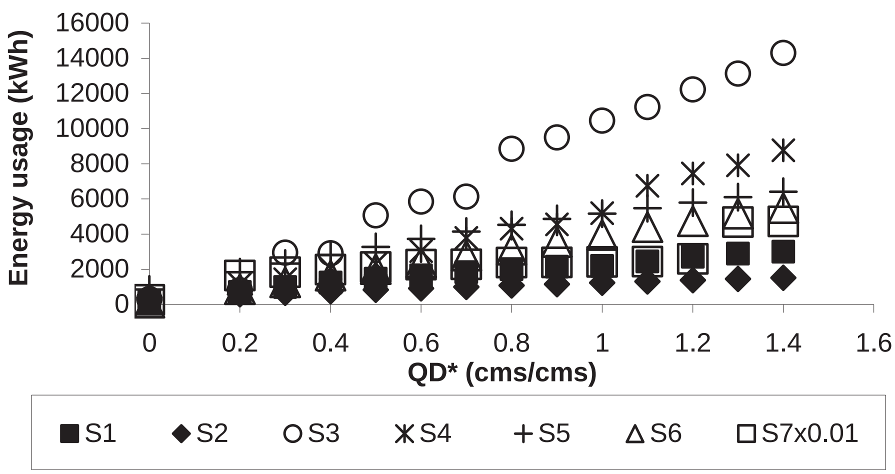

Figure 3.1 Non-normalized energy vs. normalized demand for seven systems

3.3.1.1 Analysis with Normalized Demand and Energy Values

If, however, the energy and demand are both normalized by their existing values, as described by Equations (3.1) and (3.2):

$$E^*=E/E_o \tag{3.1}$$

$$Q_D^* = Q_D/Q_{Do} \tag{3.2}$$

where, E^* = the normalized system-wide energy usage,

E = the modeled system-wide energy usage,

E_o = the current (unaltered) system-wide energy usage,

Q_D^* = the normalized global demand,

Q_D = the modeled global demand, and

Q_{Do} = the current (unaltered) global demand,

Then, the relationships are all approximately linear and collapse onto approximately the same line as seen below (Figure 3.2).

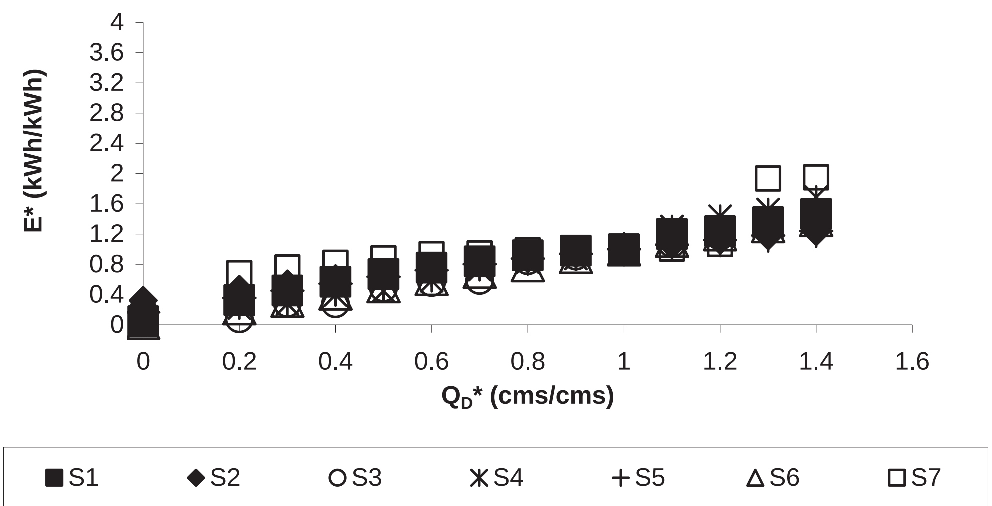

Figure 3.2 Normalized energy usage of seven systems

It can be seen that all six systems collapse in to a single coherent straight line when normalized in this way, except for S7, which is non-linear. The plot of S7 was nonlinear due the nature of Equation (3.3) as seen below.

$$E^* = AQ^{*3} + BQ^* \tag{3.3}$$

where, A and B are defined as coefficients of Q^{*3} and Q^* as in Eq. (3.4) and (3.5) below.

$$A = \frac{1}{1 + \frac{k_2}{k_1 Q_0^{\,2}}} \tag{3.4}$$

$$B = \frac{1}{\frac{k_1}{k_2} Q_0^{\,2} + 1} \tag{3.5}$$

where,

$$k_1 = \sum \frac{8\gamma fL}{\pi^2 g \eta D^5} + \sum \frac{8\gamma K_L}{\pi^2 g \eta D^4} \tag{3.6}$$

And,

$$k_2 = \frac{\gamma H}{\eta} \tag{3.7}$$

In which,

γ	=	specific weight of water (lb/ft^3, N/m^3)
f	=	*Darcy-Wiesbach* friction factor (unit less)
K_L	=	fittings coefficient (unit less)
G	=	acceleration due to gravity (m/s^2, ft/s^2)
D	=	pipe diameter (m, ft)
η	=	wire-water pump efficiency

The details of the derivation of this cubic curve fit equation matched to the EPANET simulated curve can be found in Appendix A.1-A.2 (p. 116). The results of the cubic curve fit shown in Appendix A.2 (Figure A.1, p. 120) show that the energy use and water demand in MDWDSs are approximately linearly correlated, even though theoretically it is a cubic relationship as shown in Equation (3.3) in page 45.

An equation that expresses the amount of normalized energy consumed, E*, for various amounts of normalized demand, Q_D*, was obtained by averaging the normalized energy for each normalized demand value and fitting a straight line to the averaged data, as seen in Figure 3.3 below. It can be seen that there is a low standard deviation and coefficient of variation in the data except for high values of the normalized demand, Q_D*. In addition, the R^2 value of the straight-line fit shown in Equation (3.8) is 0.9623.

$$E^* = 1.0579 \quad Q_D^* \tag{3.8}$$

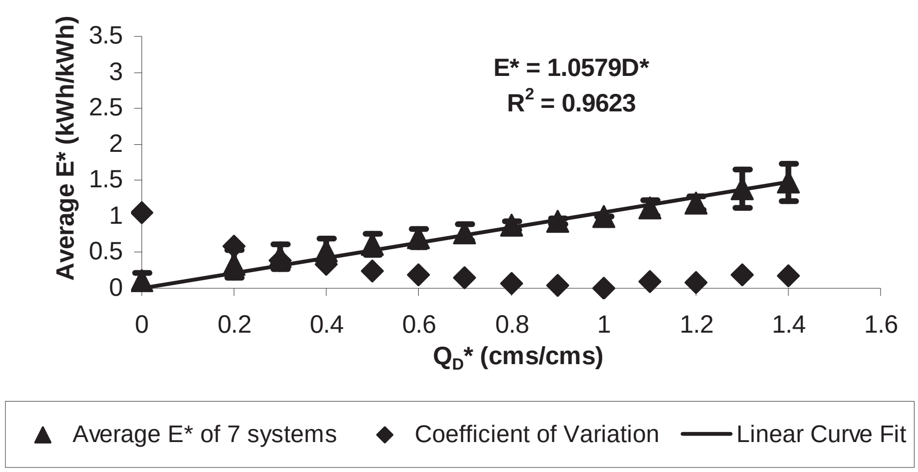

Figure 3.3 Linear relationship of average normalized energy, E*, for variation of normalized demand, Q_D*
Note: Error bars denote ± one standard deviation

During the course of changing global demand values, it was necessary to alter some of the systems to ensure sufficient pressure at all system junctions, especially at high demand values for which the existing pumps were not of sufficient capacity. Table 3.1 below gives a summary of alterations necessary for each system and global demand value. Although the theoretical energy usage with zero discharge is zero, the simulations of demand value of Q_D* = 0.0 were approximately performed by assigning a value close to zero (0.0001) for all seven of the systems. However, the system had pressure deficiency for this low value in four of the systems—S3, S4, S5, and S7. This issue for S7 was recovered by upgrading the pump head (Appendix A.3, p. 122). S3, S4, and S5 performed without any pressure deficiencies for the lowest value of Q_D* = 0.01 instead of 0.0001. The complete details of the alteration can be viewed in Tables A.1-A.4 (Appendix A.3, p.121).

Table 3.1 Summary of alterations necessary to ensure sufficient global pressure (See Appendix A.3 for complete details)

System	**Q_D* value (cms/cms)**	**Alteration**
1	1.1,1.2, 1.3, 1.4	Pump curve
4	1.1, 1.2	Pump curve
4	1.3,1.4	Pump curve and tank size
7	0.001, 0.2, 1.2, 1.3	Pump curve

For S1, there were five “Single-Point” pump curves used in order to ensure sufficient pressure values (Appendix A.3, Table A.1, p. 121). EPANET generated the complete pump curve using the single values of discharge and head of the “Single-Point” curve (EPA, 2000). The existing curve was used for the Q_D* value of 1.0. The modification of the pump curves were made by gradually increasing discharge, Q, and/or head, h, until the minimum pressure at most of the junctions in the system was at least 138 kPa (20 psi).

For S4, pump curves as well as storage tank capacity were modified in order to maintain the system pressure. As S4 employs two pumps, there are two pump curves for low-demand simulations ($Q_D^* \leq 1$) as given in Table A.2 (Appendix A.3, p. 121). The system needed pump curve modification with increased capacity as the demand factor Q_D^* increased above 1.0. For these simulations with increased pump capacities, EPANET used the "Single-Point" curves to generate the complete curves as in S1. The "Single-Point" curves are also provided in Table A.1 (Appendix A.3, p. 121).

In addition to increasing pump capacity for S4, the tank storage capacity values were also increased to maintain pressure values at most of the junctions for high-demand simulations (Table A.3, Appendix A.3, p. 122).

For S7, the normal operating condition pump curve resulted in sufficient pressures throughout the system for all the simulations of demand variations of 0.3 to 1.1. However, slight modifications for the values of D* = 0.2, 1.2 and 1.3 were made to maintain minimum system pressure. The modification of the pump curve for S7 can be found in Table A.4 (Appendix A.3, p. 122).

3.3.2 Analysis of 20% Demand Reduction Range

On the assumption that it was realistic to reduce the global demand of MDWDSs by up to 20%, the range of Q_D^* of 0.8 to 1.0 was analyzed next. The following Figure 3.4 shows a plot of Q_D^* versus E* for this range. It can be seen that all seven systems collapse onto one straight line, including S7, which did not collapse with the data from the other six systems for other ranges of Q_D*.

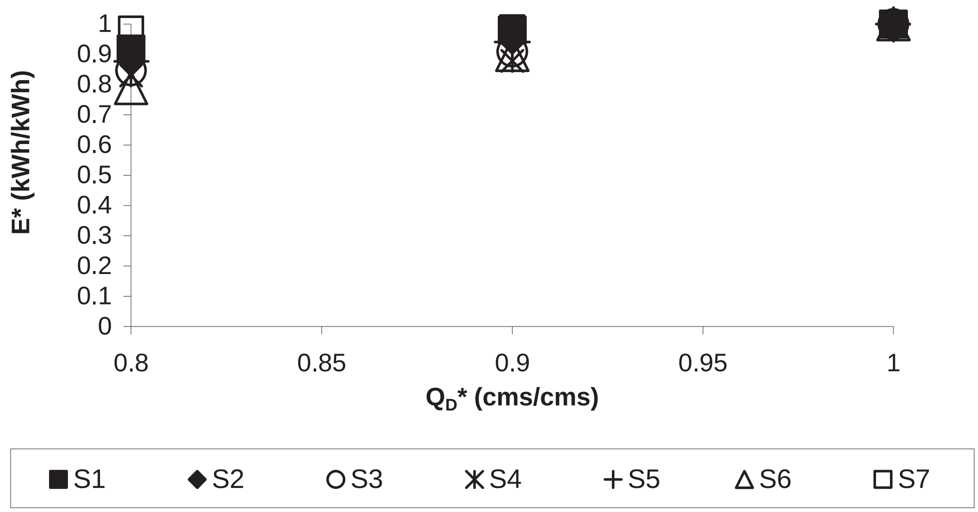

Figure 3.4 Normalized energy for variation of normalized demand for up to a 20% water demand reduction, Q_D*=0.8 to 1.0.

To find a relationship for this line, the data were averaged over the seven systems and a straight line fit to the data, which resulted in a line described by Equation (3.9) with an R^2 value of 0.9988 (Figure 3.5 below). It can be seen that there is an almost perfect linear fit and a low Coefficient of Variation for this range of demand reduction. Equation (3.9) suggests that a 20% reduction in demand will result in a 13% reduction in energy usage: the energy Elasticity Coefficient, *S*, or slope of the line in Equation (3.9), is 0.63.

$$E^* = 0.63Q_D^* + 0.37 \qquad (3.9)$$

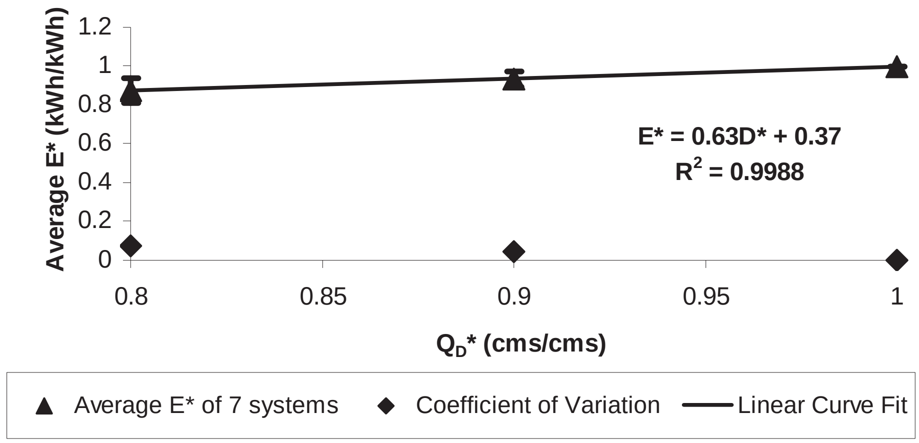

Figure 3.5 Linear relationship of average normalized energy for variation of normalized demand for up to a 20% water demand reduction, Q_D*=0.8 to 1.0 (error bars denote ± one standard deviation)

3.3.3 Reasons of increased energy use for increased water demand

It was found that energy use and the reduction of water demand in seven municipal water distribution systems were proportionally related. The increasing trend of energy use with increased water demand can be well explained by Affinity laws that relate various pump variables. The Affinity laws demonstrate the effect of pump speed (N) on pump performance values, flow (Q), head (h), and power (P) (Finnemore and Franzini, 2002). For a specific pump (diameter constant), the following equations (Equation 3.10, 3.11, and 3.12) show that the energy use in pumping water is directly proportional to the cube of flow through the pump.

$$\frac{P_1}{P_2} = \left(\frac{N_1}{N_2}\right)^3 \tag{3.10}$$

where,

P = Power supplied to the pump, or brake horsepower, and

N = Pump speed

and,

$$\frac{Q_1}{Q_2} = \left(\frac{N_1}{N_2}\right) \tag{3.11}$$

where,

Q = Pump capacity, (gpm, cms)

Therefore,

$$\frac{P_1}{P_2} = \left(\frac{Q_1}{Q_2}\right)^3 \tag{3.12}$$

Equation (3.12) shows that power supplied to pump is directly proportional to the cube of flow through the pump. This corresponds with the third-order results of Equation 3.3 above. Thus, for the increased water use, the systems will require increased energy use.

3.4 Summary and Conclusions

The change in energy usage with the change in demand for seven water distribution systems with a wide range of system characteristics was analyzed. It was found that when normalized by existing energy and demand values, the curves for all seven systems were linear and collapsed onto a single line described by Equation (3.8) (p. 47). This resulted in the conclusion that for a 20% demand reduction a 13% reduction in energy expenditures can be realized, thereby proving the Hypothesis (1) described on page 6. This energy savings in turn might have an impact on the reduction of GHG emissions thereby reducing the global warming effect.

Chapter 4

Impact of Storage Tanks on Energy Consumption in Municipal Water Distribution Systems

4.1 Introduction

Like all other optimization research in MDWDSs as described in Chapter 2 (p.11), there is much valuable research for storage tank optimization as well. Walski et al. (1987) used a hypothetical network to optimize the cost of designing pipes, pumps, and tanks. Vamvakeridou-Lyroudia et al. (2007) found that storage tank capacity and minimum normal operational level have an effect on cost and system hydraulics. In addition to other variables such as pipes and pump scheduling, Murphy et al. (1994) included tank parameters, such as size and location, in their optimal cost of a network design. Walter et al. (1999) included tank volume in their optimization study. However, the effect of tank parameters on energy consumption is still unclear. Importantly, the research mentioned above was conducted based upon a limited number of systems, as described previously in

Chapter 2 (p. 11). Thus, a study addressing the relationship between storage tank parameters and energy use based on a multiple system approach is desirable.

The present research analyzes MDWDSs by looking at the effect of altering tank maximum water level, elevation, and diameter on energy consumption. The method involved analyzing seven MDWDSs of varying size and complexity, as described previously in Chapter 2 (p. 11).

4.2 Procedure

Tank parameters that are under the MDWDS utility's control are tank maximum water level, tank elevation, and tank diameter. To examine the effect of varying storage tank parameters on MDWDS energy consumption, seven systems (see Chapter 2, p.11, for details of the systems) were modeled using the network solver EPANET 2.0 (EPA, 2000). Six of the systems were realistic and one was hypothetical. Extended period simulations of 96 hours were modeled with varying diurnal demand patterns shown previously in Section 2.1.2 (Figure 2.2- 2.7, p 16-20). This period of simulation was chosen to ensure a long enough time for initial conditions—related to tank water levels—to become insignificant.

The tank parameter analysis was carried out in three stages: (1) energy usage with varying maximum water level, (2) energy usage with varying tank elevation, and (3) energy usage with varying tank diameter. A tank, which was used for the simulation of variation of the parameters, was defined as the "variable tank". In each of the three analyses, the initial and minimum water levels of the variable tank were kept the same. The rest of the tanks were unaltered. The setting of initial water levels and minimum water levels as equal allowed the variable tank to be treated as empty at the time of simulation initiation. The initial water levels, minimum water levels, maximum water levels, and the diameters of each of the analyzed tanks of the seven systems are shown in Table 4.1.

Table 4.1 Tank levels and diameters of seven systems (Computed from the tank data from the systems described in Section 2.2, p. 20)

Systems	Tank level (m)			Diameter
	Initial	Minimum	Maximum	(m)
S1T1	0	0	6.1	13.7
S2T1	0.6	0.6	7.3	24.4
S3T1	0	0	12.8	32.3
S3T2	3	3	9.8	56.7
S4T1	0.9	0.9	6.4	24.7
S4T2	0.9	0.9	6.4	17.1
S5T1	0	0	6.1	10.7
S5T2	0	0	16.8	10.7
S6T1	1.5	1.5	32	8.7
S6T2	1.8	1.8	18.3	7.6
S7T1	0.9	0.9	45.7	30.5
S7T2	0.9	0.9	45.7	30.5
S7T3	0	0	7.2	31.7
S7T4	0	0	5.3	21.3

Note: S = System, and T = tank:

4.2.1 Systems Studied

Drawings of each of the seven systems were shown previously in Figs. 2.8-2.14 (p. 21-26) and summarized in Table 2.1 in Chapter 2 (p.12). It can be seen from these figures that there are a wide variety of system sizes, number of pumps, tanks, and complexity of systems, thereby providing a wide variety of samples for the analysis.

After simulations were performed on all seven systems, the results were analyzed. The systems were analyzed as a single statistical unit.

The following sections will describe each of the three analyses: (1) energy usage with varying maximum water level, (2) energy usage with varying tank elevation, and (3) energy usage with varying tank diameter.

4.3 Energy Usage with Varying Maximum Water Level

The following sections will describe each of the three analyses of energy usage on: (1) varying maximum water level, (2) varying tank elevation, and (3) varying tank diameter.

4.3.1 Procedure

The maximum tank water level of the variable tank was varied from 0.5 to 1.5 times the normal operating tank water level (see Table 4.2, below) and the energy usage recorded. Each simulation was begun with the variable tank being empty as explained in Section 4.2 (p. 55). The remaining initial tank water level values were unaltered. During simulations, the pumps had to be altered to ensure adequate network pressures for all of the systems except S1 and S3 (see Table 4.3, p. 62). In addition, an additional storage tank was added in S6 in order to maintain the pressure of the system.

The normalized tank water height was obtained as follows:

First, the maximum water height of the variable tank was computed by setting its minimum level and maximum level for normal operating conditions (Figure 4.1). The normal operating height is considered as the normalized height of the tank level.

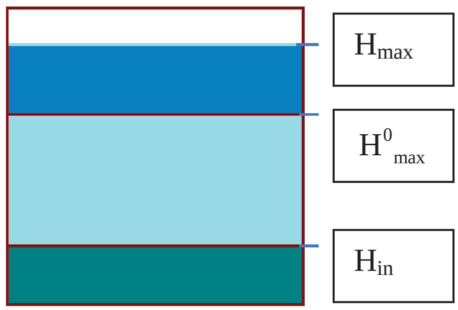

Figure 4.1 Definition sketch of tank water levels

The normalized tank water height is then calculated as:

$$H^* = \frac{H_{max} - H_{in}}{H^o_{max} - H_{in}} \tag{4.1}$$

where,

H^* = normalized tank water height

H_{max} = simulated maximum water level

H_{in} = initial water level

H^0_{max} = unchanged maximum water level: normalizing maximum water level at normal operating condition.

The normalized energy, E*, is defined as above in Section 3.3.1.1 (p. 44), Equation (3.1).

A table showing the normalized tank water height and the maximum water level of the various tanks of the seven networks is presented in Table 4.2 below.

Table 4.2 Simulated maximum water levels, H_{max}, of various tanks of the seven analyzed Networks (Computed from the tank data from the systems described in Section 2.2, p. 20)

Maximum water height, H_{max} (m)														
H*	**S1**	**S2**	**S3**		**S4**		**S5**		**S6**		**S7**			
m/m	**T1**	**T1**	**T1**	**T2**	**T1**	**T2**	**T1**	**T2**	**T1**	**T2**	**T1**	**T2**	**T3**	**T4**
0.5	3.0	4.0	6.4	4.9	3.7	3.7	3.0	8.4	16.0	9.1	22.9	23.3	3.6	2.7
0.6	3.7	4.6	7.7	5.9	4.2	4.2	3.7	10.1	19.2	11.0	27.4	27.8	4.3	3.2
0.7	4.3	5.3	8.9	6.9	4.8	4.8	4.3	11.7	22.4	12.8	32.0	32.3	5.0	3.7
0.8	4.9	6.0	10.2	7.8	5.3	5.3	4.9	13.4	25.6	14.6	36.6	36.8	5.7	4.2
0.9	5.5	6.6	11.5	8.8	5.9	5.9	5.5	15.1	28.8	16.5	41.1	41.2	6.5	4.8
1	6.1	7.3	12.8	9.8	6.4	6.4	6.1	16.8	32.0	18.3	45.7	45.7	7.2	5.3
1.1	6.7	8.0	14.1	10.8	6.9	6.9	6.7	18.4	35.2	20.1	50.3	50.2	7.9	5.8
1.2	7.3	8.7	15.3	11.7	7.5	7.5	7.3	20.1	38.4	21.9	54.9	54.7	8.6	6.3
1.3	7.9	9.3	16.6	12.7	8.0	8.0	7.9	21.8	41.6	23.8	59.4	59.2	9.3	6.9
1.4	8.5	10.0	17.9	13.7	8.6	8.6	8.5	23.5	44.8	25.6	64.0	63.6	10.1	7.4
1.5	9.1	10.7	19.2	14.7	9.1	9.1	9.1	25.1	48.0	27.4	68.6	68.1	10.8	7.9

Note: H^*: Normalized height, S = System, and T = tank

4.3.2 Results and Discussions

The results of tank water level analysis in Figure 4.2 below show that the energy usage is system specific, with some tanks exhibiting proportional and others inversely proportional behavior. The system- specific behavior of MDWDSs may be attributed to system complexity. The MDWDSs operate based upon their system aspects—storage tanks, valves, water demand, pipes, and pumping station. All of these system aspects produced a complex behavior of energy use as shown in Figure 4.3. For example, the pump operation status of S4 was controlled by the water levels in storage tanks by c*ontrols* logic supported in EPANET in such a way that if the tank water surface elevation dropped below 6 ft (1.8 m) then the Main Pump (Pump 4) comes on, and if the water level rose above 15 ft (4.6 m) then Pump 4 would shut off. This use of EPANET controls was responsible for the non-monotonic behavior of the results of S4 as seen in Fig 4.3, p. 61. To verify this, S4 was simulated separately without the use of controls (EPANET default controls), which means that by default EPANET uses the values of tank maximum and minimum water surface elevation levels—that determine the pump status. It was found that the non-monotonic behavior of both the curves (S4T1 and S4T2) were due to the use of original control values (see Figure 4.2 below). The default control values result in an increase of the water volume at the storage tank allowing more storage. This would smoothly supply water from the tank instead of supplying water from both the pump and the tank. When the pump would go off, the storage tank would be able to supply water smoothly in a non-monotonic energy use pattern, as shown in Figure 4.2 below.

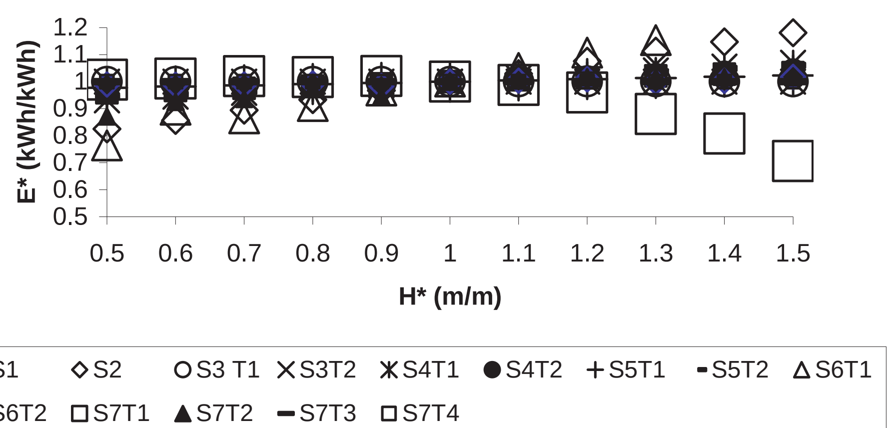

Figure 4.2 The sensitivity of energy consumption of seven systems to their tank maximum level before redesigning the pumps: with EPANET default c*ontrols*

However, to maintain the originality of the system, further analysis of S4 was based upon the use of original controls. The original controls used for S4 can be found in Appendix B.1 (p. 123). The reduction of the maximum water level of the most sensitive system resulted in a 30% change in energy use, and the least sensitive system's tank maximum water level had a negligible change in energy use, both for changes in H* values of 50 %.

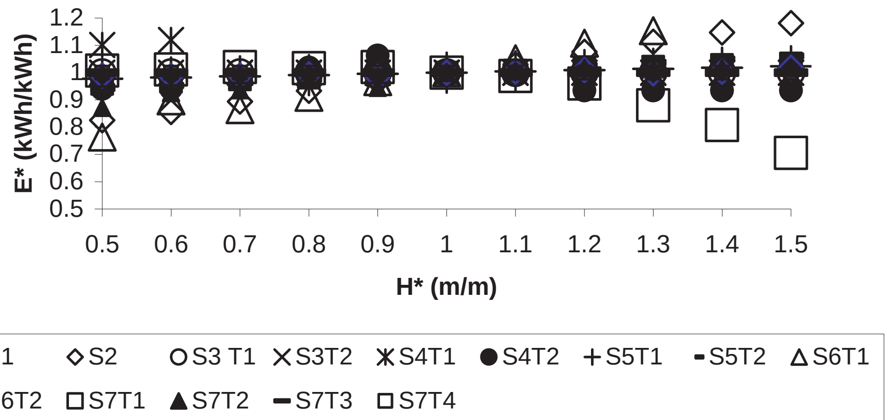

.

Figure 4.3 The sensitivity of energy consumption of seven systems to their tank maximum level before redesigning the pumps: with EPANET original controls

Next, the pump sizes were modified to determine if pump over-sizing had an influence. It was found that the pumps were overly sized for networks exhibiting a high sensitivity to tank water level (S2 and S6T1) on energy use. A summary of the modifications made to the seven systems under analysis is given in Table 4.3 below. From Table 4.3, it can be seen that the pump curves of five systems (S2, S4, S5, S6, and S7) were modified.

Table 4.3 Summary of pump curve modification for tank maximum level variation

Networks	Pump Modified	No. of Pumps in System	Pumps Adjusted
S1	No	1	0
S2	Yes	1	1
S3	No	2	0
S4	Yes	2	1
S5	Yes	8	1
S6	Yes	1	1
S7	Yes	7	2

The adjustments of these pumps are detailed in Appendix B.2 (p. 124-127). The pump curves were generated by EPANET using the "Single-point" pump curve approach (EPA 2000). A "Single-Point" is a single coordinate of a pump curve (flow and head) used by EPANET to generate the complete pump curve. The details of curve types used by the EPANET simulation can be found in Section 2.1.1 (p. 14).

After redesigning the pump sizes, separate results were obtained and presented below in Figure 4.4. Eliminating pump over-sizing resulted in little energy sensitivity in all but S7, the largest system (Figure 4.4).

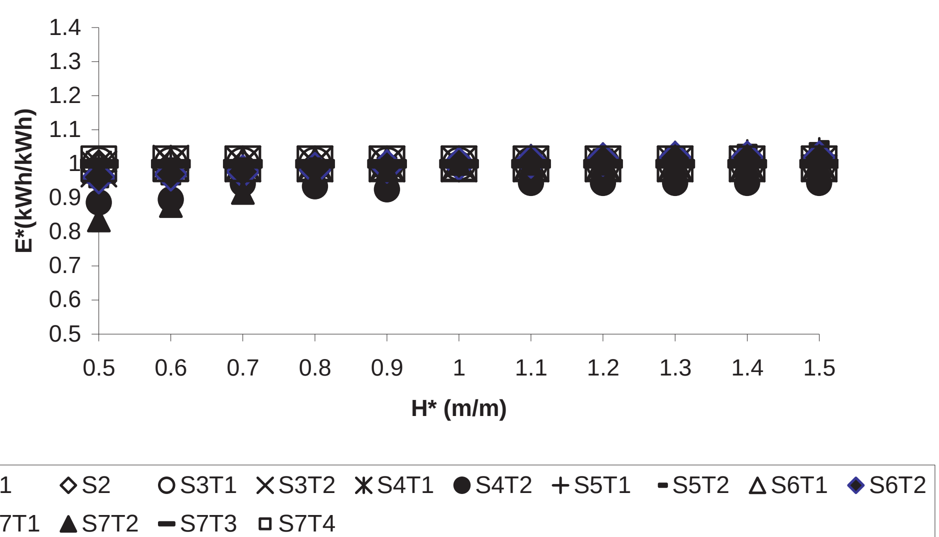

Figure 4.4 The sensitivity of seven systems and their tanks' maximum level for energy consumption after redesigning the pumps at system sources

When E* is averaged over all seven networks (Figure 4.5), it can be seen that the system-averaged E* values are linear (Equation 4.2) with an R^2 value of 0.9345 and have a coefficient of variation ranging from 0 to 0.024.

$$E^* = 0.04H^* + 0.96 \tag{4.2}$$

From Equation 4.2, it can be seen that the energy savings for a 50% water level reduction will save up to 2% of the energy consumed.

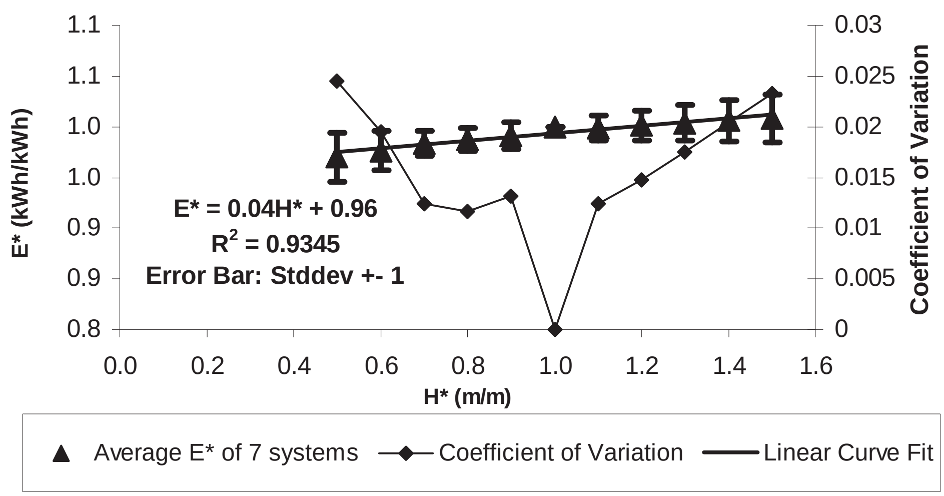

Figure 4.5 Average E* of seven systems for tank height variation after elimination of pump over-sizing (error bars denote ± 1 standard deviation)

4.3.3 Discussion of sensitivity of energy use to maximum tank water level

The reduction of tank maximum water level resulted in the reduction of energy use due to the increased static head that increased the energy use. However, this storage of water will be utilized to supply water when the pump is off—this cancels out the used extra energy utilized for greater water levels. Thus, there is not much energy savings (2% out of 50% reduction) with the variation of tank levels as manifested by Figure 4.5 above.

The results of tank water level variation were based on fixed pump efficiency as explained earlier in Chapter 2, p 11. However, in the case of the use of the efficiency curve for a pump, this can be explained by use of the following review and application of the basic pump operating theory.

The performance of a pump can be characterized by two specifications: (1) pump characteristics curve, and (2) system head curve (Finnemore and Franzini, 2002). Pump characteristics curve is the plot of head (produced by a pump) vs. flow rate through the pump. The system head curve is a plot of head required to overcome total static and friction loss of water system vs. flow. It estimates the actual head and flow rate of system. The point of intersection of system head curve and pump characteristics curve is known as the *pump operating point*. The most efficient operating point for the pump is when the *pump operating point* coincides with the peak efficiency.

The following Figure 4.6 depicts the relationship between tank maximum water level and pump efficiency for System 1 (S1). There is a shift in pump efficiency along with the rise in tank maximum water level.

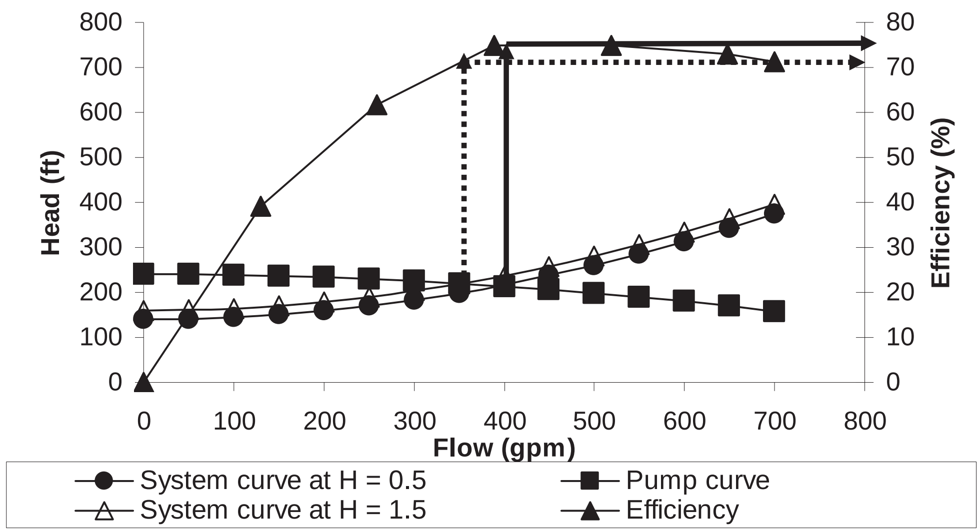

Figure 4.6 System operating points at two extreme maximum water levels of tank of S1 (Figure created from data from EPA, 2000 and Crowe et al., 2001)

Figure 4.6 above shows that the pump efficiency goes down by approximately 2% as the maximum water level of the storage tank is increased. The operating point was shifted to the left (dashed line in above figure) when the water level was increased to 1.5 times the normal operating condition water level.

The pump curve was produced using the EPANET capability of generating the pump curve based upon a Single-Point curve.

The system head curve was generated as follows:

$$H_{TOT} = \mathrm{H_{STAT}} + H_F \tag{4.3}$$

.

where,

H_{TOT} = Total system head

H_{STAT} = Static head, and

H_F = Friction headloss

Friction headloss, H_F, is proportional to the square of flow (Q) (Finnemore and Franzini 2002) and is given by:

$$H_F = \mathrm{KQ}^2 \tag{4.4}$$

In Figure 4.6 above, the static head, $\mathrm{H_{STAT}}$, is 130 ft (39.6 m) for the normal condition maximum water level. The lowest and highest simulated maximum water level values were 0.5 and 1.5 times the normal operating condition maximum water levels, respectively. The normal operating condition maximum water level of the storage tank for S1 is 20 ft (6.1 m). The corresponding values of the two extreme maximum water levels are thus equal to 140 ft or 42.7 m (see Figure 4.6 above) and 160 ft or 48.8 m respectively. Thus, the system head curve was obtained from the following Equation (4.5).

$$H_{TOT} = \mathrm{H_{STAT}} + KQ^2 \tag{4.5}$$

in which, K was computed using known values of H_{TOT}, H_{STAT}, and Q (600 gpm). The details of the computation can be found in Appendix B.3 (p. 128).

4.4 Energy Usage with Varying Tank Elevation

Next, the tank elevation (elevation of the tank bottom) was altered to examine the effect on energy usage for the seven systems.

4.4.1 Procedure

The initial and minimum water levels of each variable tank were kept constant to maintain consistency with the previous analysis of water heights. The tank elevations were varied and were normalized to analyze the results (Figure 4.7) below. The tank elevation was normalized as follows:

$$Z^* = \frac{Z_t - Z_r}{\Delta h_{max}} \qquad (4.6)$$

where,

Z^*	=	the normalized tank elevation,
Z_t	=	simulated tank elevation,
Z_r	=	reservoir or source elevation, and

and,

$$\Delta h_{max} = Z_t^N - Z_r \qquad (4.7)$$

where,

Z_t^N = normal condition tank elevation

Thus, the simulated elevation of a tank is obtained as follows:

$$Z_t = Z_r + Z^* \Delta h_{max} \tag{4.8}$$

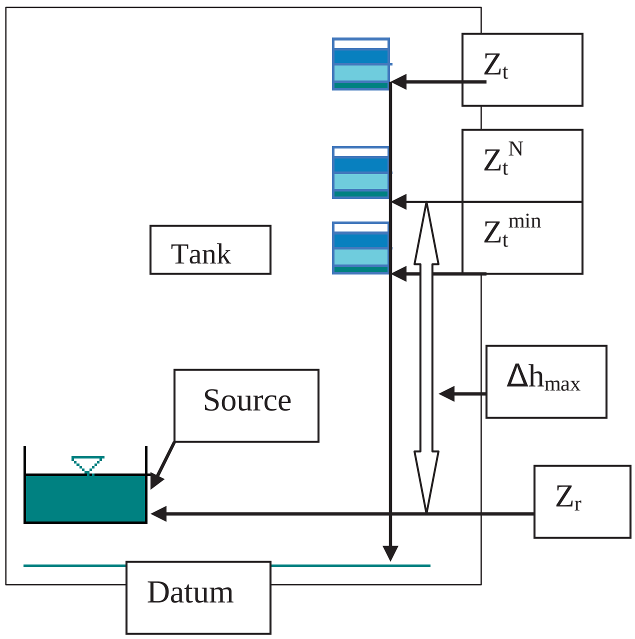

Figure 4.7 Definition sketch of tank elevation variation

All the simulations were begun with empty tanks to ensure comparability between all simulations. For Z* values above 1.0, the pump capacity was increased, if needed, to ensure acceptable system hydraulics. If lowering the tank elevation made any junction elevation higher than tank levels, these junction elevations were reduced to avoid excessively-low pressure values. This occurred for the simulations of Z* values of 0.5 to

0.9. The summary of the alteration of pump curves and junctions are given in Table 4.4 below. Details of the necessary pump and junction alterations are given in Appendix B.4 (p. 130).

Table 4.4 Summary of system modifications for tank elevation variations

System (Tank)	**Z* value m/m**	**Alteration**
1	1, 1.1,1.2, 1.3, 1.4, 1.5	Pump curve
2	1, 1.1,1.2, 1.3, 1.4, 1.5	Pump curve
3 (T1, and T2)	0.5, 0.6, 0.7, 0.8, 0.9	Junctions
3 (T2)	0.5, 0.6	Pump curve
4 (T1, T2)	0.5, 0.6, 0.7, 0.8, 0.9	Junctions
5 (T1)	0.5, 0.6	Junctions
5 (T2)	0.5, 0.6, 0.7	Junctions
5 (T2)	0.5	Pump curve
6 (T1)	1, 1.1,1.2, 1.3, 1.4, 1.5	Pump curve
6 (T2)	0.5, 0.6, 0.7, 0.8, 0.9	Junctions
7 (T2)	1.4, 1.5	Pump curve
7 (T2)	0.5, 0.6, 0.7, 0.8, 0.9	Junctions

Table 4.5 below shows the actual elevation and normalized elevation of tanks of various networks.

Table 4.5 Simulated tank elevations, Z_t (Computed from the tank data from the systems described in Section 2.2, p. 20)

Actual tank elevation, Z_t (m)														
Z*	**S1**	**S2**	**S3**		**S4**		**S5**		**S6**		**S7**			
m/m	**T1**	**T1**	**T1**	**T2**	**T1**	**T2**	**T1**	**T2**	**T1**	**T2**	**T1**	**T2**	**T3**	**T4**
0.5	233.2	196.5	238.1	193.4	232.4	222.5	206.8	194.2	361.5	349.6	36.9	36.9	9.1	4.8
0.6	237.1	199.9	259.8	206.1	241.7	229.8	216.8	201.7	364.2	350.0	44.2	44.2	10.9	5.7
0.7	241.1	203.3	281.5	218.9	251.0	237.1	226.9	209.2	367.0	350.3	51.6	51.6	12.8	6.6
0.8	245.1	206.6	303.2	231.7	260.3	244.4	236.9	216.7	369.7	350.7	58.9	58.9	14.6	7.6
0.9	249.0	210.0	324.9	244.4	269.6	251.8	246.9	224.1	372.5	351.1	66.3	66.3	16.4	8.6
1.0	253.0	213.4	346.6	257.2	278.9	259.1	256.9	231.6	375.2	351.4	73.7	73.7	18.2	9.5
1.1	256.9	216.7	368.3	270.0	288.2	266.4	267.0	239.1	378.0	351.8	81.0	81.0	20.1	10.5
1.2	260.9	220.1	390.0	282.8	297.5	273.7	277.0	246.6	380.7	352.2	88.4	88.4	21.9	11.4
1.3	264.9	223.5	411.7	295.5	306.8	281.0	287.0	254.1	383.4	352.5	95.8	95.8	23.7	12.4
1.4	268.8	226.8	433.4	308.3	316.1	288.3	297.1	261.6	386.2	352.9	103.1	103.1	25.5	13.3
1.5	272.8	230.2	455.1	321.1	325.4	295.7	307.1	269.1	388.9	353.3	110.5	110.5	27.3	14.3

4.4.2 Results and Discussions

The seven systems were simulated for tank elevation variation. The results shown in Figure 4.8 below have shown a system specific nature with a general trend of increasing energy use for higher elevation tanks.

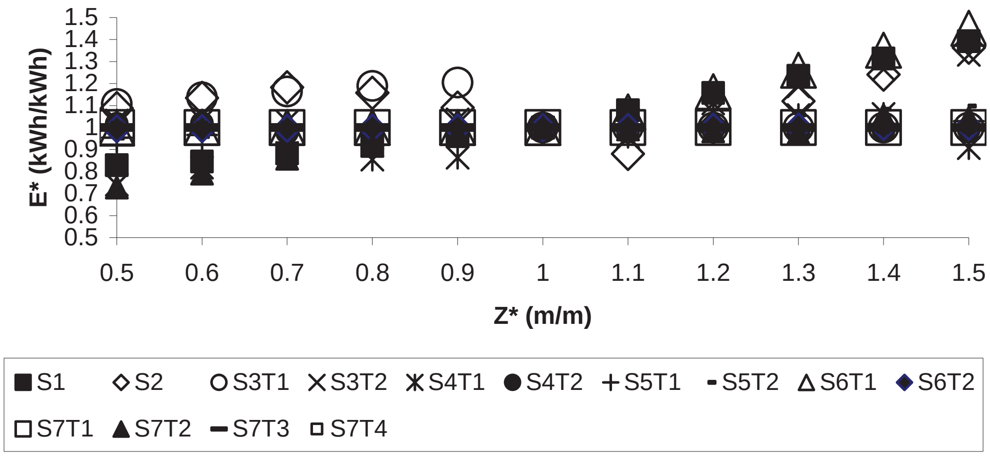

Figure 4.8 Sensitivity of energy utilization to the tank elevation variation

Statistical analysis, as performed for demand variation, for tank elevation variation was not performed due to the wide variation in results for different systems.

4.4.3 Reasons of increased energy use for increased maximum tank elevation

The increasing trend of energy use for increasing tank elevation is due to a rise in static head of the system as described in Section 4.3.3 (p. 64). As the tank elevation was increased, the static head was increased by the same quantity producing a similar condition to tank maximum water level variation. However, the system would utilize all or part of this energy when the pump would turn off. This would cancel out part of the additional use of energy along with the rise in tank elevation. There could also be a reduced pump efficiency at this new operating point, as mentioned above in the discussion of maximum tank water elevation.

4.5 Energy Usage with Varying Tank Diameter

4.5.1 Procedure

The MDWDSs were analyzed to understand the relationship between tank diameters and energy use. Tank diameter was varied on each variable tank separately, some systems having multiple tanks. Altering the tank diameter changed the hydraulics of the network for some cases and, therefore, it was necessary to alter the pump characteristics (head versus discharge) in order to ensure adequate pressure (at least 14 m of head) at all junctions at all times. Reservoirs, tanks, and some junctions near the storage tanks were not included in this pressure requirement. The details of pump modification can be found in Appendix B.5 (p. 142). The tank diameter was altered in the range of 0.5 to 1.5 times the normal operating condition diameter of each variable tank. The corresponding energy use for each simulated diameter was then recorded for analysis. The diameter was normalized as described below.

The normalized tank diameter, D', was defined as follows:

$$D' = \frac{D}{D_o} \tag{4.9}$$

where,

D = diameter modeled, and,

D_o = original tank diameter.

Similarly, the normalized consumed energy, E*, during the simulation period was as defined earlier in Section 3.3.1.1 (p. 44).

Table 4.6 below shows the normalized tank diameter and actual tank diameter of various systems.

Table 4.6 Table showing the variation of tank diameters, D, of the seven systems (Computed from the tank data from the systems described in Section 2.2, p. 20)

	Diameter, D (m)													
D'	**S1**	**S2**	**S3**		**S4**		**S5**		**S6**		**S7**			
	T1	**T1**	**T1**	**T2**	**T1**	**T2**	**T1**	**T2**	**T1**	**T2**	**T1**	**T2**	**T3**	**T4**
0.5	6.9	12.2	16.2	28.3	12.4	8.5	5.3	5.3	2.2	3.8	15.2	15.2	15.9	10.7
0.6	8.2	14.6	19.4	34.0	14.8	10.2	6.4	6.4	2.6	4.6	18.3	18.3	19.1	12.8
0.7	9.6	17.1	22.6	39.7	17.3	11.9	7.5	7.5	3.0	5.3	21.3	21.3	22.2	14.9
0.8	11.0	19.5	25.8	45.4	19.8	13.7	8.5	8.5	3.5	6.1	24.4	24.4	25.4	17.1
0.9	12.3	21.9	29.1	51.0	22.3	15.4	9.6	9.6	3.9	6.9	27.4	27.4	28.6	19.2
1	13.7	24.4	32.3	56.7	24.7	17.1	10.7	10.7	4.4	7.6	30.5	30.5	31.7	21.3
1.1	15.1	26.8	35.5	62.4	27.2	18.8	11.7	11.7	4.8	8.4	33.5	33.5	34.9	23.5
1.2	16.5	29.3	38.8	68.0	29.7	20.5	12.8	12.8	5.2	9.1	36.6	36.6	38.1	25.6
1.3	17.8	31.7	42.0	73.7	32.2	22.2	13.9	13.9	5.7	9.9	39.6	39.6	41.2	27.7
1.4	19.2	34.1	45.2	79.4	34.7	23.9	14.9	14.9	6.1	10.7	42.7	42.7	44.4	29.9
1.5	20.6	36.6	48.5	85.0	37.1	25.6	16.0	16.0	6.6	11.4	45.7	45.7	47.6	32.0

Note: S = System; T = Tank

The results are plotted below in Figure 4.9. It can be seen that the energy utilization of nine of the tanks is less sensitive to the variation of tank diameter than the remaining five tanks (S2, S3T1, S3T2, S4T1 and S4T2).

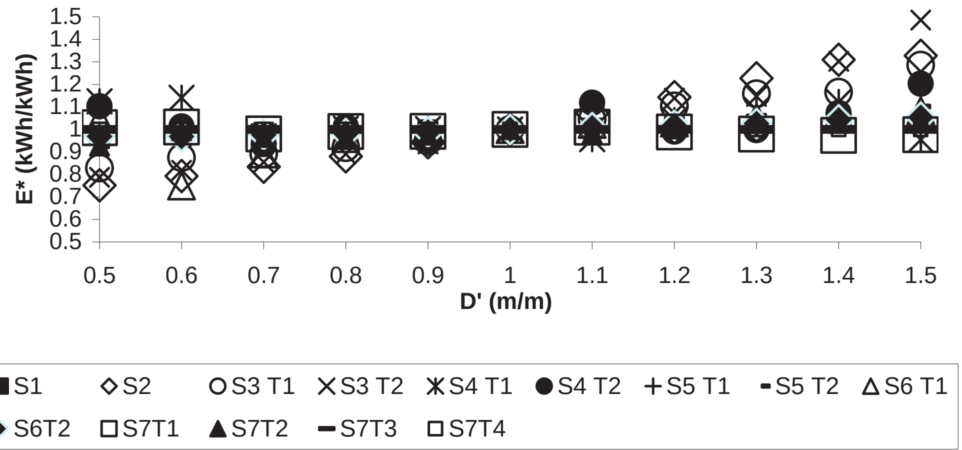

Figure 4.9 The sensitivity of energy consumption to tank diameter of original systems: ‘S’ represents ‘System’ and ‘T’ represents ‘Tank’.

A closer-look at the diameter-sensitive tanks reveals that the greater energy use was caused by an oversized pump(s) for those networks. Pump curves were adjusted to have the smallest pump that satisfied minimum pressures (Table 4.7 below). It is seen in Table 4.7 below that S1, S5, and S7 did not require any modifications. S6 suffered from low pressure at several locations because of the insufficient tank size for D’ = 0.5 for the unmodified condition. This challenge was overcome by increasing the maximum water level of Tank 1 to 146 ft from its original level of 105ft. The increase in tank level will increase the tank volume and thus help to provide enough pressure at the junctions of low pressure. However, this increased tank level increased energy use for S6. No modifications were made while looking at the pump over sizing as opposed to S2, S3 and S4.

Table 4.7 Systems with pump curve variation for tank diameter variation

Systems	Pump variation	No. of Curves	No. of curves adjusted
S1	No	1	0
S2	Yes	1	1
S3	Yes	2	2
S4	Yes	2	2
S5	No	8	0
S6	No	1	0
S7	No	7	0

After adjusting the pump curves, the energy usage declined (Figure 4.10 below). This supports the fact that pumps are more efficient at near-maximum discharge values. Figure 4.10 shows that the normalized energy can be altered by as much as 10% for a 50% change in normalized tank diameter, or have almost no effect, depending on the network and if the pumps are operating at peak efficiency.

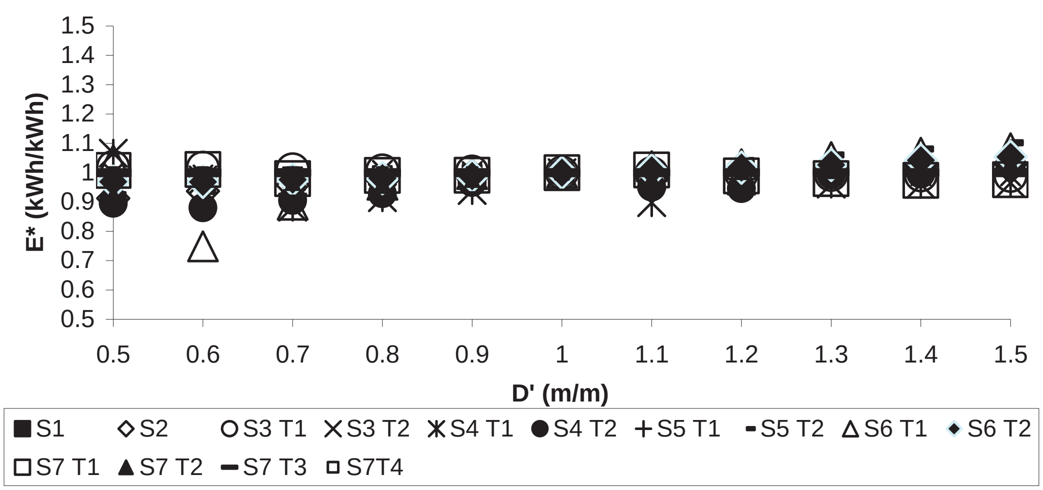

Figure 4.10 The sensitivity of energy consumption to tank diameter of systems with non-oversized pumps: 'S' represents 'System and 'T' represents 'Tank'

Analyzing all seven systems by taking the average E* value averaged over D' reveals that (Figure 4.11 below) energy utilization for the variation of diameter is given by an equation:

$$E^* = 0.12D' + 0.87 \tag{4.10}$$

with an R^2 value of 0.9480 and the error bars denoting ± 1 of standard deviation. From Eq. 4.5 it can be observed that the average energy saving for a 50% reduction of tank diameter of seven systems is approximately 7%. Both the standard deviation and coefficient of variation (COV) exhibit a wider variation of the network energy consumption values at values below D' = 1.0.

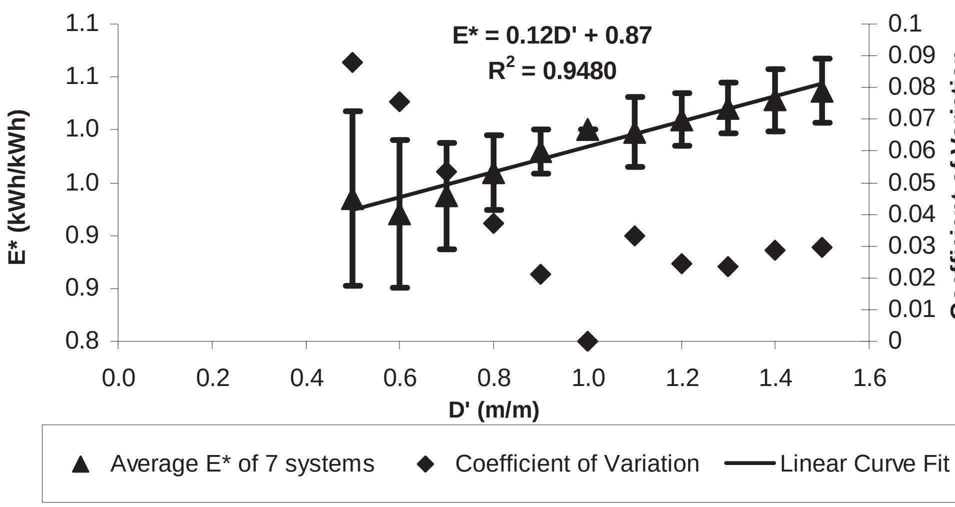

Figure 4.11 Average E* of networks with non-oversized pumps for tank diameter variation. (Error bars denote ± 1 standard deviation).

4.5 Conclusions

Seven water distribution systems were analyzed to observe the impact of storage tank parameters (tank maximum water level, tank elevation, and tank diameter) on energy use. From the results, it was found that the tank maximum water levels have a relatively smaller impact on energy use compared with the tank diameters for the seven systems analyzed. The relationship between tank maximum water level and diameters was observed to be linear while the impact of tank elevation on energy use was observed to be system specific. It was found that the reduction of tank diameter by 50% saved up to 7% of average energy use, whereas reduction of tank maximum water levels by 50% saved a smaller amount of average energy use (about 2%). Based on these results, it can be concluded that more energy savings can be attained through tank diameter reduction than the alteration of other tank parameters. The results also proved the Hypothesis (2) described on page 7. However, lowering the tank diameter should be given first preference in order to save energy over changing the tank maximum water level and/or tank elevation.

4.6 Future Work

The results of tank parameter variation were based upon the empty initial status of the variable tank, and the results were independent of each other. Further research on variation of composite tank parameters should be the next step. Composite tank parameter variation means altering multiple tank parameter values simultaneously.

Chapter 5

The Role of Pumping Stations in the Reduction of Energy Use in Municipal Drinking Water Distribution Systems

5.1 Introduction

Among several components of MDWDSs as described earlier in Chapter 2 (p.11), the effect of the variation of the number of pumping stations and pump horsepower on energy use is an important issue.

Energy consumption depends on many factors in a MDWDS. Among them are pump scheduling (Lansey and Awumah, 1994), tank size and water levels (Gyergyek and Presern 1982). The current study is unique in that it uses energy consumption as the target and alters the number of booster stations and pump power as independent variables. The sensitivity of energy use of MDWDSs to the variation of the above-mentioned components of the systems needs to be analyzed to investigate the possibility of reducing electrical energy use and is described below.

5.2 Procedure

A network solver EPANET 2.0 was used to analyze the role of seven municipal drinking water distribution systems (MDWDSs) on energy use as mentioned above in Section 2.4 (p. 36-40). The analysis was carried out in two steps: (1) sensitivity of energy use to the variation of pump horsepower (hp), and (2) sensitivity of energy use to the variation in number of booster pumping stations and their location. The seven analyzed systems were described earlier in Chapter 2 (p. 11).

5.2.1 Sensitivity of energy use to the variation of pump horsepower (hp)

Seven MDWDSs were used to study the impact of the variation of pump horsepower (hp) on energy use. During the modeling, the system hydraulics was maintained by modifying the systems where necessary. The following Sections 5.2.1.1 to 5.2.1.7 will describe a brief introduction to the systems and necessary modifications in order to maintain the minimum pressure followed by network modeling and results of the analysis.

5.2.1.1. System 1 (S1)

System S1 consists of one Main pump station by the reservoir (Figure 5.3 (a), p. 90), six junctions, eight pipes, and a tank. The simplest system, S1 was taken from the EPANET manual example (EPA 2000). The normal operating condition system used for tank maximum water level was used without any additional modification to the necessary pressure limit.

5.2.1.2 System 2 (S2)

Moderately bigger than S1, S2 consists of one Main pump station that pumps water to the network of 44 junctions, 62 pipes and one tank (Figure 5.4, p. 93). S2 did not need any modifications to provide enough pressure to the system.

5.2.1.3 System 3 (S3)

The S3 is made of 126 junctions and 168 pipes, 8 valves and 2 tanks, and a reservoir. S3 consists of two pumps; the Main pump station is located near the reservoir (Figure 5.5, p. 95), and the other is located near Tank 1. S3 was taken from Ostfeld et al. (2006). In order to maintain the system hydraulics, the system needed some modification to run it successfully with sufficient pressure. The tank water levels were maintained using EPANET software original controls logic. The Main pump station required modification of the original controls (see Appendix C.1.1, p. 146) to EPANET default controls in order to run the system with enough pressure. The EPANET default controls turned the pump on and off depending upon the storage tank minimum and maximum levels. However, the original controls overrode the default tank levels as can be seen in Appendix C.1.1, p.146, thereby allowing less volume of water to be stored in the tank. The modification was applied for all simulations scenarios of pump station 1— variation of horsepower, to nullify the impact of control logic for the whole system. However, there was no change in original controls for pump station 2 simulations. Moreover, the simulations of pump station 2 needed a modification of pump 1 (see Appendix C.1.2, p 147).

5.2.1.4 System 4 (S4)

There are 126 junctions, 144 pipes, and 4 valves in S4. System 4 consists of a Main pump station near Reservoir 1 and an existing Booster 1 near Reservoir 2 as shown in Figure 5.6 (p. 96). Each station has three pumps: one operating pump and the other two for emergency supply. The pump scheduling controls of S4 were also modified to run with appropriate pressure for the system for both pumping station simulations. There were no any other modifications in S4 pump horsepower simulations.

5.2.1.5 System 5 (S5)

347 junctions, 394 pipes, and a reservoir are the main components of System 5. Additionally, S5 consists of a Main pump station near the Reservoir, and two boosters at two different locations as seen in Figure 5.7 (p. 97). There are three pumps at the Main pump station of which two are reserved for emergency supply. The booster stations, Booster 1 and Booster 2, consist of two and three pumps, respectively. The pumps of Booster 1 and 2 of System 5 were modified in order to ensure sufficient pressure to the system (Table 5.1). All of the pumps at each booster station were modified to be identical. However, the pumps at the Main pump station were not modified.

Table 5.1 Pump modification of System 5 for horsepower variation (Modified from pump data of S5 as described in Section 2.2, p. 20)

Pump Station		**Old**		**New**	
		flow	**head**	**flow**	**head**
	Pump#	**gpm**	**ft**	**gpm**	**ft**
	Booster 1				
Curve-7	4				
		0	230	0	400
		250	160	250	250
		400	110	600	110
Curve-8	5				
		0	200	0	400
		250	160	250	250
		320	110	600	110
	Booster 2				
Curve-1	1	0	210	0	250
		100	200	100	210
		200	152	200	190
Curve-2	2				
		0	260	0	250
		300	225	100	210
		620	130	200	190
Curve-3	3				
		0	260	0	250
		300	225	100	210
		620	130	200	190

5.2.1.6 System 6 (S6)

System 6, S6, has 873 junctions, 958 pipes and 6 valves along with a Main pump station with three pumps. Two pumps are reserved for emergency supply (Figure 5.8, p. 98). The diameter of Tank 1 by the Main pump station was doubled to maintain adequate system pressure. In addition, Tank 2 was added to S6 to obtain desired pressure (> 138 kPa) for most of the junctions in the system. S6 is unique from the rest of the systems for its pump location. The location of the Main pump station of S6 is different from the remaining systems in the sense that it lifts the water to storage Tank 1, and the whole system is fed by gravity.

5.2.1.7 System 7 (S7)

System 7, taken from Ostfeld et al. (2006), is the largest system used for the analysis. It consists of 12,525 junctions and 14,825 pipes, and 5 valves. System 7 consists of four pumping stations (Figure 5.9, p. 100). Like S6, S7 is also fed by gravity, but it has three booster stations with a small amount of energy utilization. The pump at the Main pump station is the most important pump with the highest energy cost, being the most active. Thus, the simulations were carried out only for the main pump station (S7PS3), (see Table 5.2, p.85 and Figure 5.1, p. 86).

5.2.1.8 Network Modeling

The seven systems were modeled using the network solver EPANET 2.0 (EPA, 2000). The simulation period was 96 hours to achieve clear repeating patterns of pressure and flow. The pressure at the majority of the junctions was maintained between 138 kPa (20 psi) and 621 kPa (90 psi) except where noted later. The high pressure at many junctions could be an issue for energy loss, and it was not addressed in this study. The high pressure in a system may cause more leakage, as the leakage is related to the pressure of the system (Haestad Methods, 2004) thereby consuming more energy in a MDWDS.

Various diurnal curves and pump efficiency curves were used for the seven analyzed systems as described previously (see Chapter 2, p. 11). A typical pump efficiency curve was developed using the pump efficiency curve and motor efficiency curve as described in Section 2.1.1 (p.14).

To obtain the effect of the horsepower of the existing pumps in the systems, the analysis of variation in pump horsepower (hp) relative to energy use was performed without the addition of any booster pumps. This will help guide the study of the horsepower variation from additional booster pumps described later.

The pump curve for normal operating conditions was used to compute the required hp for the normal operating condition for a specific pump. This normal operating hp was then used for the simulations of variation of horsepower ranging from 1 to 2 times the normal operating condition hp (Table 5.2 below). The computed hp was based on the middle point of flow, Q, and head H, of a pump curve. A pump curve consists of a wide range of discharge values while the hp (fixed energy) is computed from a single flow. Thus, replacing a pump curve by hp requires some modifications in pump curves in some systems.

The following equation was used to compute the hp (Haestad Methods, 2004).

$$WP = C_f Q H_p \gamma \tag{5.1}$$

where,

WP	=	Water power (hp, Watt)
C_f	=	Conversion factor (4.056×10^{-6} English, 0.001SI)
Q	=	Flow (gpm, l/s)
Hp	=	Head added at pump (ft, m)
γ	=	Specific weight of water (lb/ft^3, N/m^3)

5.2.1.9 Pump Efficiency

The network solver EPANET requires as input a pump efficiency curve or a fixed pump efficiency in order to compute the energy use in association with the pump-horsepower or pump curve (EPA, 2000). Thus, energy use in a MDWDS is dependent on a pump efficiency curve or fixed pump efficiency. The pump efficiency curve is a plot of flow rate vs. efficiency of the pump, whereas fixed efficiency is the specified efficiency of a pump regardless of flow or head provided by the pump. The efficiency curve or fixed pump efficiency is used to compute the energy use in EPANET. The pump efficiency curve was used for this analysis and was determined as follows:

A typical wire-to-water pump efficiency curve (Fig 2.1, p.15) was generated using the following two typical curves: (1) Typical pump efficiency (Crowe et. al., 2001, Daugherty and Franzini, 1957) and (2) Typical motor efficiency (UPPCO, 2007) (Section 2.1.1 p. 14). The curve was then used for the simulations of all seven systems. A constant energy (horsepower) of pumps was used in lieu of pump curves for this part of the analysis.

5.2.1.10 Simulations

Simulations were begun with the tanks full in all cases. Pump horsepower hp, values were varied systematically one at a time and the energy usage recorded.

The energy usage output at each simulation was normalized with respect to the normal operating condition energy usage as defined below:

$$E^* = E/E_o \qquad (5.2)$$

where, E^* = the normalized system-wide energy usage,

E = the modeled system-wide energy usage,

E_o = the current (unaltered) system-wide energy usage,

Likewise, the pump horsepower of each simulation was also normalized, and the results were plotted against each other for further analysis. The normalized horsepower (hp*) was defined below:

$$h^*_p = \frac{\text{Simulated horsepower}}{\text{Normal condition horsepower}} = \frac{hp}{hp_0} \qquad (5.3)$$

where,

hp = pump horsepower at simulated condition, and

hp_o = normal condition (unaltered) pump horsepower.

The variation in pump horsepower for the various systems is provided in Table 5.2 below.

Table 5.2 Energy usage values, hp, with horsepower variation of pumping stations of the seven systems (Computed from the pump data from the systems described in Section 2.2, p. 20)

Normalized	**Actual horsepower, hp, (ft)**										
	S1	**S2**	**S3P1**	**S3P2**	**S4P1**	**S4P2**	**S5P1**	**S5P2**	**S5P3**	**S6PS1**	**S7PS3**
hp*	**hp**	**hp**	**hp**	**hp**	**hp**	**hp**	**hp**	**hp**	**hp**	**hp**	**hp**
1	27.4	16.7	177.3	63	195.1	26.6	44.3	15.8	5.3	83.2	3062.8
1.1	30.14	18.37	195.03	69.3	214.61	29.26	48.73	17.38	5.83	91.52	3369.08
1.2	32.88	20.04	212.76	75.6	234.12	31.92	53.16	18.96	6.36	99.84	3675.36
1.3	35.62	21.71	230.49	81.9	253.63	34.58	57.59	20.54	6.89	108.16	3981.64
1.4	38.36	23.38	248.22	88.2	273.14	37.24	62.02	22.12	7.42	116.48	4287.92
1.5	41.1	25.05	265.95	94.5	292.65	39.9	66.45	23.7	7.95	124.8	4594.2
1.6	43.84	26.72	283.68	100.8	312.16	42.56	70.88	25.28	8.48	133.12	4900.48
1.7	46.58	28.39	301.41	107.1	331.67	45.22	75.31	26.86	9.01	141.44	5206.76
1.8	49.32	30.06	319.14	113.4	351.18	47.88	79.74	28.44	9.54	149.76	5513.04
1.9	52.06	31.73	336.87	119.7	370.69	50.54	84.17	30.02	10.07	158.08	5819.32
2	54.8	33.4	354.6	126	390.2	53.2	88.6	31.6	10.6	166.4	6125.6

Note: hp= Normalized horsepower defined as:*

$$h^*_p = \frac{\text{Simulated horsepower}}{\text{Normal condition horsepower}}$$

5.2.1.11 Results and Discussion

The results of energy sensitivity of the seven systems to the variation in pump horsepower are presented in Figure 5.1 below. It can be seen that the energy usage of the system is more sensitive to horsepower of the main system pump and not to any existing booster pumps, except for S6, which is primarily gravity fed with the highest elevation of the system being the main storage tank by the main pumping station (Figure 5.8, p. 98). In addition, the positive slopes of all the curves (Figure 5.1) prove that increased pump horsepower results in the rise of energy use for all of the seven systems.

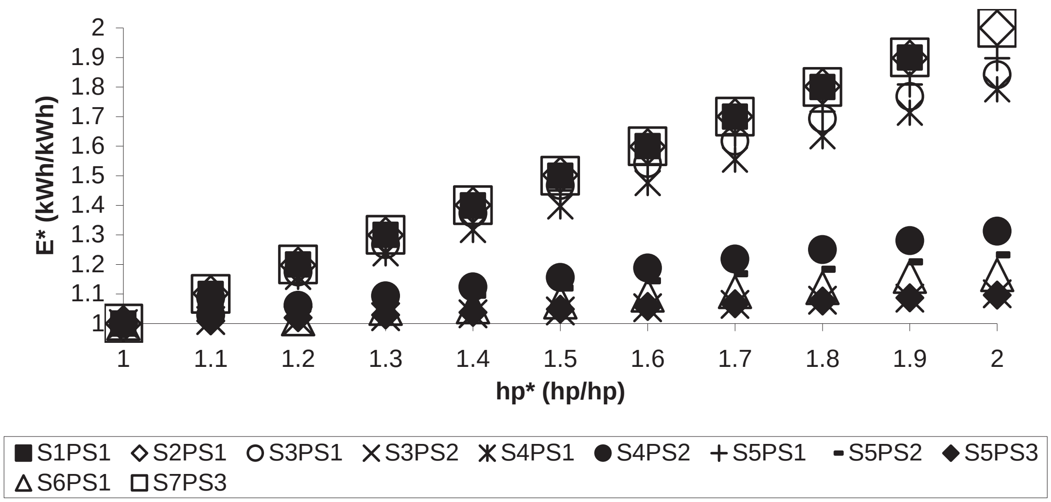

Figure 5.1 Energy sensitivity of seven systems to pump horsepower

5.2.2 Sensitivity of energy use to the variation in number of booster pumping stations and their location

After establishing that increased horsepower increases energy consumption in a linear fashion, the effect of the variation in number and location of booster pump stations on energy use were examined. The first step of this process was to identify the category of existing pumping stations in a water system. A municipal water distribution system is equipped with two categories of pumping stations: (1) only a main pumping station, or (2) both a main pumping station and booster station(s). In the current study, three systems (S1, S2, and S6) were equipped with only a main pumping station. The remaining four systems (S3, S4, S5, and S7) were equipped with one or more booster stations along with the main pump stations.

The two categories of systems were simulated by adding or removing pumping stations at various locations. In the case of the first category of systems consisting of only the main station, a booster station was added at the bottom of the highest elevation zone of the system. The new scenario was then simulated with a booster pump station to compute the required energy utilized. Additional booster pumps were added at the rest of the highly-elevated zones until a clear pattern of energy use was observed to conclude the impact of booster stations to a system. The boosters were added at various locations in the systems depending on the elevation difference between the highest point and a booster location (Figure 5.2, p. 88).

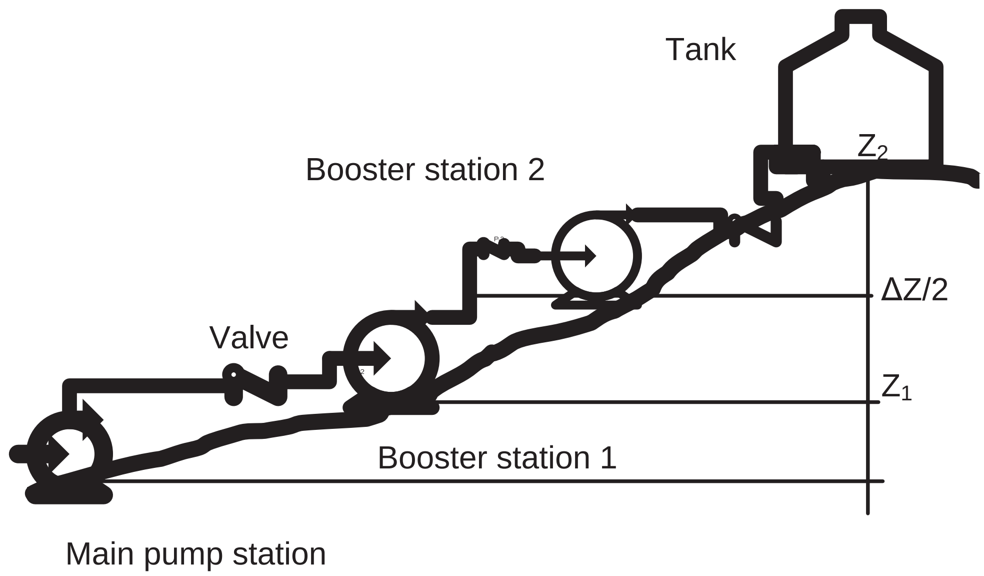

Figure 5.2 Installation of booster stations: $\Delta Z/2 = (Z_2 - Z_1)/2$, and Z = elevation

The first additional booster was installed at the bottom of the highest hill with a tank. Subsequent boosters were placed either at mid elevation between the first booster elevation and the tank bottom elevation or at the bottom of the next highest hill, whichever elevation difference was greater.

In some situations, however, it was not possible to find many suitable locations for a booster site. In that case, additional boosters were added at a point between a previously selected location and the highest-elevation point in linear increments of elevation.

In the case of the second category of systems with existing booster pump-stations, boosters were gradually removed one at a time to simulate the single or multiple booster scenarios to record the energy use. However, it may have been necessary to add more stations depending on the number of existing pumping stations to observe a clear pattern of energy use. The system modifications such as pump capacity modification and/or addition of a bypass pipe were needed along with the addition or removal of booster stations. The addition of a bypass pipe was needed whenever a booster pump was added at a location where water flows were of a single path, thereby allowing flow in both directions as needed, since a pump allows flow only in one direction. The details of the simulations and modification of the seven systems are described in sections 5.2.2.1 to 5.2.2.7 below followed by the results and discussions of the analysis:

5.2.2.1 System 1 (S1)

The existing system, S1 (Figure 5.3 (a) below) had a single pump station. Several pump stations were gradually added to the system as described above in Section 5.2.2. All the boosters were added between the tank and its base junction assuming that the elevation was linearly increased. The system needed modification along with the additions of boosters to ensure enough pressure. The modifications included controlling the main pump using controls logic, time patterns, addition of a bypass pipe, and modification of pump curves. The addition of a bypass pipe would allow the flow to direct it in reverse direction of pump flow. The addition of a bypass pipe allowed the tank drainage. The use of controls logic turned off the pump as the water level in the tank approached its maximum level and turned on again when it approached the minimum level. The details of the pump modifications and controls logic are found in Appendix C.2.1, p.148. The boosters added for the analysis are presented in Figure 5.3 (a-e) below. The optimal booster station consisted of the main pump only and is shown below in Figure 5.3 (a).

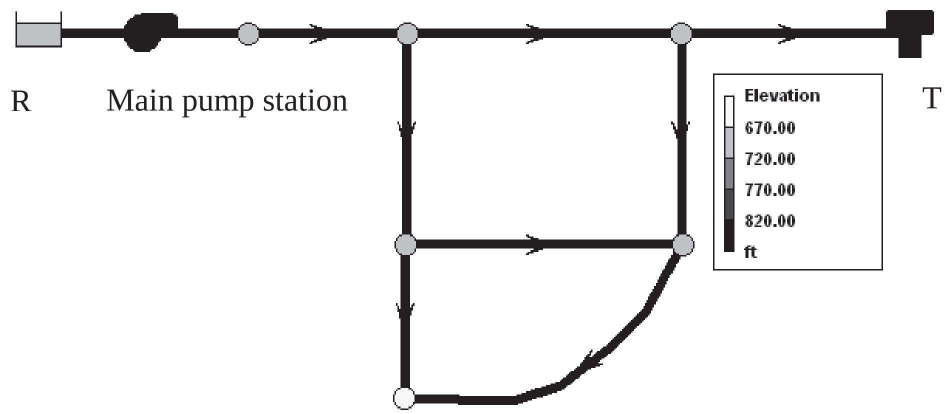

Figure 5.3 (a) Main pump station—the optimum pumping arrangement of S1 (Figure created from data from EPA, 2000): R = Reservoir, T = Tank

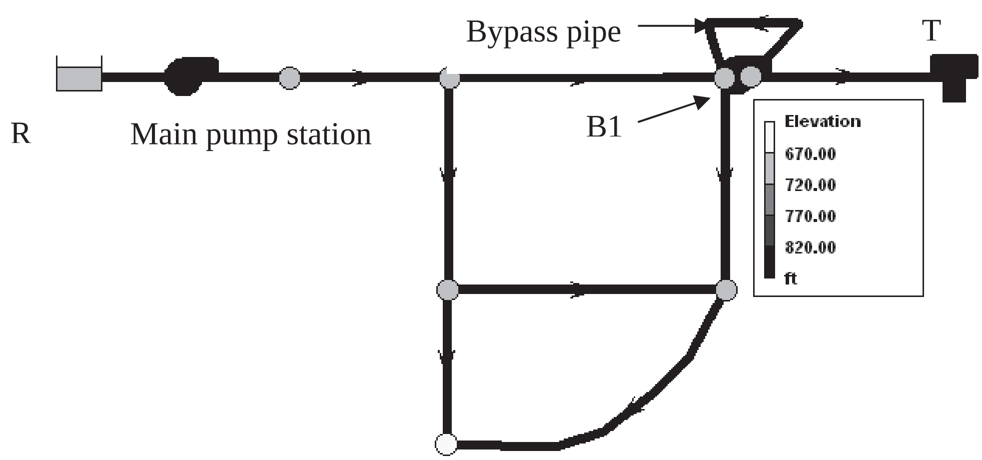

Figure 5.3 (b) Booster 1 of S1 (Figure created from data from EPA, 2000): R = Reservoir, T = Tank, B = Booster

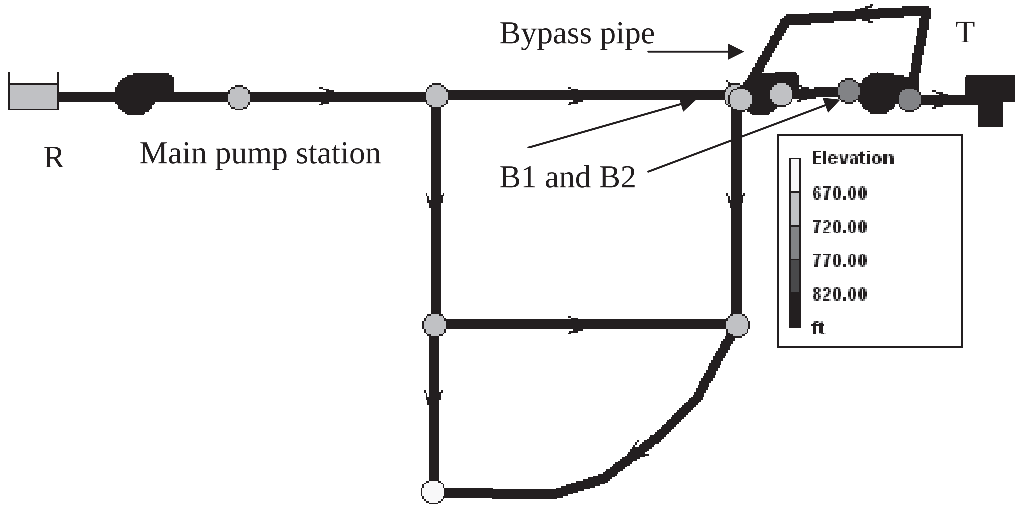

Figure 5.3 (c) Boosters 1 and 2 of S1 (Figure created from data from EPA, 2000):
R = Reservoir, T = Tank, B = Booster

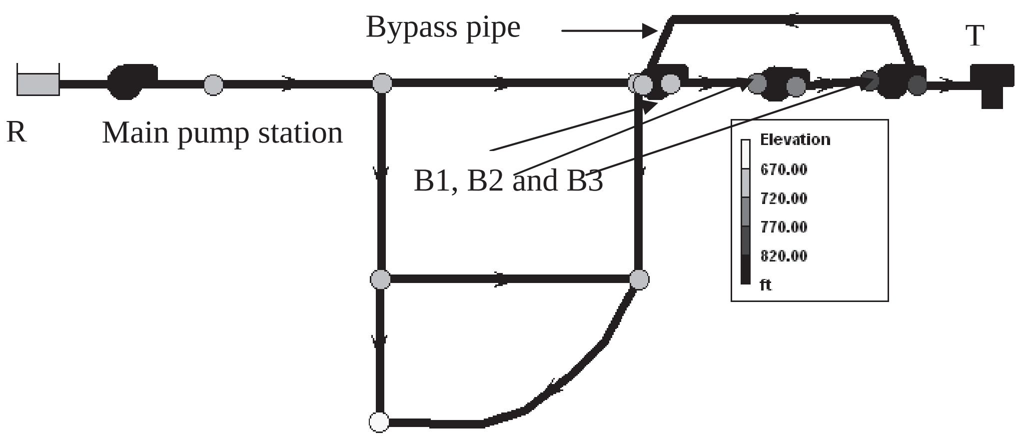

Figure 5.3 (d) Boosters 1, 2 and 3 of S1 (Figure created from data from EPA, 2000):
R = Reservoir, T = Tank, B = Booster

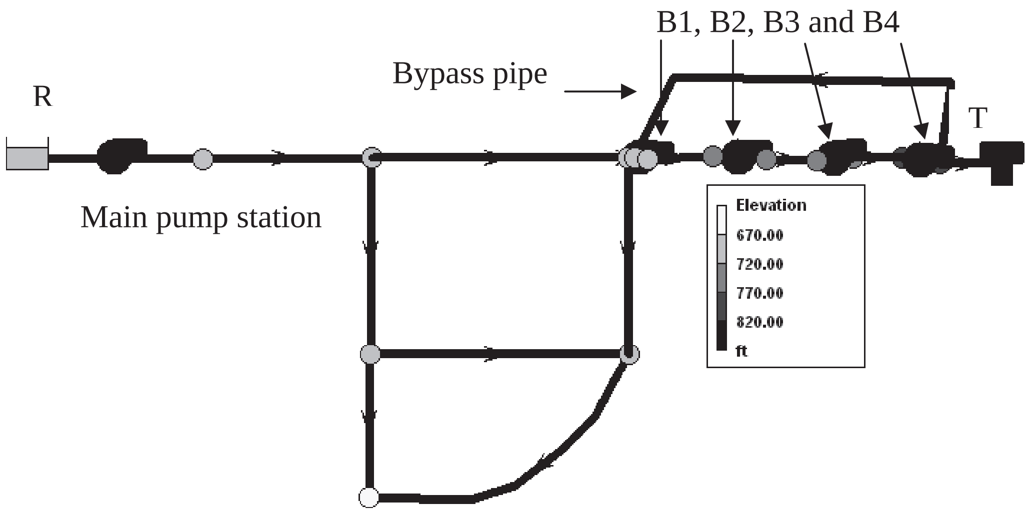

Figure 5.3 (e) Boosters 1, 2, 3 and 4 of S1 (Figure created from data from EPA, 2000): R = Reservoir, T = Tank, B = Booster

For this simple system, S1, the highest (and only) hill is the hill with the storage tank, T. Five separate maps were shown above in order to explain the booster installation methodology. From these five figures (Figures 5.3 (a)-(e)), it can be seen that boosters were added in progression by always keeping the elevation change between sets of two successive boosters equal as described in Figure 5.2, p. 88. For example, in Figure 5.3 (e), the bottom of the hill is at an elevation of 700 ft, and the top is 830 ft. The first booster was added at the elevation of 700 ft, the bottom of the hill, and the remaining three boosters (B2, B3, and B4) were added at the locations of 732.5 ft, 765 ft, and 797.5 ft of elevation.

However, the installation of boosters depends upon the hills and the elevation change as shown in the following six systems. If there are more than a single hill in a system, the succeeding boosters may be installed at the bottom of succeeding hills as desired by the systems (see below Sections 5.2.2.2-5.2.2.7).

The rest of the systems were analyzed in a similar fashion as shown in the following sections (5.2.2.2-5.2.2.7)

5.2.2.2 System 2 (S2)

Several pump stations were gradually added to System 2, S2, which originally had a single pump station (Main pump station) (see Figure 5.4). In order to ensure enough pressure to the system, the main pump was modified, and the modifications can be found at Appendix C.2.2, p 149. S2 also needed a bypass pipe when the booster was added at the bottom of the tank. This helped water flow from the tank to the system. The optimum booster for S2 consisted of the main pump only and is shown in Figure 5.4 below.

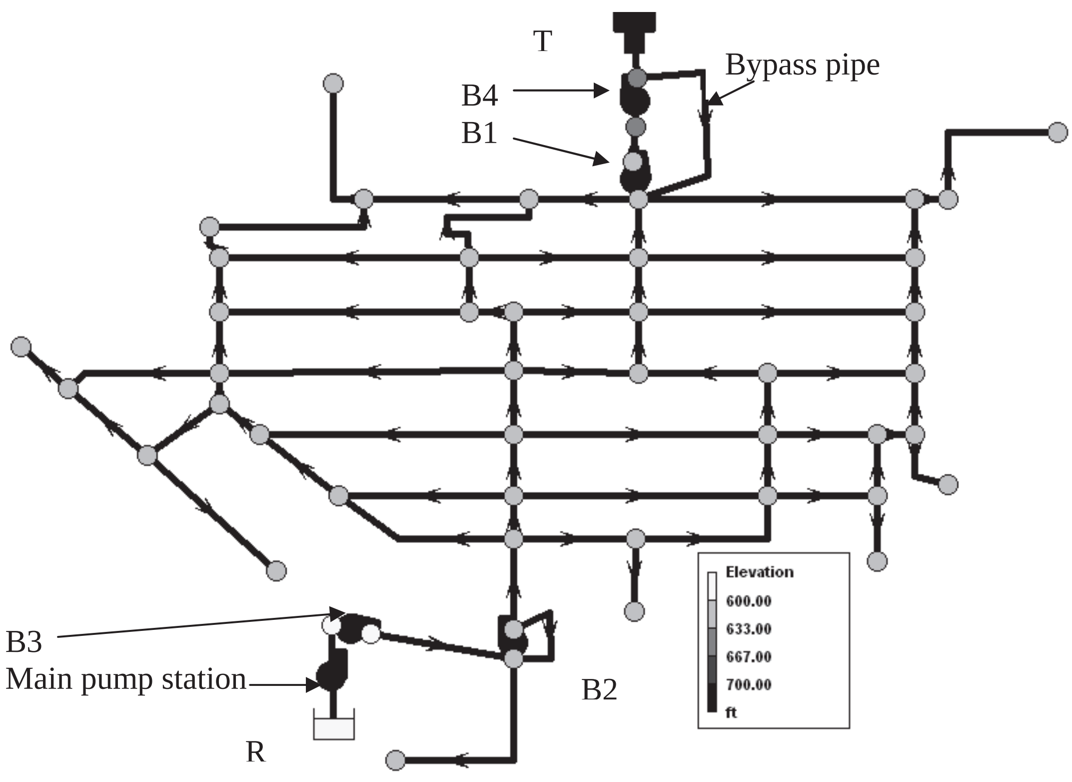

Figure 5.4 Modeled booster arrangement of S2. Optimal booster arrangement consisted of main pump station only.: R = Reservoir, T = Tank, B = Booster

5.2.2.3 System 3 (S3)

System 3, S3, originally had two pumping stations. One of them was considered to be the main pump and the other to be a booster, B1 (Figure 5.5). For a two-booster scenario, one additional pumping station was added. A bypass pipe (see Figure 5.5 below) was added to drain Tank 1 when Booster 2 was installed. The first booster was an existing booster at the base of Tank 1 (elevation 1137 ft). The rest of the boosters were installed by determining the elevation difference between the peak elevation of a hill and its base (Figure 5.5). In the original data file, the elevation of Booster 2 was located at an elevation of 0 ft, but was changed to the elevation of the surrounding junctions (846 ft) for these pump simulations due to its unrealistic original value.

The hydraulics for the various simulations was made consistent with the normal condition hydraulics. To bring the system above the acceptable pressure of 138 kPa (20 psi), it was sometimes necessary to make some changes in pumps such as the use of a pump schedule according to a time pattern. A time pattern allows the network modeler to control the pump operation schedule. The details of the modifications can be found in Appendix C.2.3, p. 150. Like S1 and S2, S3 also needed bypass piping when a booster was added near the storage tank T1. The optimal booster configuration consisted of a main pump and two boosters (B1 and B2) located as shown in Figure 5.5.

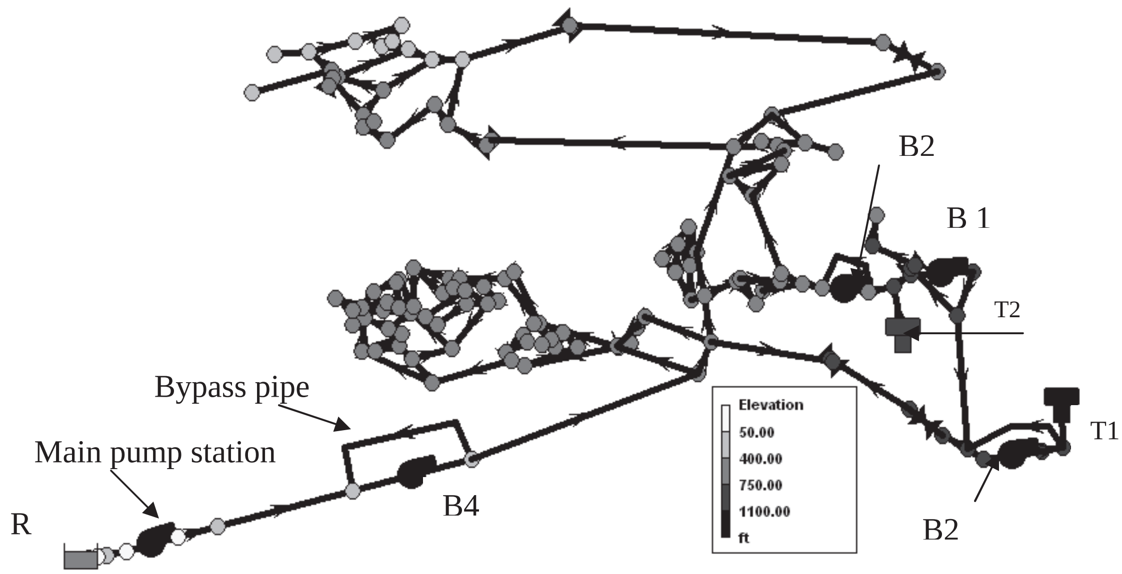

Figure 5.5 Modeled booster arrangement of S3 (Figure created from data from Ostfeld et al. 2006). Optimal booster arrangement consisted of main pump station and boosters B1 and B2: R = Reservoir, T = Tank, B = Booster

5.2.2.4 System 4 (S4)

The existing System 4, S4, also consists of a main pumping station and a booster station by the second reservoir (Figure 5.6). However, there are two emergency pumps at each location, which are both closed. One of the closed pumps at the main station was opened for the third and succeeding booster simulations.

For the no-booster case, the existing booster was removed and the main pump head was increased. The pump (Booster 1, Figure 5.6) was considered the first booster. S4 is slightly different from the rest of the systems in the sense that there are several pumps turning off and on during the simulation period depending on the tank water level. In order to run the system with sufficient pressure, the system required the pumps to turn on when the water level of the tanks dropped below the assigned water level. However, a few junctions near the water tower for short periods dropped below the minimum pressures of 20 psi. S4 required some modifications in pump as shown in Appendix C.2.4, p. 151 and the addition of a bypass pipe along with the installation of Booster 3. The most efficient booster arrangement consisted of a main pumping station and a single booster (B1) as shown in Fig. 5.6.

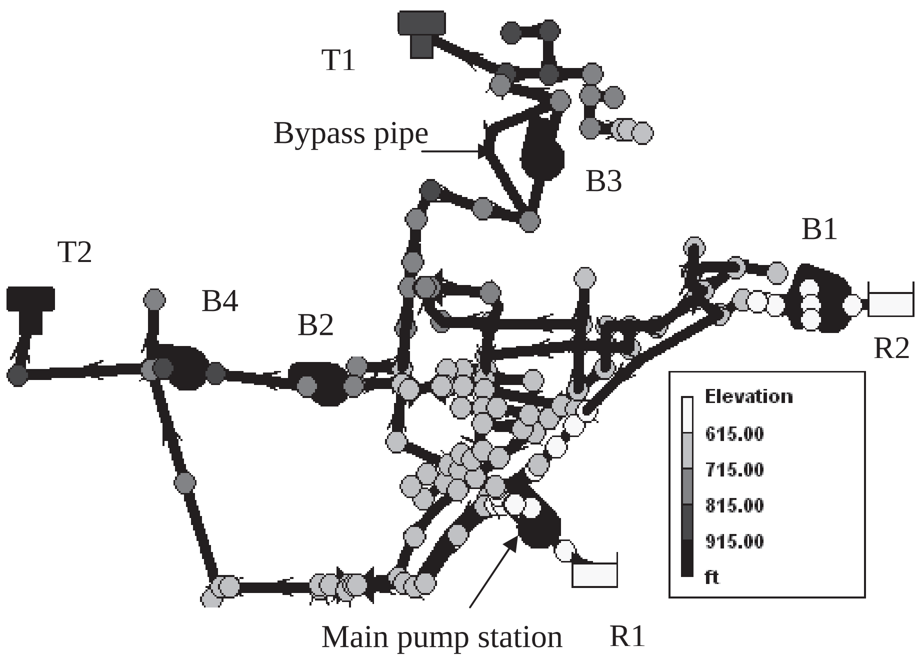

Figure 5.6 Modeled booster arrangement of S4. Optimal booster arrangement consisted of main pump station and booster B1: R = Reservoir, T = Tank, B = Booster

5.2.2.5 System 5 (S5)

System 5, S5, originally had three pumping stations (Main pump station, B1, and B2) with several emergency pumps in each of the stations (Figure 5.7). However, the emergency pumps were not in use for the simulations of the zero-booster case. The other two stations were gradually removed one at a time to simulate the single-and two-booster scenarios. An additional booster (B4) was added to simulate the four-booster case as shown in Figure 5.7 below. The pump curves were modified to their lowest capacity capable of maintaining system hydraulics when changing the number of boosters. S5 pumps were modified in order to maintain the system pressure for various simulations scenarios. The modifications are described in Appendix C.2.5, p. 152. The most efficient arrangement of pumps consists of a main pump and three boosters (B1, B2, and B3) as shown in Fig. 5.7.

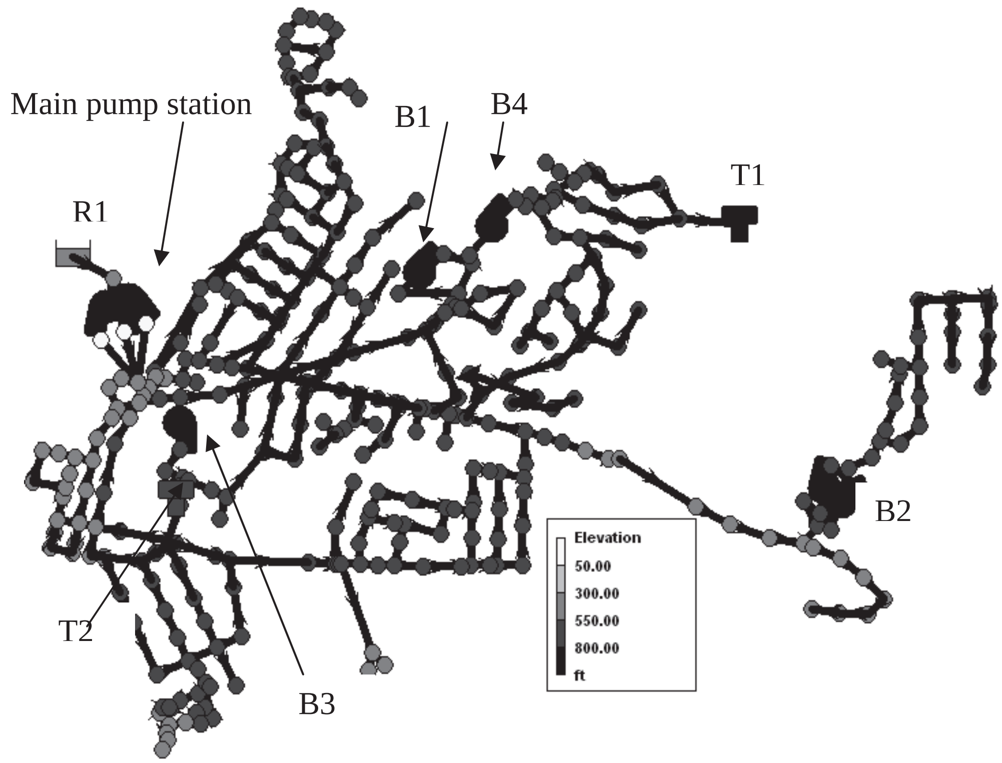

Figure 5.7 Modeled booster arrangement of S5. Optimal booster arrangement consisted of main pump station and boosters B1, B2, and B3: R = Reservoir, T = Tank, B = Booster

5.2.2.6 System 6 (S6)

System 6, S6, originally had a pump station with two emergency pumps and a pump for normal operation near the reservoir, which pumps water to a storage tank and feeds water to the system (Figure 5.8). The two emergency pumps are closed all the time and are only for emergency operations. The highest point for booster pump installation for S6 is near the second storage tank. By observing the several junctions near the tank, the first booster, Booster 1, was added at a junction located at the bottom of the highest hill (Figure 5.8). Likewise, succeeding boosters were added as can be seen from Figure 5.8 below. S6 required some pump modifications along with the addition of boosters (see Appendix C.2.6, p. 154). The most efficient pump arrangement consists of the main pump station and a booster (B1) as shown in Fig. 5.8.

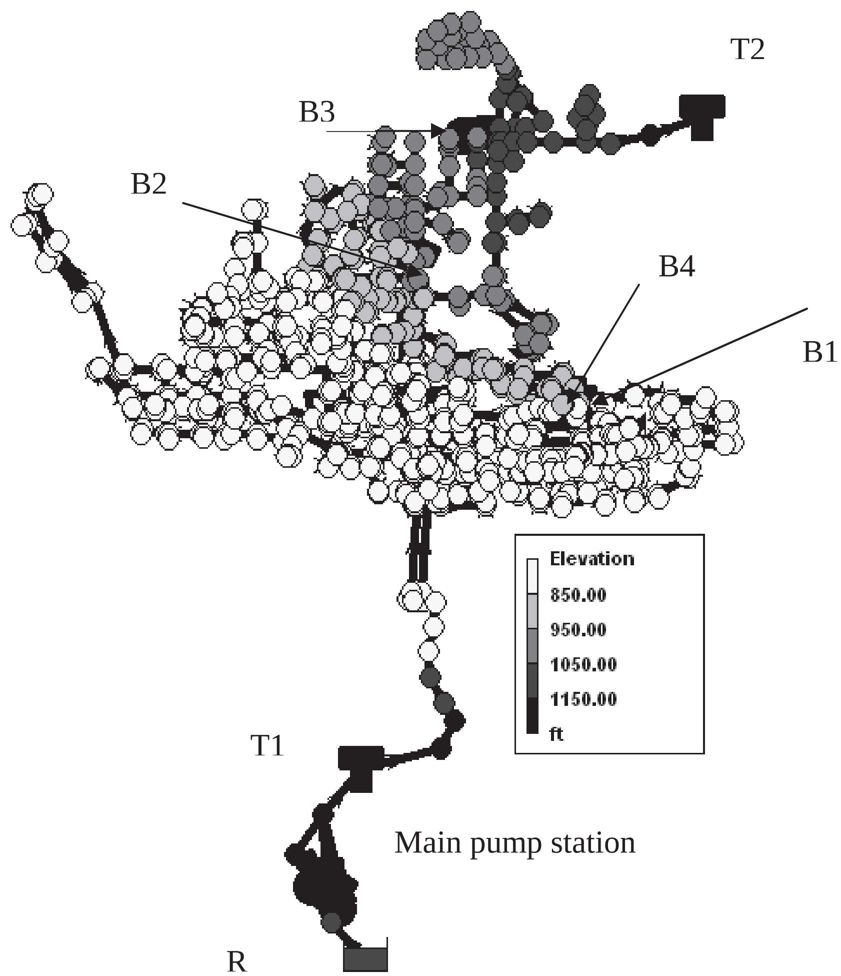

Figure 5.8 Modeled booster arrangement of S6. Optimal booster arrangement consisted of main pump station and booster B1: R = Reservoir, T = Tank, B = Booster

5.2.2.7 System 7 (S7)

System 7, S7, is a huge system in contrast to the rest of the systems. S7 originally consisted of four pumping stations. The first main pumping station pumps water to the storage tank and feeds the whole system by gravity. There is a booster station (Booster 1 in Figure 5.9) which operates with a small amount of energy use. The third closed station drains water from storage tank, T3 in case of emergency. Likewise, the fourth closed pumping station may be used for emergency water supply from the storage tank, T4 (see Figures 2.14, p. 26).

The main pumping station and Booster 1 were considered to be as the existing condition scenario (one booster case), keeping the rest of the pump stations unchanged (closed) for the simulations. Additional boosters were added as described below. As in the rest of the systems, the placements of the booster pumping stations of S7 were based on the elevation contours of the system (Figure 5.9). The first booster was already installed at the base of a hill with an elevation change of 45 ft. The second booster was installed at the bottom of a hill with an elevation difference of 38 ft. The pump curve for Booster 2 was generated by considering the flow at normal operation conditions in the pipe connecting the junction and head difference between the two junctions.

Likewise, the third booster was installed at the bottom of a hill with an elevation difference of 30.8 ft. The third booster pump was added here, as this was the next highest hill in the system. The pump curve for Booster 3 was generated by adding the required head to lift the water to an elevation of 105 ft, the top of the hill from the base of the hill at 74 ft. The flow required for the pump was the flow of the pipe connecting these two junctions. However, the flow was insufficient. To overcome the situation, the flow in the pump curve was increased gradually to successfully run the system with enough flow and pressure. Fourth booster (B4) was installed at an elevation of 65.4 ft to pump water to the top of a hill at an elevation of 85 ft. (Figure 5.9). The modifications of pumps of S7 are found at Appendix C.2.7, p. 154). The most efficient pumping arrangement consists of a main pump and three boosters (B1, B2, and B3) as can be seen in Fig. 5.9.

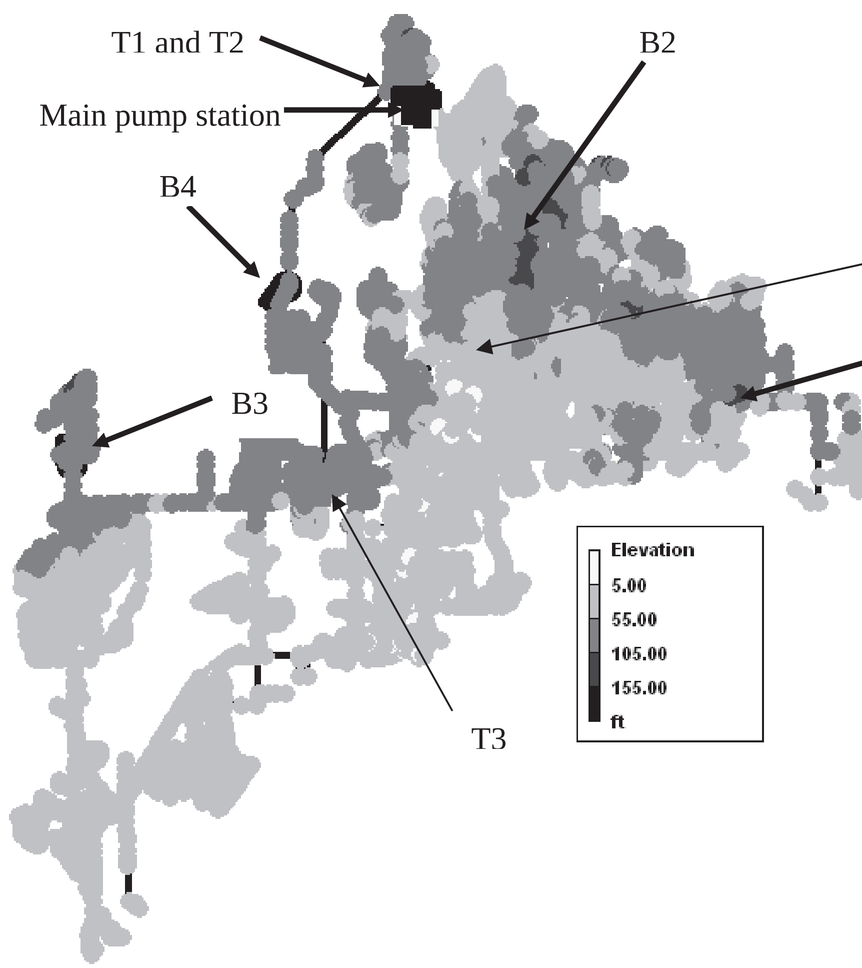

Figure 5.9 Modeled booster arrangement of S7 (Figure created from data from Ostfeld et al. 2006). Optimal booster arrangement consisted of main pump station and boosters B1, B2, and B3: R = Reservoir, T = Tank, B = Booster

5.2.2.8 Results and Discussion

The results of the analysis of variation in booster pump stations at different locations and its effect on energy use is presented in Figure 5.10 below. It can be seen that adding booster stations at a high altitude on most of the analyzed systems, S3, S4, S5, S6, and S7, saved energy. The savings were in the range of 6% to 66% for these five systems (Table 5.3). However, no savings were observed from the addition of a booster for S1 and S2. For S3 significant saving of 53.7% was realized after the addition of the second booster. Succeeding booster addition did not make any significant savings for S3. For S4, an energy savings of 11.1% was observed at the first booster addition. For S5, a savings of 66.4% was observed after the addition of two boosters. For S6, 5.6% savings was realized after the addition of the first booster with no savings resulting from adding the succeeding boosters. For S7, there is no savings in energy after the addition of the first booster; however, there is a significant savings after the second booster addition and not much change in savings after that. A 27.8% savings was realized after the third booster was installed in S7.

In summary, energy savings from the addition of booster(s) was realized for five of the analyzed systems, and no savings was found for the remaining two systems due to the nature of the system. The optimal number of boosters and their locations is, however, dependent on system characteristics. The topography and head of the systems are the major two differences in these five energy savings systems (S3, S4, S5, S6, and S7) and non-energy saving systems (S1 and S2). In other words, the change in system elevation (see Figures 2.8-2.14, p. 21-26), and range of energy grade line (EGL) (see Figures 2.16-

2.22, p. 30-36) are the major causes for this energy savings for the addition of boosters ("boosterification") of these five systems. The remaining two systems, S1 and S2, have less elevation and EGL variation (see Figures 2.16-2.22 and Figures 5.3-5.9). In addition, from Figure 5.10, it is also seen that the slope of the curves for the five energy saving systems was maximized when the first booster was added. This means that maximum energy savings occurred when the first booster was added to the system. The optimal number of booster stations and energy savings for the seven systems can be found in Table 5.3 below.

Table 5.3 Energy savings of seven systems for the addition of booster stations

Systems	**Energy savings (%)= (1-C/N)*100**						
	Pump station #					**Optimal Pump**	**Optimal % savings**
	1	2	3	4	5		
S1	0.0	-145.9	-147.0	-146.2	-146.5	Main pump	n/a
S2	0.0	-12.4	-22.3	-22.3	-25.5	Main pump	n/a
S3	0.0	51.8	53.7	53.7	53.7	2	53.7
S4	0.0	11.1	-39.0	-39.2	-50.4	1	11.1
S5	0.0	36.9	63.1	66.4	62.8	3	66.4
S6	0.0	5.6	-0.2	0.8	2.6	1	5.6
S7	0.0	-0.1	25.9	27.8	25.1	3	27.8

Note: Energy savings (%) = (1-C/N)*100,

Where, C/N is the normalized energy (E*) and is obtained from Figure 5.10.

C= Current energy utilized, and N= Normal operating condition energy utilized.

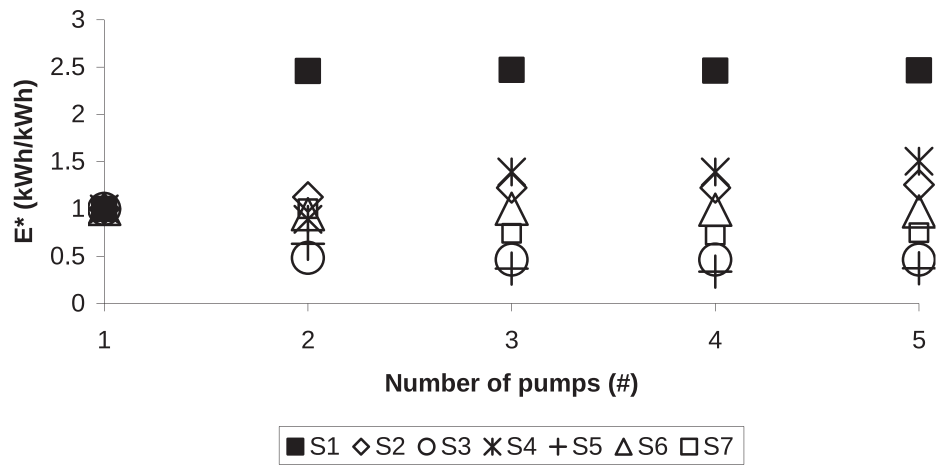

Figure 5.10 Energy sensitivity of seven systems to their number of booster stations

5.3 Reasons of increased energy use for decreased booster stations

The energy used by a pump is largely dependent on the nature of a system such as topography—the elevation variation, and the head of a system. The rapid variation of elevation of a system and the rapid drop of head are primarily the main factors to consume more energy. This can be seen by observing the system maps (Figure 2.8-2.14, p. 21-26) and head plots (Figure 2.16-2.22, p. 30-36). From Figure 2.16 and Figure 2.17, it is evident that the elevation change of S1 and S2 is smaller than the rest of systems (S3, S4, S5, S6, and S7). This justifies the energy savings from the addition of boosters in these five systems with highly elevated hills. The change of head of these five systems is also of a similar nature—S1 and S2 being a small range of head variation and the rest with larger head variation.

The increased energy use for the increased number of booster stations for these five systems can also be explained by understanding the pump performance curves for pumps in series. S1 is used here to demonstrate this point, but the same concept applies to the other systems as well. The concept of pumps in series allows the generation of a pump curve by adding the head values for the two pumps for a given flow rate as shown in Table 5.4 below. When a booster pump was added, the original pump capacity was reduced (‘modified original’ in Table 5.4), and the added booster pump was made identical to the modified main pump.

Table 5.4 Pump curve data for pumps in series for S1: heads added for series (Computed based on S1 pump data as described in Section 2.2, p.20)

Flow	Original	Modified original	Booster 1	series
Q (gpm)	Head (ft)	Head (ft)	Head (ft)	Head (ft)
0	240.0	220.0	220.0	440.0
50	239.6	219.6	219.6	439.2
100	238.3	218.5	218.5	436.9
150	236.2	216.6	216.6	433.1
200	233.3	213.9	213.9	427.8
250	229.6	210.5	210.5	420.9
300	225.0	206.2	206.2	412.5
350	219.6	201.3	201.3	402.6
400	213.3	195.6	195.6	391.1
450	206.2	189.1	189.1	378.1
500	198.3	181.8	181.8	363.6
550	189.6	173.8	173.8	347.6
600	180.0	165.0	165.0	330.0
650	169.6	155.4	155.4	310.9
700	158.3	145.1	145.1	290.3

From Figure 5.11 below, it can be seen that the efficiency of the operation of a pump depends upon the system requirements. This means, if the system curve rapidly increases, the pump efficiency will increase as the pumps are operated in series, or if it does not change rapidly as seen in Figure 5.11 below, the pump operation efficiency begins decreasing slowly. Figure 5.11 below shows that the pump operating points shifted to a lower efficiency (75% to 72%) as the additional booster was added to the system—partly responsible for the increased energy use with increased number of boosters. The pump operating points are the intersection point of the pump and system head curve, and the pump operating point changes with the variation of demand with time (Bosserman, 2000).

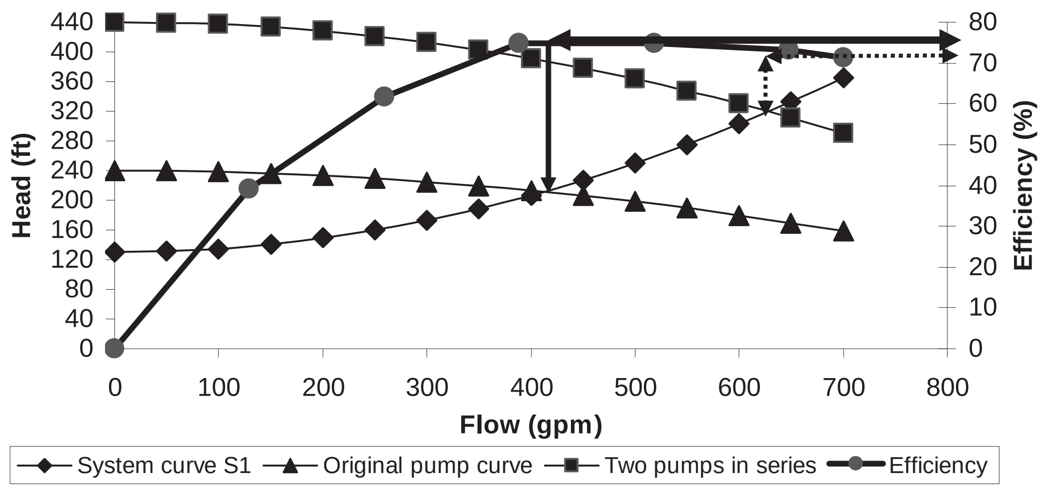

Figure 5.11 Pump performance curves for S1 depicting the efficiency for pumps in series: (Figure created from data from EPA, 2000 and Crowe et al., 2001)

5.4 Conclusions

The sensitivity of energy use in seven municipal water distribution systems to the pumps horsepower, number of booster stations and their locations were studied. Energy use is more sensitive to the variation in horsepower of the main pumps than to the booster pumps in the analyzed seven systems. The results of booster addition at various locations showed that from 5 percent to as much as 66 percent of energy consumption could be saved for the five systems (S3, S4, S5, S6, and S7). In addition, it was found that the savings after the installation of the first booster is greater than the energy savings from the additional boosters. However, the energy savings from the booster addition was not possible for S1 and S2 due to the relatively flat topography and EGL. However, the energy savings from the number of boosters at various locations may vary from system to system. Thus, the results supported the Hypothesis (3) described on page 7.

Chapter 6

Summary and Conclusions

6.1 Summary

A network solver, EPANET 2.0, was used to analyze seven municipal drinking water distribution systems to observe the impact of various aspects of MDWDSs. The various aspects of the systems included water demand, storage tank parameters (maximum water level, tank elevation or location, and tank diameter), and pumping stations. The findings of the study are summarized on Table 6.1 below.

Table 6.1 Summary of results of the study

MDWDS aspect	% Reduction	Maximum Energy Savings
Demand reduction	50%	47%
Tank maximum water level reduction	50%	2%
Tank elevation reduction	50%	30%
Tank diameter reduction	50%	7%
Booster pump	n/a	66%

The summary of the results presented in Table 6.1, proved the hypotheses as defined in page 6-7.

6.2 Conclusions

1. Reducing system-wide demand by 50% results in a 47% reduction in average energy use for the analyzed seven systems. An equation relating water demand and energy use was found as shown in Equation 3.8 (p. 47) repeated here as follows:

$$E^* = 1.0579 \quad Q_D^*$$

2. A 20% reduction in demand results in a 13% reduction in energy use for the analyzed seven systems. The equation obtained for a 20% demand reduction was as shown in Equation 3.9, (p. 50), and presented below. The energy Elasticity Coefficient, *S*, or slope of the line in Equation 3.9, is 0.6292.

$$E^* = 0.6292Q_D^* + 0.3695$$

3. The relationship between maximum tank water level variation and energy use is linear for the analyzed seven systems as shown in Equation 4.2 (p. 63). The equation is also repeated below.

$$E^* = 0.04H^* + 0.96$$

From Equation 4.2, it is evident that for the seven systems analyzed, a 50% reduction in tank maximum water levels saves 2% of the average energy use.

4. Lowering the tank elevation 50% saves up to 30% of the energy usage for the analyzed seven systems (Figure 4.8, p. 70).

5. A linear relationship between tank diameter and average energy use exists for the analyzed seven systems (Equation 4.10 (p 75), and is repeated below.

$$E^* = 0.12D' + 0.87$$

A 50% reduction in tank diameters saves up to 7% of energy used for the analyzed seven systems making it more sensitive than the other two tank parameters.

6. Multiple booster stations can result in more energy savings than a single high-horsepower pump for the analyzed seven systems with a high-elevation neighborhood.

7. The energy savings by adding multiple booster stations is system specific and ranges from 5% to 66% for the analyzed five systems (S3, S4, S5, S6, and S7), with no savings for the other two systems (S1 and S2), which had no higher-elevation neighborhoods.

8. Using analysis of several MDWDSs and analyzing results on a statistical basis may lead to generalizable results for many systems.

9. The presented results will aid researchers in understanding the relationship between variable MDWDS aspects and energy use in order to further more energy-efficient-design. This energy-efficient design will help to reduce energy use, thereby reducing the GHG emissions to mitigating global warming. In turn, this will help in meeting the United Nations Millennium Development Goals (MDG) of ensuring environmental sustainability.

References

Arpke, Angela and Hutzler, Neil (2005) "Operational life-cycle assessment and life-cycle cost analysis for water use in multioccupant buildings," *Journal of Architectural Engineering*, 11(3), 99-109.

Babayan, Artem V., Savic, Dragan A., Walters, Godfrey A., and Kapelan, Zoran S. (2007). "Robust least-cost design of water distribution networks using redundancy and integration-based methodologies." *Journal of Water Resources Planning and Management*, 133(1), 67-97.

Bosserman, B.E. (2000). "Pump system hydraulic design", *Water Distribution Systems Handbook,* Mays, Larry W, McGraw-Hill, New York, 5.1-5.40.

Brion, L.M., Mays, L.W. (1991). "Methodology for optimal operation of pumping stations in water distribution systems." *Journal of Hydraulic Engineering*, 117(11), 1551-1569.

Crowe, Clayton T., Elger, F. Donald, Roberson A., (2001). *Engineering Fluid Mechanics,* Seventh Edition, John Wiley & Sons, Inc.

Chase, Donald V. (2000). "Operation of water distribution systems." *Water Distribution Systems handbook,* L. W. Mays, ed., McGraw-Hill, Inc., Two Penn Plaza, New York, 15.1-15.16.

Colombo, Andrew F., and Karney, Bryan W., (2001). “Energy and costs of leaky pipes: towards comprehensive picture.” *Journal of Water Resources Planning and Management*, 128(6), 441-450.

Cunha, Maria da Conceição and Joaquim, Sousa (2001). “Hydraulic infrastructures design using simulated annealing.” *Journal of Infrastructure Systems,* 7(1), 32-39.

Daugherty, Robert L., and Joeseph B. Franzini (1957). *Fluid Mechanics with Engineering Applications.* McGraw-Hill, New York.

Ellis, Robert H. (1978). “New considerations for municipal water network planning” *Water Resources Bulletin,* 14(3), 542-553.

EPA (2000). *EPANET 2, Users Manual*, by Lewis A. Rossman, Water Supply and Water Resources Division National Risk Management Research Laboratory Cincinnati, OH 45268.

EPRI (2002). Electric Power Research Institute, *Water and Sustainability (volume 4): U.S. Electricity Consumption for Water Supply and Treatment – The Next Half Century*. EPRI, Palo Alto, CA: 2000. 1006787. Topical Report, March 2002.

Energy Information Administration (2007). *Form EIA-826*, "Monthly electric sales and revenue report with state distributions report.”

Farmani, R.; Savic, D.A.; Walters, G.A. (2004). “The simultaneous multi-objective optimization of anytown pipe rehabilitation, tank sizing, tank siting and pump operation schedules.” *Proceedings of the 2004 World Water and Environmental Resources Congress: Critical Transitions in Water and Environmental Resources Management*, Salt Lake City, UT, 4663-4672.

Filion, Y.R, MacLean, H.L., and Karney, B.W. (2004). “Life-cycle energy analysis of a water distribution system,” *Journal of Infrastructure Systems*, 10(3), 120-130.

Finnemore, John E., and Franzini, Joseph B. (2002). *Fluid Mechanics with Engineering Applications*, Tenth Edition, McGraw Hill Companies Inc., New York.

Ghimire, Santosh R., and Barkdoll, Brian, D (2008). “Effect of demand on energy use in municipal water distribution systems” *Proceedings, World Environmental & Water Resources Congress*, ASCE, Honolulu, Hawaii.

Gyergyek, L. and Presern, S. (1982). “Simulation and optimal control of large water distribution systems.” *Mathematics and Computers in Simulation*, 24(5), 385-392.

Haestad Methods (2004). *Advanced Water Distribution Modeling and Management*, Haestad Press, Waterbury, CT

Lansey, Kevin E. (2000). “Optimal design of water distribution systems”, *Water Distribution Systems Handbook*, Mays, Larry W, McGraw-Hill, New York.

Lansey, Kevin E. and Awumah, Kofi, (1994). “Optimal pump operations considering pump switches”, *Journal of Water Resources Planning and Management*, 120(1), 17-35.

Levin, Ronnie B., Epstein, Paul R., Ford, Tim E., Harrington, Winston, Olson, Eric, and Reichard, Eric G. (2002). U.S. Drinking water challenges in the twenty-first century, *Environmental Health Perspectives*, 110(1), 43-52.

Meier, R.W. and Barkdoll, B.D. (2000). “Sampling design for network model calibration using genetic algorithms.” *Journal of Water Resources Planning and Management*, 126(4), 245-250.

Mohapatra, P.K., Siebel, M.A., Gijzen, H.J., Van der Hoek, J.P., and Groot, C.A. (2002). “Improving eco-efficiency of Amsterdam water supply: A LCA approach” *Journal of Water Supply: Research and Technology*-AQUA, 51(4), 217-227.

Millennium Development Goals, (2000). “Goals, targets and indicators”. http://www.unmillenniumproject.org/goals/gti.htm#goal7, accessed on 03/12/08.

Murphgy, L.J., Dandy, G.C., and Simpson, A.R. (1994). “Optimum design and operation of pumped water distribution systems”, *Proceedings, Conf. on Hydraulics in Civil/ Engineering*, Institution of Engineers, Brisbane, Australia. National Conference Publication of Engineers Australia NCP, 94(1), 149-155.

Ostfeld A., Uber J., and Salomons E. (2006). "Battle of the water sensor networks (BWSN): a design challenge for engineers and algorithms." *Proceedings of 8th Annual Water Distribution System Analysis Symposium*, Cincinnati, Ohio, USA, published on CD.

Pezeshk, S., Helweg, O.J. (1996). “Adaptive search optimization in reducing pump operating costs” *Journal of Water Resources Planning and Management*, 122(1), 57-63.

Reis, L.F.R., Porto, R.M., and Chaudhry, F.H. (1997). “Optimal location of control valves in pipe networks by genetic algorithm.” *Journal of Water Resources Planning and Management*, 123(6), 317-326.

Savic, Dragan A., and Walters, Godfrey A., (1997). “Genetic algorithms for least-cost design of water distribution networks”. *Journal of Water Resources Planning and Management*, 123(2), 67-77.

Simpson, Angus R., Dandy Graeme C., and Murphy, Laurence J. (1994). “Genetic algorithms compared to other techniques for pipe optimization.” *Journal of Water Resources Planning and Management*, 120 (4), 423-443.

Skipworth, P., Engelhardt, M., Cashman, A., Savic, D., Saul, A., and Walters, G. (2002). *Whole life costing for water distribution network management*. Thomas Telford, London.

Tarquin, A. J.and Dowdy, J. (1989). “Optimal pump operation in water distribution” ASCE *Journal of Hydraulic Engineering*, 115(2), 158-168.

Ulanicki, B., Kahler, J., and See, H. (2007). “Dynamic optimization approach for solving an optimal scheduling problem in water distribution systems.” *Journal of Water Resources Planning and Management*, 133(1), 23-32.

United Nations Secretariat, (2007). World Population Prospects: The 2006 Revision. *Population Newsletter,* Issued by Population Division, Department of Economic and Social Affairs New York, Number 83

Upper Peninsula Power Company (UPPCO) (2007). http://www.uppco.com/business/eba_35.asp, accessed on 12/2007.

Vamvakeridou-Lyroudia, L. S., Savic, D. A., and. Walters, G. A (2007). “Tank simulation for the optimization of water distribution networks” *Journal of Hydraulic Engineering.* 133(6), 625-636

Vickers, Amy (2001). *Handbook of Water Use and Conservation,* Water Plow Press, Amherst, Massachusetts, USA, First Edition, ISBN 1-931579-07-5

Visesman Warren Jr., and Hammer, Mark J. (1998). *Water Supply and Pollution Control* 6th Edition, Addison Wesley Longman, Inc. CA.

Walski, Thomas M.; Brill, E. Downey Jr.; Gessler, Johannes; Goulter, Ian C.; Jeppson, Roland M.; Lansey, Kevin; Lee, Han-Lin; Liebman, Jon C.; Mays, Larry; Morgan, David R.; Ormsbee, Lindell (1987). "Battle of the network models: epilogue". *Journal of Water Resources Planning and Management*, 113(2), 191-203.

Walski, T.M. (2000). "Hydraulic design of water distribution storage tanks". *Water Distribution Systems Handbook*, L. W. Mays, ed., McGraw-Hill, Inc., Two Penn Plaza, New York, 10.1-10.20.

Wolff, J.B. (1961). "Peak demand in residential areas". *Journal of the American Water Works Association*, 1251-1260.

Walters, Godfrey A., Halhal, Driss, Savic, Dragan, Ouazar, Driss (1999). "Improved design of ``Anytown'' distribution network using structured messy genetic algorithms" *Urban water* 1 (1999), 23-38.

Yu, G., Powell, R.S., and Sterling, J.H. (1994). "Optimized pump scheduling in water distribution systems." *Journal of Optimization Theory and Applications*, 83(3), 463-488.

Zecchin, Aaron C., Maier, Holger R., Simpson, Angus R., Leonard, Michael, and Nixon, John B., (2007). "Ant colony optimization applied to water distribution system design: Comparative study of five algorithms." *Journal of Water Resources Planning and Management*, 133(1), 87-92.

Appendices

Appendix A: Chapter 3-Energy Savings through Water Conservation in Municipal Water Distribution Systems

A.1 Derivation of 3rd Degree Polynomial Equation of Energy Use Rate

Assuming that the pipe line flow (Q) and system-wide water demand rate (Q_D) have the same degree of relation with the energy use rate, Equation (A.12) may be derived as follows:

Total rate of energy (E) transferred from wire to water is the amount of energy rate required to pump water overcoming the friction losses along all of the pipes and elevation changes. It can be written as in Equation A.1 (Finnemore and Franzini, 2002).

$$E = \frac{1}{\eta} Q \gamma H_T \qquad \text{(A.1)}$$

where,

Q = pipeline flow rate (ft^3/s, m^3/s)

η = wire-water efficiency (%)

H_T = Total head added by pump (ft, m)

The term H_T, can be split into three components: (1) Static head *(H)* (m, ft), (2) Total head loss due to friction, *(*H_L*)* (m, ft), can be computed using Darcy-Weisbach equation (Haestad Methods, 2004), and (3) Other minor losses due to fittings and appurtenances (m, ft) *(*H_m*)* (Haestad Methods 2004).

Thus, the equation for total rate of energy can be rewritten as:

$$E = H + H_L + H_m \qquad \text{(A.2)}$$

Or,
$$E = \frac{1}{\eta} Q\gamma \left[H + \Sigma\left(\frac{8fL}{\pi^2 g D^5} Q^2 \right) + \Sigma\left(\frac{K_L}{2gA^2} Q^2 \right) \right] \qquad \text{(A.3)}$$

Or,
$$E = \frac{1}{\eta} Q\gamma \left[H + \sum\left(\frac{8fL}{\pi^2 g D^5} Q^2 \right) + \sum\left(\frac{8K_L}{\pi^2 g D^4} Q^2 \right) \right] \qquad \text{(A.4)}$$

Or,
$$E = k_1 Q^3 + k_2 Q \qquad \text{(A.5)}$$

where,

$$k_1 = \sum \frac{8\gamma fL}{\pi^2 g\eta D^5} + \sum \frac{8\gamma K_L}{\pi^2 g\eta D^4} \tag{A.6}$$

and,

$$k_2 = \frac{\gamma H}{\eta} \tag{A.7}$$

in which,

K_L = minor loss coefficient

A = cross section area (m^2, ft^2)

g = acceleration due to gravity (m/s^2, ft/s^2)

f = Darcy-Weisbach frictional factor (unit less)

γ = fluid (water) specific weight (N/m^3, lb/ft^3)

L = pipe length (m, ft)

D = pipe diameter (m, ft)

η = wire-water pump efficiency (unit less)

π = mathematical constant (approximately, 3.1416)

Therefore, the ratio of two energies, the normalized energy can be written as

$$E^* = \frac{E}{E_0} = \frac{k_1 Q^3 + k_2 Q}{k_1 Q^3 + k_2 Q} \tag{A.8}$$

Or, by dividing by Q_0^3 on numerator and denominator,

$$E^* = \frac{E}{E_0} = \frac{k_1 * \frac{Q^3}{{Q_0}^3} + k_2 * \frac{Q^3}{{Q_0}^3}}{k_1 + k_2 * \frac{1}{{Q_0}^2}} \qquad \text{(A.9)}$$

Or, replacing, $\frac{Q}{Q_0} = Q^*$ and also dividing by k_1 in numerator and denominator,

$$E^* = \frac{{Q^*}^3 + \frac{k_2}{k_1 {Q_0}^2} Q^*}{1 + \frac{k_2}{k_1 {Q_0}^2}} \qquad \text{(A.10)}$$

Finally, separating the terms in numerator,

$$E^* = \frac{1}{1 + \frac{k_2}{k_1 {Q_0}^2}} {Q^*}^3 + \frac{1}{\frac{k_1}{k_2} {Q_0}^2 + 1} Q^* \qquad \text{(A.11)}$$

Or,

$$E^* = A{Q^*}^3 + BQ^* \qquad \text{(A.12)}$$

where, A and B are defined as coefficients of ${Q^*}^3$ and Q^* as in Equation A.13, and A.14 below.

i.e,

$$A = \frac{1}{1 + \frac{k_2}{k_1 {Q_0}^2}} \qquad \text{(A.13)}$$

$$B = \frac{1}{\frac{k_1}{k_2} {Q_0}^2 + 1} \qquad \text{(A.14)}$$

A.2 Comparison of Cubic Curve Fit Equation with EPANET Simulations

It can be seen that the results of the cubic curve fit equation as defined in Equation (A.12) yielded almost the same value of R^2 as the linear trend line of E* obtained from EPANET simulations (Figure A.1). More importantly, the slopes of both the lines are the same, if the cubed term and squared term of cubic curve fit E* is neglected, being negligible numbers ($6x10^{-14}$ and $1x10^{-13}$). This leads to conclude that the relationship between water demand reduction and energy use for the seven systems can be described as linear.

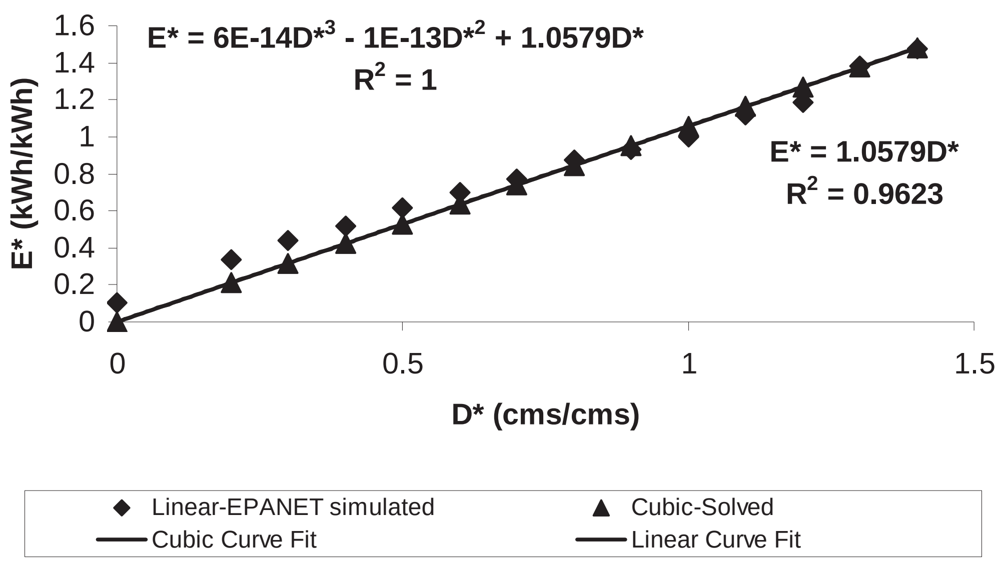

Figure A.1 Cubic curve fit match: Polynomial relationship between cubic curve fit average normalized energy, (as defined in Equation A.12), and linear average normalized energy, E*, simulated from EPANET, for the variation of normalized demand, Q_D*

The values of the curve fit normalized energy (E*) were computed using Equation (A.12) above. An Excel solver function was used to estimate the coefficients of D^{*3} and D* of the equation setting a constraint for non negative values of A and B.

A.3 Pump Curves and Tank Levels Modification for High-Demand Simulation

The alterations of pump curves and tanks for various systems during the simulations of variations in water demands are provided below:

Table A.1 Alteration of pump curves for high-demand simulations for System 1 (Modified from the pump data of S1 as described in Section 2.2, p. 20): Q = flow, h = head, Q_D* = 1 is the original.

Q_D*	Q	h
	m^3/s (gpm)	m (ft)
1	0.038 (600)	45.7 (150)
1.1	0.038 (600)	54.9 (180)
1.2	0.039 (620)	54.9 (180)
1.3	0.043 (680)	54.9 (180)
1.4	0.042 (660)	64.0 (210)

Table A.2 Alteration of pump curves for high-demand simulations for System 4 (Modified from the pump data of S4 as described in Section 2.2, p. 20): Q = flow, h = head

	Curve 1		Curve 2	
Q_D* m/m	Q m^3/s (gpm)	h m (ft)	Q m^3/s (gpm)	h m (ft)
1.0	0.014 (222)	128 (420)	0.0 (0.1)	128 (420)
	0.027 (426)	125 (409)	0.027 (426)	125 (409)
	0.041 (650)	118 (388)	0.041 (649)	118 (388)
	0.057 (897)	106 (346)	0.057 (897)	106 (346)
	0.075 (1,185)	79.6 (261)	0.075 (1,185)	79.6 (261)
Single point curves				
1.1	0.095 (1,500)	128 (420)	0.011 (175)	128 (420)
1.2	0.098 (1,550)	128 (420)	0.013 (200)	128 (420)
1.3	0.132 (2,100)	128 (420)	0.016 (250)	128 (420)
1.4	0.139 (2,200)	128 (420)	0.019 (300)	128 (420)

Table A.3 Alteration of tank maximum and minimum water levels for S4 (Q_D* = 1.3 and 1.4 needed modifications) (Modified from the tank data of S4 as described in Section 2.2, p. 20): Q = flow, h = head, D = diameter

Q_D*	**Tank 1**				**Tank 2**			
	IL m (ft)	**Min L m (ft)**	**Max L m (ft)**	**D m (ft)**	**IL m (ft)**	**Min L m (ft)**	**Max L m (ft)**	**D m (ft)**
1.0,1.1,1.2	3.0 (10)	1.8 (6.0)	4.6 (15)	17.7 (58.0)	3.0 (10)	1.8 (6.0)	4.6 (15)	6.1 (20)
1.3	3.0 (10)	1.8 (6.0)	6.1 (20)	23.4 (75.4)	3.0 (10)	0.9 (3.0)	5.90 (19.5)	7.9 (26)
1.4	3.0 (10)	0.9 (3.0)	6.4 (21)	24.7 (81.2)	3.0 (10)	0.9 (3.0)	6.4 (21)	17 (56)

IL = Initial tank water level

Min L = minimum tank water level

Max L = maximum tank level

Table A.4 Alteration of pump curves for demand variation simulations for S7 (Modified from the pump data of S7 as described in Section 2.2, p. 20): Q = flow, h = head, Q_D* = 1 is the original

	Curve 3		**Curve 4**	
Q_D*	**Q m^3/s (gpm)**	**h m, (ft)**	**Q m^3/s (gpm)**	**h m, (ft)**
0.0001	1.9 (30,740)	91.4 (300)	3.0 (48,340)	96.6 (317)
0.2	1.9 (30,740)	82.3 (270)	3.0 (48,340)	96.6 (317)
1	1.9 (30,740)	76.5 (251)	3.0 (48,340)	96.6 (317)
1.2	1.9 (30,740)	83.8 (275)	3.0 (48,340)	96.6 (317)
1.3, 1.4	2.3 (36,300)	96.0 (315)	3.6 (57,100)	112.8 (370)

Appendix B: Chapter 4-Impact of Storage Tanks on Energy Consumption in Municipal Water Distribution Systems

B.1 Example of Controls Used in EPANET

The c*ontrols* are the Rules that control the pump status depending on the tank water levels of a system. The c*ontrols* used in S4 are provided below.

Rule 1

If tank 1 level above 15.0

Then pump 5 status is closed

And pump 4 status is closed

Rule 2

If tank 1 level below 6.0

Then pump 4 status is open

And pump 5 status is open

Rule 3

If tank 5 level above 15.0

Then pump 10 status is closed

And pump 9 status is closed

Rule 4

If tank 5 level below 6.0

Then pump 10 status is open

And pump 9 status is open

B.2 Pump alterations for tank maximum water level sensitivity modeling

Below are the pump curves modifications for various systems. The curves were generated by EPANET using "Single-point" (EPA 2000). A single point is a single coordinate of the pump curve (flow and head) which is utilized by EPANET to generate the complete pump curve by considering zero flow at shutoff head (133% of design head), and a maximum flow (twice the design flow) at zero head.

B.2.1 S2 Pump Modification

Figure B.1 following represents the pump head modification for S2. The original pump curve (C2) was modified to curve (C6) with lower head.

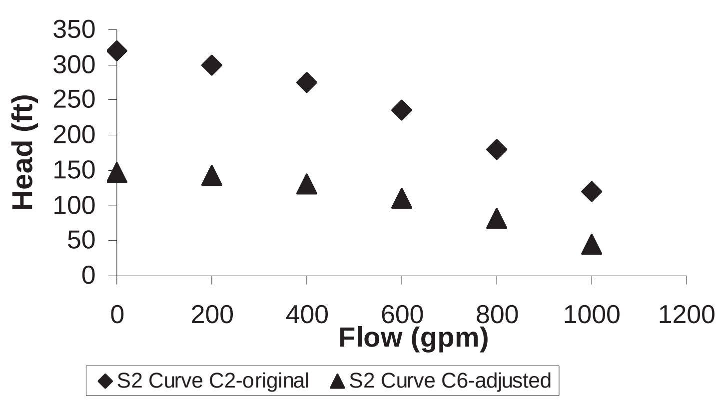

Figure B.1 Pump curves for S2 before and after adjustments (Adjusted from the pump data of S2 as described in Section 2.2, p. 20)

B.2.2 S4 Pump Modification

S4 consists of two pump curves (C1, and C2) for six pumps, and both curves were modified as shown below. Only head was adjusted for both the curves. Following Figure B.2 is a plot of pump curve C1 for network S4 with modification of head.

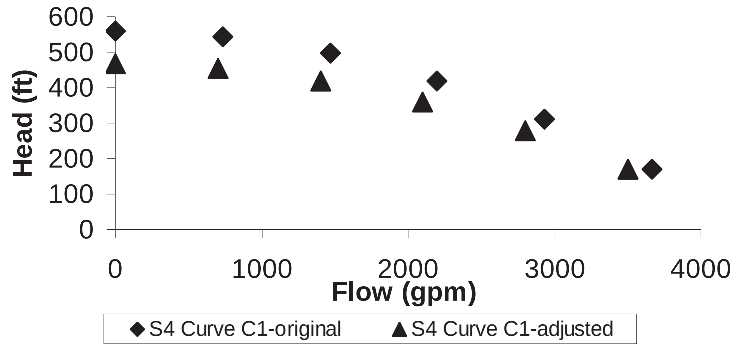

Figure B.2 Pump curves (C1) for S4 before and after adjustments (Adjusted from the pump data of S4 as described in Section 2.2, p. 20)

Following Figure B.3 represents the pump curve C2 for S4 before and after the adjustment of pump characteristics.

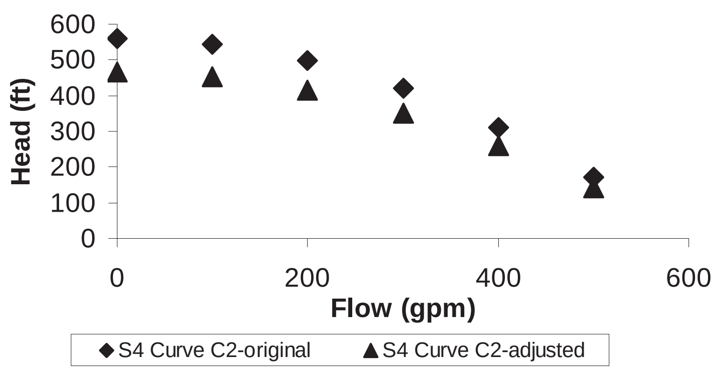

Figure B.3 Pump curves (C2) of S4 before and after adjustments (Adjusted from the pump data of S4 as described in Section 2.2, p. 20)

B.2.3 S5 Pump Modification

The following Figure B.4 represents a modification of head of a pump curve for S5.

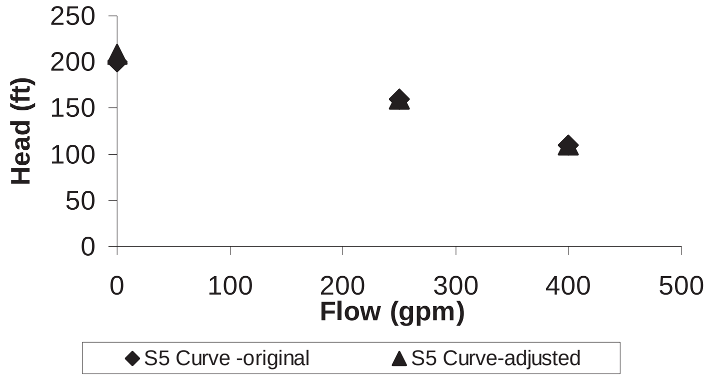

Figure B.4 Pump curves of S5 before and after adjustments of head (Modified from the pump data of S5 as described in Section 2.2, p. 20).

B.2.4 S6 Pump Modification

Originally, no pump curves were modified for both tanks of S6. The modifications to check the pump oversize are depicted below in Figure B.5. In this case, both head and flow were adjusted.

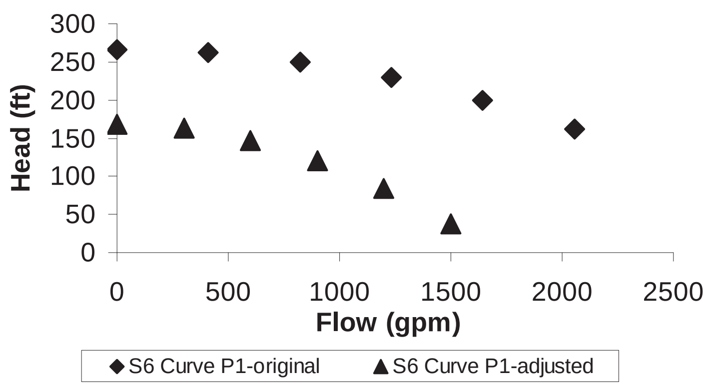

Figure B.5 Pump curves P1 of S6 before and after adjustments (Modified from the pump data of S6 as described in Section 2.2, p. 20)

B.2.5 S7 Pump Modification

Pump curve modifications for S7 are shown below in Figure B.6, and B.7. The adjusted curve (C3) has a very small flow in comparison to the original flow of the original curve (C3), and is hardly extended in its axis (Figure B.6).

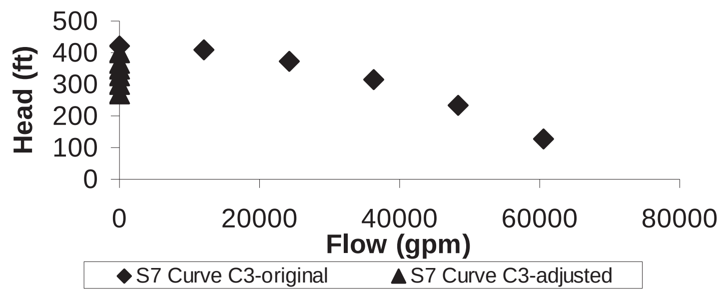

Figure B.6 Pump curves C3 of S7 before and after adjustments (Modified from the pump data of S7 as described in Section 2.2, p. 20)

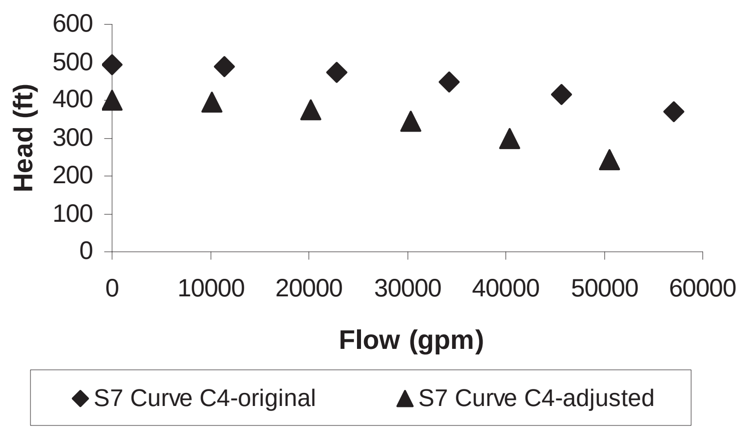

Figure B.7 Pump curves C4 of S7 before and after adjustments (Modified from the pump data of S7 as described in Section 2.2, p. 20)

B.3 Computation of System Curve for Tank Maximum Water Level Variations

Friction loss (h_L) through a pipe was computed using Hazen-Williams Equation (B.1) given as follows (Haestad Methods, 2004):

$$h_L = \frac{C_f L}{C^{1.852} D^{4.87}} Q^{1.852} \quad \text{(B.1)}$$

See Chapter 2 (p. 11) for details.

Total head loss was computed by adding the total friction loss through all of the pipes through the system, S1 (in this case) (Table B.1 below). This was used for the computation of K in Equation 4.1, Chapter 4 (p. 54).

Table B.1 Friction head loss through S1 (Calculated from the pump data of S1 as described in Section 2.2, p. 20)

Link ID	Length	Diameter	Roughness	Flow	Friction loss
	L	D	C	Q	h_L
	m	m		cms	m
Pipe 1	914.4	0.356	100	0.048	1.1
Pipe 2	1,524.0	0.305	100	0.002	0.0
Pipe 3	1,524.0	0.203	100	0.031	12.1
Pipe 4	1,524.0	0.203	100	0.001	0.0
Pipe 5	1,524.0	0.203	100	0.031	12.1
Pipe 6	2,133.6	0.254	100	0.033	6.3
Pipe 7	1,524.0	0.152	100	0.013	10.6
Pipe 8	2,133.6	0.152	100	0.011	10.6
Total Head loss →					52.7

Thus, the *K* can be calculated as:

$$K = \frac{h_L}{Q^2} \tag{B.2}$$

Then, the system curve is developed using following Equation (B.3):

$$H_{TOT} = \mathrm{H_{STAT}} + h_L \tag{B.3}$$

.

The system curve and pump curve data are provided in Table B.2 below.

Table B.2 System curve and pump curve data (Computed from the pump data of S1 as described in Section 2.2, p. 20)

System Curve		**Pump Curve**		**System Curve**		**Pump Curve**	
H*=0.5				**H*=1.5**			
Flow	**Head**	**Flow**	**Head**	**Flow**	**Head**	**Flow**	**Head**
cms	**m**	**cms**	**m**	**cms**	**m**	**cms**	**m**
0.000	42.67	0.000	73.15	0.000	48.77	0.000	73.15
0.003	43.04	0.003	73.02	0.003	49.13	0.003	73.02
0.006	44.14	0.006	72.64	0.006	50.23	0.006	72.64
0.009	45.97	0.009	72.01	0.009	52.06	0.009	72.01
0.013	48.53	0.013	71.12	0.013	54.63	0.013	71.12
0.016	51.83	0.016	69.98	0.016	57.92	0.016	69.98
0.019	55.85	0.019	68.58	0.019	61.95	0.019	68.58
0.022	60.61	0.022	66.93	0.022	66.71	0.022	66.93
0.025	66.11	0.025	65.02	0.025	72.20	0.025	65.02
0.028	72.33	0.028	62.86	0.028	78.43	0.028	62.86
0.032	79.29	0.032	60.45	0.032	85.39	0.032	60.45
0.035	86.98	0.035	57.78	0.035	93.08	0.035	57.78
0.038	95.40	0.038	54.86	0.038	101.50	0.038	54.86
0.041	104.56	0.041	51.68	0.041	110.65	0.041	51.68
0.044	114.44	0.044	48.26	0.044	120.54	0.044	48.26

B.4 Pump and Junctions Alterations for Tank Elevation Sensitivity Modeling

The analyzed seven systems needed pump modifications as summarized in Table B.3 below:

Table B.3 Summary of system modifications for tank elevation variations

System	Z* value m/m	Alteration
1	1, 1.1,1.2, 1.3, 1.4, 1.5	Pump curve
2	1, 1.1,1.2, 1.3, 1.4, 1.5	Pump curve
3 (T1, and T2)	0.5, 0.6, 0.7, 0.8, 0.9	Junctions
3 (T2)	0.5, 0.6	Pump curve
4 (T1, T2)	0.5, 0.6, 0.7, 0.8, 0.9	Junctions
5 (T1)	0.5, 0.6	Junctions
5 (T2)	0.5, 0.6, 0.7	Junctions
5 (T2)	0.5	Pump curve
6 (T1)	1, 1.1,1.2, 1.3, 1.4, 1.5	Pump curve
6 (T2)	0.5, 0.6, 0.7, 0.8, 0.9	Junctions
7 (T2)	1.4, 1.5	Pump curve
7 (T2)	0.5, 0.6, 0.7, 0.8, 0.9	Junctions

B.4.1 System 1 (S1)

In order to achieve the sufficient pressure, S1 required modification in pump head as given in Table B.4 below.

Table B.4 Pump modification for S1 (Modified from pump data of S1 as described in Section 2.2, p. 20)

Q	H	Z*
gpm	**ft**	**ft/ft**
600	180	1
600	193	1.1
600	206	1.2
600	219	1.3
600	232	1.4
600	245	1.5

B.4.2 System 2 (S2)

S2 also needed pump modification as shown in Table B.5 below.

Table B.5 Pump head modification for S2 (Modified from the pump data of S2 as described in Section 2.2, p. 20)

Q	H	Z*
gpm	ft	ft/ft
600	110	1
600	110	1.1
600	121.1	1.2
600	132.1	1.3
600	143.2	1.4
600	154.2	1.5

B.4.3 System 3 (S3)

The simulations of System 3 tank 1 (S3T1) required only junction alteration as shown in Table B.6 below. Many junctions were required to lower their location to a lower level of elevation in order to bring them at the level of lowest simulation of Z* = 0.5 (tank elevation = 781.1 ft) (Table B.6).

Table B.6 Alteration of the elevation of junctions for S3T1 simulations (Modified from the elevation data of S3 as described in Section 2.2, p. 20)

Node ID	**Elevation**	**Lower T1 (Z* times)**				
	(ft)	**0.9**	**0.8**	**0.7**	**0.6**	**0.5**
Tank -131 (T1)	1,137.1	1065.9	994.7	923.5	852.3	781.1
Junction-102	1,094.07	X	X	X	X	X
Junction-103	1,031.73		X	X	X	X
Junction-121	957			X	X	X
Junction-122	957			X	X	X
Junction-104	860.64				X	X
Junction-119	849					X
Junction-120	849					X
Junction-29	846.28					X
Tank -130 (T2)	843.9	Tank				
Junction-46	820.24					X

However, the junction alterations were required for T2 simulations Z* = 0.5 to 0.9 values (Table B.7).

Table B.7 Modification of the elevation of junctions for S3T2 simulations (Modified from the elevation data of S3 as described in Section 2.2, p. 20)

Node ID	**Elevation**	**Lower T2 (Z*x)**				
	ft	**0.9**	**0.8**	**0.7**	**0.6**	**0.5**
Tank -131 (T1)	1,137.1					
Junction-102	1,094.07	X	X	X	X	X
Junction-103	1,031.73	X	X	X	X	X
Junction-121	957	X	X	X	X	X
Junction-122	957	X	X	X	X	X
Junction-104	860.64	X	X	X	X	X
Junction-119	849	X	X	X	X	X
Junction-120	849	X	X	X	X	X
Junction-29	846.28	X	X	X	X	X
Tank -130 (T2)	843.9	802	760.1	718.2	676.3	634.5
Junction-46	820.24	X	X	X	X	X
Junction-123	758			X	X	X
Junction-124	758			X	X	X
Junction-45	747.32			X	X	X
Junction-40	741.63			X	X	X
Junction-42	728.05			X	X	X
Junction-39	703.19				X	X
Junction-28	701.69				X	X
Junction-41	700.22				X	X
Junction-27	690.65				X	X
Junction-26	683.43				X	X
Junction-44	678.5				X	X
Junction-37	677.05				X	X
Junction-25	653.93					X
Junction-43	653.09					X
Junction-21	652.42					X
Junction-35	651.97					X
Junction-38	646.51					X
Junction-101	645.09					X
Junction-90	644.09					X
Junction-93	643.74					X
Junction-98	643.05					X
Junction-99	641.89					X
Junction-47	640.47					X
Junction-100	637.9					X
Junction-48	637.45					X
Junction-91	637.44					X
Junction-24	636.61					X
Junction-30	636					X

The simulations of Z* = 0.5 and 0.6 of S3T2 also required modification in Pump 2 (Table B.8). However, S3T2 simulations did not need any modifications for the normal operation simulation and greater value of Z*.

Table B.8 Pump 2 modification for Z*=0.5, 0.6 of S3T2 (Modified from the pump data of S3 as described in Section 2.2, p. 20)

Z*					
0.5		**0.6**		**1**	
Q	**H**	**Q**	**H**	**Q**	**H**
gpm	**ft**	**gpm**	**ft**	**gpm**	**ft**
0	499	0	457	0	445
790	365	790	365	790	365
1,460	120.0	1,460	120.0	1,460	120.0

B.4.4 System 4(S4)

System 4 Tank 1 (S4T1) required alteration in junction elevation (Table B.9) in order to maintain the required pressure of the majority of the systems except reservoir, tanks, and a few junctions near the tanks. S4T1 simulations did not require any pump modifications.

Table B.9 Modification of the elevation of junctions of S4T1 simulations (Modified from elevation data of S4 as described in Section 2.2)

Node ID	**Elevation**	**Lower T1 (Z*x)**				
	ft	**0.9**	**0.8**	**0.7**	**0.6**	**0.5**
Tank 1 (T1)	915	884.5	854	823.5	793	762.5
J-95	880		X	X	X	X
Tank 5 (T2)	850	No need				
J-970	828			X	X	X
J-1000	826			X	X	X
J-940	820				X	X
J-980	817				X	X
J-990	817				X	X
J-1080	789					X
J-930	787					X
J-90	784					X
J-80	784					X
J-10F	784					X
J-960	779					X
J-950	779					X
J-1010	768					X

The following Table B.10 consists of the modification of System 2 Tank 2 (S4T2) elevations. S4T2 simulations required opening all other standby pumps to maintain the system pressure for most of the junctions for the simulations of Z* = 1.1 to 1.5. The normal operating pumps were used for all simulations without any modifications.

Table B.10 Modification of the elevation of junctions of S4T2 simulations (Modified from the elevation data of S4 as described in Section 2.2, p. 20)

Node ID	**Elevation**	**Lower T2 (Z*x)**				
	ft	**0.9**	**0.8**	**0.7**	**0.6**	**0.5**
Tank 1 T1)	915	915	915	915	915	915
J-95	880	X	X	X	X	X
Tank 2 (T2)	850	826	802.0	778.0	754.0	730.0
J-970	828	X	X	X	X	X
J-1000	826		X	X	X	X
J-940	820		X	X	X	X
J-980	817		X	X	X	X
J-990	817		X	X	X	X
J-1080	789			X	X	X
J-930	787			X	X	X
J-90	784			X	X	X
J-80	784			X	X	X
J-10F	784			X	X	X
J-960	779			X	X	X
J-950	779			X	X	X
J-1010	768				X	X
J-60	755				X	X
J-200	755				X	X
J-1020	751					X
J-100	748					X
J-1030	745					X
J-340	738					X
J-910	738					X
J-920	738					X
Junc 1PRV-3	738					X
Junc 2PRV-3	738					X
J-1040	737.7					X

B.4.5 System 5 (S5)

The simulations of System 5 Tank 1 (S5T1) for Z* = 0.7 to 1.5 did not have any issues. There were several junctions that needed to be adjusted in the case of Z* = 0.5 and 0.6. The adjustments are shown below in Table B.11. This network did not have any issues for the simulations of Z* = 0.7, even though there were 17 junctions with higher elevation than the elevation of lowered tank elevation (Table B.11).

Table B.11 Modification of the elevation of junctions of S5T1 simulations (Modified from the elevation data of S5 as described in Section 2.2, p. 20)

Node ID	**ft**	**Tank1**				
	Elevation	**0.9**	**0.8**	**0.7**	**0.6**	**0.5**
Junc 67	793			X	X	X
Junc 68	792			X	X	X
Junc 63	787			X	X	X
Junc 64	784			X	X	X
Junc 65	782			X	X	X
Junc 69	782			X	X	X
Junc 196	775			X	X	X
Junc 61	772			X	X	X
Junc 62	772			X	X	X
Junc 66	772			X	X	X
Junc 70	770			X	X	X
Junc 57	764			X	X	X
Junc 55	763			X	X	X
Junc 56	760			X	X	X
Tank 345 (T2)	760			X	X	X
Junc 53	757			X	X	X
Junc 54	757			X	X	X
Junc 58	751			X	X	X
Junc 59	714				X	X
Tank 344 (T1)	**843**	**810.1**	**777.2**	**744.3**	**711.4**	**678.5**
Junc 52	707					X
Junc 51	702					X
Junc 3	700					X
Junc 4	698					X

Junc 2	690					X
Junc 7	690					X
Junc 15	690					X
Junc 50	690					X
Junc 60	690					X
Junc 93	687					X
Junc 233	686					X
Junc 5	685					X
Junc 38	685					X
Junc 1	684					X
Junc 230	684					X
Junc 229	682					X
Junc 231	682					X
Junc 331	682					X
Junc 8	680					X
Junc 9	680					X
Junc 29	680					X
Junc 77	680					X
Junc 81	680					X
Junc 117	680					X
Junc 232	680					X
Junc 234	680					X

S5T2 simulations did not need any junction elevation modification for Z*= 0.7 to 1.5. There were 26 junctions above the Tank 2 elevation for Z*= 0.7. However, there was insufficient pressure in the system for the simulations of Z* = 0.6, which was solved by modifying the junctions (See Table B.12). For Z*=0.5, pump curve 7 was slightly modified as well (See Table B.13).

Table B.12 Modification of the elevation of junctions of S5T2 simulations (Modified from the elevation data of S5 as described in Section 2.2, p. 20)

Node ID	ft	Tank2				
	Elevation	0.9	0.8	0.7	0.6	0.5
Tank 344 (T1)	843					
Junc 67	793				X	X
Junc 68	792				X	X
Junc 63	787				X	X
Junc 64	784				X	X
Junc 65	782				X	X
Junc 69	782				X	X
Junc 196	775				X	X
Junc 61	772				X	X
Junc 62	772				X	X
Junc 66	772				X	X
Junc 70	770				X	X
Junc 57	764				X	X
Junc 55	763				X	X
Junc 56	760				X	X
Junc 53	757				X	X
Junc 54	757				X	X
Junc 58	751				X	X
Junc 59	714				X	X
Junc 52	707				X	X
Junc 51	702				X	X
Junc 3	700				X	X
Junc 4	698				X	X
Junc 2	690				X	X
Junc 7	690				X	X
Junc 15	690				X	X
Junc 50	690				X	X
Junc 60	690				X	X
Junc 93	687				X	X
Junc 233	686				X	X
Junc 5	685				X	X
Junc 38	685				X	X
Junc 1	684				X	X
Junc 230	684				X	X
Junc 229	682				X	X
Junc 231	682				X	X
Junc 331	682				X	X
Junc 8	680				X	X
Junc 9	680				X	X

Junc 29	680				X	X
Junc 77	680				X	X
Junc 81	680				X	X
Junc 117	680				X	X
Junc 232	680				X	X
Junc 234	680				X	X
Junc 40	672				X	X
Junc 49	672				X	X
Junc 6	670				X	X
Junc 28	670				X	X
Junc 41	670				X	X
Junc 235	668				X	X
Junc 10	667				X	X
Junc 30	665				X	X
Junc 39	665				X	X
Junc 42	665				X	X
Junc 45	665				X	X
Junc 44	662				X	X
Tank 345 (T2)	**760**				**661.16**	**637**
Junc 26	660					X
Junc 27	660					X
Junc 31	660					X
Junc 43	660					X
Junc 24	657					X
Junc 32	655					X
Junc 35	655					X
Junc 71	655					X
Junc 33	652					X
Junc 36	650					X
Junc 11	648					X
Junc 225	645					X
Junc 226	643					X
Junc 12	642					X
Junc 224	642					X
Junc 23	640					X
Junc 37	640					X

Table B.13 Pump head modification for Z*=0.5 of S5T2 (Modified from the pump data of S5 as described in Section 2.2, p. 20)

New		Old	
Flow(gpm)	Head (ft)	Flow(gpm)	Head (ft)
0	208	0	200
250	160	250	160
400	110	400	110

B.4.6 System 6 (S6)

The main pump was modified for the simulations of System 6 Tank 1 (S6T1) variations. The modification for S6T1 simulations was only for the values of Z* above 1.0. The normal pump curve is applicable for the lower Z* values (0.5 – 1.0). The pump head was gradually increased based upon the increased tank elevation (Table B.14).

Table B.14 Pump modification for S6T1 simulations (Modified from the pump data of S6 as described in Section 2.2, p. 20).

Flow	Head	head modified	Z*
gpm	ft		ft/ft
850	126	126	1
850	135.0	136.0	1.1
850	144.0	149.0	1.2
850	153.0	163.0	1.3
850	162.0	176.0	1.4
850	171.0	191.0	1.5

Unlike S6T1, S6T2 did not require pump modification for the simulation of the values of Z*= 1.0 to 1.5. However, it required junction modification for the lower values of Z* (0.5 to 0.9) (Table B.15)

Table B.15 Modification of the elevation of junctions of S6T2 simulations (Modified from elevation data of S6 as described in Section 2.2)

Node ID	ft	Tank2				
	Elevation	0.9	0.8	0.7	0.6	0.5
Junc 2	1,231	X	X	X	X	X
Junc 3	1,231	X	X	X	X	X
Junc 4	1,231	X	X	X	X	X
Junc 5	1,231	X	X	X	X	X
Tank 1 (T1)	1,231	No need	X	X	X	X
J-125	1,203	X	X	X	X	X
J-390	1,203	X	X	X	X	X
Tank 2 (T2)	1,153	1,151.8	1,150.6	1,149.4	1,148.2	1,147.0
J-60	1,152	X	X	X	X	X

B.4.7 System 7 (S7)

System 7 Tank 1, (S7T1), did not need any sort of modifications.

System 7 Tank 2, (S7T2), did not require any modifications in pump curves and alteration of junctions for the simulations of Z*= 0.6 to 1.3. However, S7T2 required modification of pump head for the simulations of Z* = 1.4 and 1.5 (Table B.16). For the lowest value of Z* = 0.5, the junctions above the tank elevation were required to be lowered to the level of tank elevation (Table B.17). In addition, there was one other junction at a location of the system that was needed to lower its elevation in order to provide non-negative pressure to the system. The junction was lowered to 80 ft of elevation from its original elevation of 118ft, even though it is below the tank elevation of 120.9 ft at Z*= 0.5.

Table B.16 Pump head modifications for S7T2 simulation (for Z* = 1.4 and 1.5) (Modified from the pump data of S7 as described in Section 2.2, p. 20)

Curve 3			Curve 4		
Old		New	Old		New
Flow (gpm)	Head (ft)	Head (ft)	Flow (gpm)	Head (ft)	Head (ft)
7	300	324.2	40,299	300	324.2

Table B.17 Modification of elevation of junctions for S7T2 simulations (for Z*= 0.5) (Modified from elevation data of S7 as described in Section 2.2, p. 20)

Node ID	ft	Tank2				
	Elevation	**0.9**	**0.8**	**0.7**	**0.6**	**0.5**
Tank 2 (T2)	241.7	217.5	193.4	169.2	145	120.9
Tank1 (T1)	241.7					X
Junction-6806	133.4					X
Junction-6812	132.5					X
Junction-6801	130.2					X
Junction-6072	130.0					X
Junction-2809	130.0					X
Junction-6104	129.9					X
Junction-10782	129.8					X
Junction-6138	129.7					X
Junction-6802	129.0					X
Junction-6142	128.9					X
Junction-6143	128.8					X
Junction-6112	128.8					X
Junction-6068	128.6					X
Junction-6103	128.1					X
Junction-6069	128.0					X
Junction-6110	127.9					X
Junction-6811	127.9					X
Junction-7353	127.6					X
Junction-6105	127.5					X
Junction-7351	127.5					X
Junction-6808	127.5					X
Junction-7334	127.3					X
Junction-6109	127.2					X
Junction-6804	127.0					X
Junction-6800	127.0					X
Junction-6075	126.0					X
Junction-6073	125.8					X
Junction-6135	125.6					X
Junction-6803	125.0					X
Junction-6805	124.8					X

Junction-6070	124.3					X
Junction-7344	124.0					X
Junction-5945	123.1					X
Junction-6813	123.0					X
Junction-7291	122.5					X
Junction-7333	122.5					X
Junction-6107	122.2					X
Junction-3205	121.9					X
Junction-6115	121.9					X

System 7 Tank 3, (S7T3), did not need any modifications.

System 7 Tank 4, (S7T4), did not need any modifications.

B.5 Pump Alterations for Tank Diameter Sensitivity Modeling

The following modifications were made for various systems for sensitivity modeling of storage tank diameters.

Table B.18 Systems with pump curve variation for tank diameter variation

Systems	Pump variation	No. of Curves	No. of curves adjusted
S1	No	1	0
S2	Yes	1	1
S3	Yes	2	2
S4	Yes	2	2
S5	No	8	0
S6	No	1	0
S7	No	7	0

The following pump curves were generated using EPANET using the single values of discharge and head (EPA 2000) for the three systems, S2, S3, and S4.

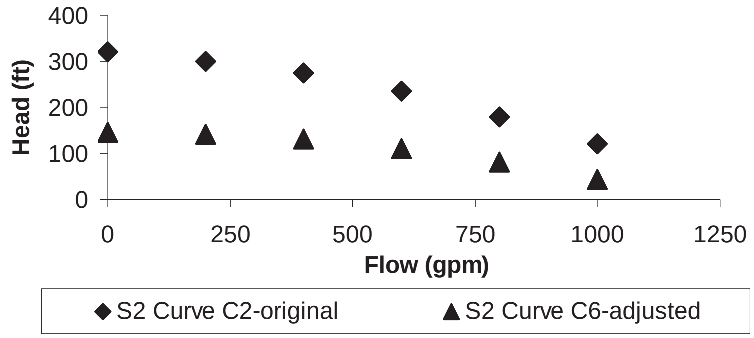

Figure B.8 Pump curve C2 adjustment for the diameter variation of S2 (Modified from the pump data of S2 as described in Section 2.2, p. 20)

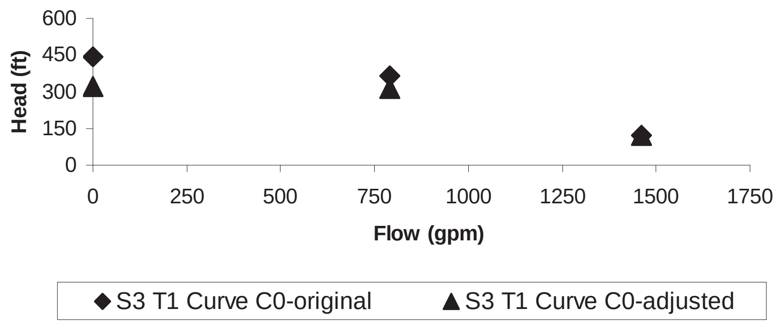

Figure B.9 Pump curve C0 adjustment for the diameter variation of S3T1 (Modified from the pump data of S3 as described in Section 2.2, p. 20)

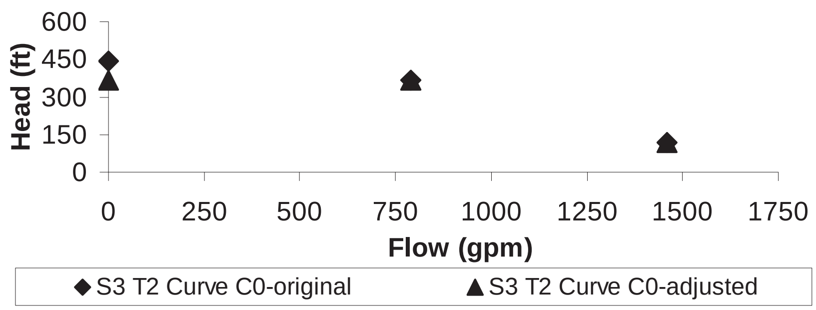

Figure B.10 Pump curve C0 adjustment for the diameter variation of S3T2 (Modified from the pump data of S3 as described in Section 2.2, p. 20)

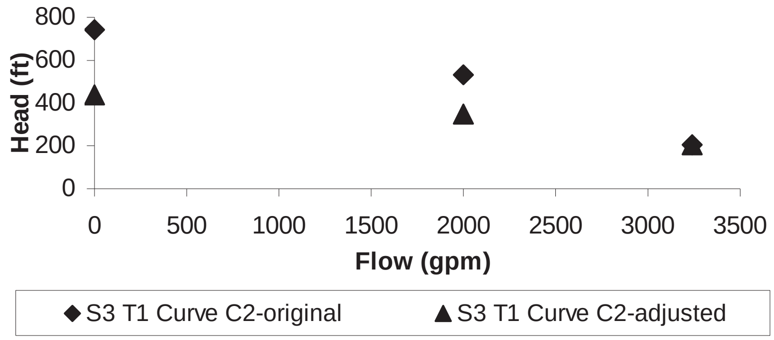

Figure B.11 Pump curve C2 adjustment for the diameter variation of S3T1 (Modified from the pump data of S3 as described in Section 2.2, p. 20)

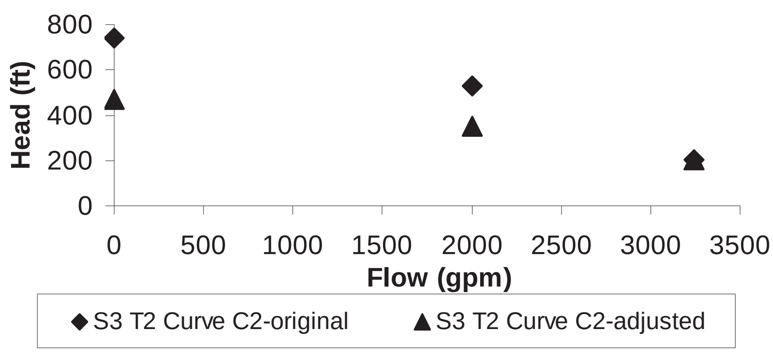

Figure B.12 Pump curve C2 adjustment for the diameter variation of S3T2 (Modified from the pump data of S3 as described in Section 2.2, p. 20)

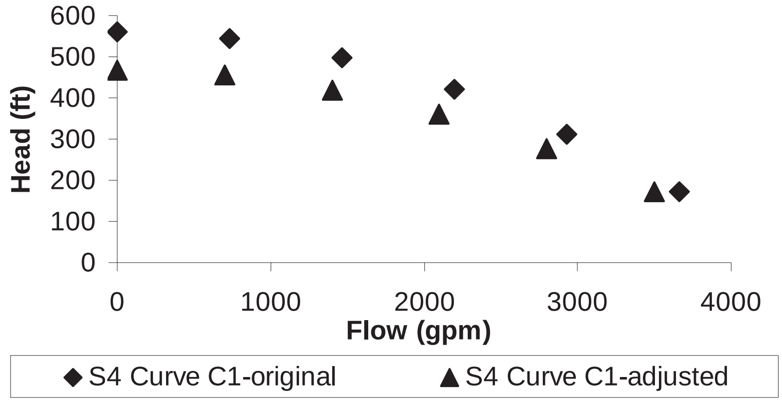

Figure B.13 Pump curve C1 adjustment for the diameter variation of S4T1 and S4T2 (Modified from the pump data of S4 as described in Section 2.2, p. 20)

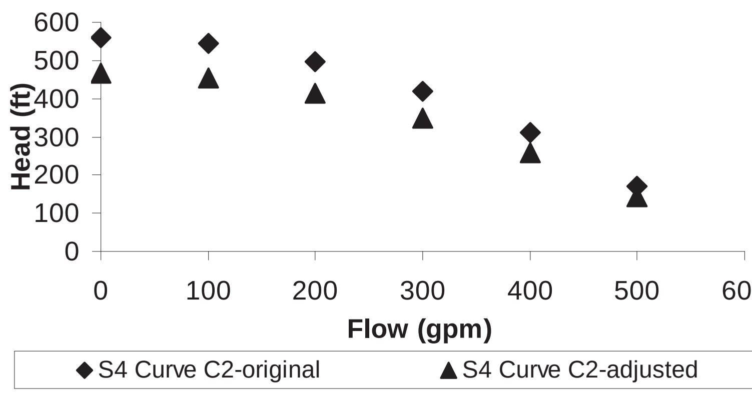

Figure B.14 Pump curve C2 adjustment for the diameter variation of S4T1 and S4T2 (Modified from the pump data of S4 as described in Section 2.2, p. 20)

Appendix C: Chapter 5- The Role of Pumping Stations in the Reduction of Energy Use in Municipal Drinking Water Distribution Systems

C.1 Horsepower Variation

C.1.1 Original controls of S3 (Ostfeld et al. 2006)

RULE RULE-0

IF TANK TANK-130 LEVEL >= 16.000000

THEN PUMP PUMP-172 STATUS IS CLOSED

PRIORITY 1.000000

RULE RULE-1

IF TANK TANK-130 LEVEL <= 12.100000

THEN PUMP PUMP-172 STATUS IS OPEN

PRIORITY 1.000000

RULE RULE-3

IF TANK TANK-131 LEVEL >= 18.400000

THEN PUMP PUMP-170 STATUS IS CLOSED

PRIORITY 1.000000

RULE RULE-4

IF TANK TANK-131 LEVEL <= 15.400000

THEN PUMP PUMP-170 STATUS IS OPEN

Priority 1.000000

C.1.2 Pump Modifications

The following Table C.1 shows the modifications of pump-1 for the simulations of pumping station 2 for System 3 (S3PS2).

Table C.1 Modification of Pump 1 for the simulation of S3PS2 (Modified from the pump data of S3 as described in Section 2.2, p. 20)

Old		New	
Flow	**Head**	**Flow**	**Head**
gpm	**ft**	**gpm**	**ft**
0	440	0	460
2,000	350	2,000	400
3,240	205	3,240	205

C.2 Booster Station Variation

The description of modifications of systems for the booster stations variation is presented below.

C.2.1 Modifications of System 1 (S1)

C.2.1.1 Addition of controls logic

The added controls logic for S1 are given below:

Rule 1

If tank 8 level above 15

Then pump 9 status is closed

Rule 2

If tank 8 level below 6

Then pump 9 status is open

C.2.1.2 Pump Modifications of S1

Table C.2 below shows the modifications of pump curves for various simulations of booster additions. The modified pumps are shown in the fifth column of the table.

Table C.2 Modifications of S1 for booster additions (Modified from the pump data of S1 as described in Section 2.2, p. 20)

S1				Modified Pump #	Modified Curve	
Pump#	Curve #	Flow (gpm)	Head (ft)		Q (gpm)	H (ft)
1	1	600	180	N/A	N/A	N/A
2	b1	600	165	1	600	165
3	b2	600	10	1	600	165
				b1	600	10
4	b3	600	10	1	600	165
				b1	600	10
				b2	600	10
5	b4	600	10	all same as b4	600	165

Note: In Table C.2, second column, b_i *= Curve number for a booster, i = 1, 2, 3, and 4.*

C.2.2 Modifications of System 2 (S2)

C.2.2.1 Pump Modifications of S2

Table C.3 below shows the modifications of pumps for the simulations of booster additions of S2.

Table C.3 Modifications of S2 for booster additions (Modified from the pump data of S2 as described in Section 2.2, p. 20)

S2				Modified pump #	Modified curve	
Pump#	Curve #	Flow (gpm)	Head (ft)		Q (gpm)	H (ft)
1	C6	600	70	N/A	N/A	N/A
2	b1	600	10	1	600	70
3	b2	600	10	1	600	70
				b1	600	10
4	b3	600	10	1	600	60
				b1	600	10
				b2	600	10
5	b4	600	10	Same as b3	600	60

Note: In Table C.3, second column, b_i *= Curve number for a booster, i = 1, 2, 3, and 4.*

C.2.3 Modifications of System 3 (S3)

C.2.3.1 Pump Modifications of S3

The pumps of S3 were modified as described below.

The two existing pump curves used for the normal condition system with one booster station are provided in Table C.4 below. The modifications of the pump curves are provided in the following Table C.5.

Table C.4 Two existing pump curves for S3 (Computed from the pump data of S3 as described in Section 2.2, p. 20)

	Flow (gpm)	Head (ft)		Flow (gpm)	Head (ft)
b1 (CURVE-0)	0.0	445.0	CURVE-2	0	740
	790.0	365.0		2,000	530
	1,460	120.0		3,240	205

Table C.5 Modifications of S3 for booster additions (Modified from the pump data of S3 as described in Section 2.2, p. 20)

S3				Modified pump #	Modified curve	
	Curve #					
Pump#	CURVE-2	Flow (gpm)	Head (ft)	CURVE-2	Q (gpm)	H (ft)
1		0	740	Main pump-1	0	1,185
		2,000	530		2,790	895
		3,240	205		4,700	325
2	b1 (CURVE-0)			CURVE-2		
3	b2	790	150	1	2,000	4,60
				b1	790	250
4	b3	790	150	1	2,000	460
				b1	790	250
				b2	790	100
5	b4	2,000	450	same as b3		

Note: In Table C.5, second column, b_i = Curve number for a booster, i = 1, 2, 3, and 4.

C.2.4 Modifications of System 4 (S4)

C.2.4.1 Pump Modifications of S4

The two existing pump curves used for the normal condition system with one booster station are provided in Table C.6 below. The modifications of the pump curves are provided in the following Table C.7.

Table C.6 Two existing pump curves for S4 (Computed from the pump data of S4 as described in Section 2.2, p. 20)

	Main pump			Booster pump	
curve	Flow (gpm)	Head (ft)	curve	Flow (gpm)	Head (ft)
1	2,200	780	2	300	780

Table C.7 Modifications of S4 for booster additions (Modified from the pump data of S4 as described in Section 2.2, p. 20)

S4				Modified pump #	Modified curve	
	Curve #			Curve #		
Pump#	1	Flow, Q (gpm)	Head, H (ft)		Q (gpm)	H (ft)
1		2,200	780	main1	2,200	800
2	b1	300	780		2,200	780
3	b2	700	140	1	2,000	710
				b1	300	310
4	b3	456	71	1	2,200	710
				b1	300	290
				b2	700	140
5	b4	1,039	65.5	1	2,200	700
				b1	300	260
				b2	700	140
				b3	456	71

Note: In Table C.7, second column, b_i = Curve number for a booster, i = 1, 2, 3, and 4.

C.2.5 Modifications of System 5 (S5)

C.2.5.1 Pump Modifications of S5

Table C.8 Three existing pump curves for S5 (Curves 4, 5, and 6 are identical) (Computed from the pump data of S5 as described in Section 2.2, p. 20)

Main pump station			Booster pump Station1			Booster pump Station 2		
curve	**Flow (gpm)**	**Head (ft)**	**curve**	**Flow (gpm)**	**Head (ft)**	**curve**	**Flow (gpm)**	**Head (ft)**
5	0	450	7 (open)	0	230	1(open)	0	210
4,5,6	500	350		250	160		100	200
	700	168		400	110		200	152
			8	0	200	2	0	260
				250	160		300	225
				320	110		620	130
						3	0	260
							300	225
							620	130

Table C.9 Modifications of S5 for booster additions (Modified from the pump data of S5 as described in Section 2.2, p. 20)

S5				Modified pump #	Modified curve	
	Curve #			Curve #		
Pump#		Flow (gpm)	Head (ft)	mainpump	Q (gpm)	H (ft)
1	5	0	450		0	1480
	(3 4,5,6)	500	350		500	1310
		700	168		700	1200
2	7 as 7b1	0	420	5 as 5b1	0	660
		250	370		500	640
		400	330		700	630
3	b2	0	210	5 as 5	0	450
		100	200		500	350
		200	152		700	168
				7 as 7	0	230
					250	160
					400	110
4	b3	178	204	5 as mainb3	500	260
				7 as 7	0	230
					250	160
					400	110
				1 as 1	0	210
					100	200
					200	152
5	b4	500	117	5 as mainb4	500	290
				7 as 7	0	230
					250	160
					400	110
				1 as 1	0	210
					100	200
					200	152
				b3	178	204

Note: In Table C.9, second column, b_i = Curve number for a booster, i = 1, 2, 3, and 4.

C.2.6 Modifications of System 6 (S6)

C.2.6.1 Pump Modifications of S6

Table C.10 Modifications of S6 for booster additions (Modified from the pump data of S6 as described in Section 2.2, p. 20)

S6				Modified pump #	Modified curve	
	Curve #			Curve #		
Pump#		Flow, Q (gpm)	Head, H (ft)		Q (gpm)	H (ft)
1	P1	2043	200	N/A		
2	b1	30	116	P1 as P1	2043	150
3	b2	154	114	1	2043	150
				b1	30	16
4	b3	158	95	P1 as P1	2043	150
				b1	30	16
				b2	154	14
5	b4	59	58	P1 as P1	2043	150
				b1	59	16
				b2	154	14
				b3	158	15

Note: In Table C.10, second column, b_i = Curve number for a booster, i = 1, 2, 3, and 4.

C.2.7 Modifications of System 7 (S7)

C.2.7.1 Pump Modifications of S7

Table C.11 Three existing pump curves for S7 (Modified from the pump data of S7 as described in Section 2.2, p. 20)

Main pump station				Booster pump Station1	
Curve	Flow, Q (gpm)	Head, H (ft)	Curve	Q (gpm)	H (ft)
4	40,299	300	CURVE-4	0	47
3	7	300		200	40.2
				353	33

Table C.12 Modifications of S7 for booster additions (Modified from pump the data of S7 as described in Section 2.2, p. 20)

S7				Modified pump #	Modified curve	
	Curve #			Curve #		
Pump #		Flow, Q (gpm)	Head, H (ft)		Q (gpm)	H (ft)
1	4	40,299	300	N/A		
	3	7	300			
2	(b1) CURVE-4	0	47	4 as 4	40,299	300
		200	40.2	3 as 3	7	300
		353	33			
3	b2	95	140	4 as 4	40,299	230
				3 as 3	7	300
				b1 as b1	N/A	
4	b3	150	30.8	4 as 4	40,299	225
				3 as 3	7	300
				b1 as b1	N/A	
				b2 as b2	95	140
5	b4	9,600	22.26	4 as 4	40,299	225
				3 as 3	7	300
				b1 as b1	N/A	
				b2 as b2	95	110
				b3 as b3	150	20.8

Note: In Table C.12, second column, b_i = Curve number for a booster, i = 1, 2, 3, and 4.